

2017

Development of Immunotherapy Strategies: Targeting Gram-positive and Gram-negative Pathogenic Bacteria

Mary J. Sabulski
Lehigh University

Follow this and additional works at: <http://preserve.lehigh.edu/etd>



Part of the [Chemistry Commons](#)

Recommended Citation

Sabulski, Mary J. ., "Development of Immunotherapy Strategies: Targeting Gram-positive and Gram-negative Pathogenic Bacteria" (2017). *Theses and Dissertations*. 2790.
<http://preserve.lehigh.edu/etd/2790>

This Dissertation is brought to you for free and open access by Lehigh Preserve. It has been accepted for inclusion in Theses and Dissertations by an authorized administrator of Lehigh Preserve. For more information, please contact preserve@lehigh.edu.

**Development of Immunotherapy Strategies:
Targeting Gram-positive and Gram-negative Pathogenic Bacteria**

by

Mary J. Sabulski

A Dissertation

Presented to the Graduate and Research Committee

Of Lehigh University

In Candidacy for the Degree of

Doctor of Philosophy

In

Chemistry

Lehigh University

May 2017

© 2017 Copyright
Mary J. Sabulski

Approved and recommended for acceptance as a dissertation in partial fulfillment
of the requirements for the degree of Doctor of Philosophy

Mary J. Sabulski

Development of Immunotherapy Strategies: Targeting Gram-positive and Gram-negative
Pathogenic Bacteria

April 21, 2017

Defense Date

Approved Date

Dissertation Director
Marcos M. Pires, PhD

Committee Members

Damien Thevenin, PhD

David Vicic, PhD

Kathryn Iovine, PhD
Outside Committee Member

Acknowledgements

To my advisor, Professor Marcos Pires, I would like to express my deepest gratitude. Throughout my graduate studies, he continually conveyed enthusiasm in regard to research, scholarship, and mentorship. I am honored to have been part of a team under the direction of Dr. Pires, whose ability to critically examine every aspect of a project is truly admirable. Thank you for the immense guidance and counsel during my study: I am a stronger scientist because of it.

I would also like to thank my committee members, Dr. Damien Thévenin, Dr. David Vicic, and Dr. Kathy Iovine. I deeply appreciate your willingness to serve on my committee, as well as the guidance and insightful suggestions throughout my graduate career.

These years have been blessed with wonderfully creative and knowledgeable fellow graduate students, whom I hold in the highest regard. To my lab mate, Sean Pidgeon, and former lab mate, Dr. Jon Fura, it has been a joy to work alongside both of you. Thank you for the meaningful scientific discussions and all the laughs. Our new lab mates, George Ongwae and Noel Ferraro, thank you for the words of encouragement and support. My fellow graduate students, Dr. Kelly King, Betty Bloch, Janessa Gerhart, Eden Reichard, and Sarah Plucinsky Gilson, thank you for being a constant force of positivity. In earning this degree, I have found friendships in all of you and, for that, I will be forever grateful to Lehigh University.

My most heartfelt thanks are given to my family. To my parents, Michael and Jennifer Sabulski, thank you for making the sacrifices so I could pursue my highest dreams. All that I am is because of you. To my sister, Sarah, my brother, Michael, and

my brother-in-law, Mike, I am forever blessed to have a strong, faith-filled, loving family in all of you. Thank you for the unwavering support throughout my academic career and continued support throughout life. Finally, thank you to my fiancé, Max, who believed when I doubted, championed when I failed, and who didn't say "I told you so" when I succeeded. Thank you for being my rock.

Dedication

*To my mom and dad, Jen and Mike,
Thank you for everything – I had the time of my life.
All my love.*

Table of Contents

List of Figures	xii
List of Tables	xvii
List of Reaction Schemes	xviii
Abstract	1
Chapter 1. Pathogenic Bacteria	4
1.1 Microbes	4
1.2 Antibiotic Treatment for Bacterial Infections	5
1.3 Mechanisms of Antibiotic Resistance in Bacteria	12
1.4 Treatment of Antibiotic Resistant Bacteria Infections	20
1.5 References	24
Chapter 2. Bacterial Immunotherapy	28
2.1 Introduction	28
2.2 Bacteria and the Human Host	30
2.3 Bacterial Immunotherapy	31
2.3.1 Antibody-Recruiting Small Molecules (ARMs) for Bacteria Targeting	32
2.4 References	40
Chapter 3. Immuno-Targeting of <i>Staphylococcus aureus</i> via Sortase A-Mediated Incorporation of Vancomycin-Antigen Complexes	43

3.1 Abstract	43
3.2 Introduction	45
3.3 Results and Discussion	49
3.3.1 Fluorescent Labeling of <i>S. aureus</i> using vancomycin-BODIPY	49
3.3.2 SrtA-mediated Incorporation in <i>S. aureus</i>	52
3.3.3 Vancomycin-conjugated SrtA Recognition Peptide Incorporation in <i>S. aureus</i>	56
3.3.4 DNP-Conjugate Mediated Opsonization of <i>S. aureus</i>	68
3.3.5 <i>In vivo</i> Labeling of <i>S. aureus</i> Sc01 in <i>C. elegans</i>	75
3.3.6 SrtB-mediated Incorporation in <i>L. monocytogenes</i>	77
3.4 Conclusion	79
3.5 References	81
Chapter 4. Synthetic Immuno-Attractants against Gram-Negative Pathogens	83
4.1 Abstract	83
4.2 Introduction	84
4.3 Results and Discussion	88
4.3.1 Fluorescent Labeling of <i>E. coli</i> using PMN-FITC	88
4.3.2 PMBN-DNP Mediated Opsonization of <i>E. coli</i>	96
4.3.3 PMBN-DNP Potentiation of Antibiotics	106
4.3.4 PMBN-DNP Mediated Opsonization of <i>P. aeruginosa</i>	108

4.3.5 Induced Toxicity with Fatty Acid Derivative	112
4.3.6 Pooled Human Serum Bacterial Cell Opsonization	115
4.4 Future Work	118
4.5 Conclusion	119
4.6 References	121
Chapter 5. Fluorescence-based Assay Monitors PAD2 and PAD4 Activity	123
5.1 Abstract	123
5.2 Introduction	124
5.2.1 Post-Translational Modifications	124
5.2.2 Peptidylarginine Deiminases	125
5.3 Materials and Methods	130
5.4 Results and Discussion	134
5.4.1 Assay reports on PAD2 / PAD4 Activity	134
5.4.2 Assay Optimization for High-Throughput Screening	138
5.4.2.1 Assay Miniaturization at Room Temperature	138
5.4.2.2 Reagent Stability	140
5.4.2.3 Kinetics of Reaction	142
5.4.2.4 Trypsin Inhibition	144
5.4.3 Assay Response to Known PAD Inhibitors	148

5.5 Conclusions	149
5.6 References	151
Chapter 6. Materials and Methods	154
6.1 Materials	154
6.2 Mammalian Cell Culture	154
6.3 Bacterial Cell Culture	155
6.4 Bacterial Strains	155
6.5 Synthesis of FITC-conjugated anti-DNP Antibody	155
6.6 Solid Phase Peptide Synthesis of FITC-Conjugated Sortase Recognition Peptides	156
6.7 Solid Phase Peptide Synthesis of DNP-Conjugated Sortase Recognition Peptides	157
6.8 Synthesis of Vancomycin-conjugated SrtA Recognition Peptides	159
6.9 Synthesis of PMBN-FITC	160
6.10 Synthesis of PMBN-PEG _x -DNP	160
6.11 Synthesis of PMBN-PEG _x -DNP(Oct)	161
6.12 SrtA Mediated Fluorescent Labeling	162
6.13 Antibody Binding Assay in <i>S. aureus</i> (Wood Strain)	162
6.14 Antibody Binding Assay in <i>S. aureus</i>	153
6.15 Bacterial Labeling in live <i>C. elegans</i>	163

6.16 Minimal Inhibitory Concentration Assay	164
6.17 Mammalian Cell Viability Assay	165
6.18 Fluorescent Imaging	165
6.19 PMBN-FITC <i>E. coli</i> Labeling	166
6.20 Dissociation of PMBN-FITC from <i>E. coli</i> Surface	166
6.21 PMBN-PEGx-DNP Antibody Binding Assay	167
6.22 Bacterial Opsonization with Pooled Human Serum	167
6.23 Time-kill Studies of Stationary-phase <i>E. coli</i>	168
6.24 Antibiotic Potentiation Assay	168
Appendix	170
Curriculum Vitae	177

List of Figures

Chapter 1

1.1 Bacterial Classification	9
1.2 Bacterial Antibiotic Resistance Mechanisms	13
1.3 Lack of New Classes of Antibiotics	20
1.4 Pathogen Priority Level	23

Chapter 2

2.1 Primary Modes of Pathogen Clearance based on Immunomodulators	34
2.2 Chemical Structures of Antigens Capable of Recruiting Endogenous Antibodies	36

Chapter 3

3.1 Remodeling of Bacterial Surface via Sortase A	47
3.2 Schematic Representation of <i>S. aureus</i> Immunotherapy	48
3.3 Mechanism of Vancomycin	50
3.4 Vancomycin-BODIPY Dissociation from <i>S. aureus</i> Surface	51
3.5 Incorporation of FITC Conjugated SrtA Recognition Peptides	54

3.6 DIC and Fluorescent Microscopy Image of FITC-KLPMTG Labeled <i>S. aureus</i>	55
3.7 Cartoon representation of SrtA incorporation of Vancomycin-peptide conjugates	57
3.8 Vancomycin Acid Susceptibility	59
3.9 Vancomycin-conjugated SrtA Recognition Peptide Incorporation in <i>S. aureus</i>	62
3.10 Vancomycin-conjugated SrtA Recognition Peptide Incorporation in <i>S. aureus</i>	63
3.11 Vancomycin-conjugated SrtA Recognition Peptide Incorporation in Various Bacterial Strains	64
3.12 Toxicity of Vancomycin in Gram-positive Bacteria	65
3.13 DIC and Fluorescent Microscopy Image of FITC-2PEG1Vanc Labeled <i>S. aureus</i>	67
3.14 Antibody Recruitment to the Surface of <i>S. aureus</i> -Wood Strain	71
3.15 Antibody Recruitment to the Surface of <i>S. aureus</i> Sc01	72
3.16 DNP-2PEG1Vanc Toxicity towards <i>S. aureus</i> Sc01	73
3.17 Induced Mammalian Toxicity	74
3.18 <i>In vivo</i> Labeling of <i>S. aureus</i> Sc01 in <i>C. elegans</i>	76
3.19 SrtB-mediated Fluorescent Peptide Incorporation in <i>Listeria monocytogenes</i>	78

Chapter 4

4.1 Structure of LPS	85
4.2 Representation of PMB and LPS Binding	86
4.3 Schematic Representation of Gram-negative Bacterial Immunotherapy	87
4.4 Structures of Polymyxin B and PMB-Nonapeptide (PMBN)	88
4.5 PMBN-FITC Labeling of <i>E. coli</i>	90
4.6 PMBN-FITC Labeling of <i>E. coli</i> over Time	91
4.7 PMBN-FITC Dissociation from <i>E. coli</i> Surface	92
4.8 Cation Effect on PMBN-FITC Labeling of <i>E. coli</i>	94
4.9 DIC and Fluorescent Microscopy Image of PMBN-FITC Labeled <i>E. coli</i>	95
4.10 Gram-negative bacterial Outer Membrane Molecular Complexity	96
4.11 Structures of Polymyxin B and PMBN-DNP conjugates with PEG linkers.	97
4.12 PMBN-PEG _x -DNP mediated antibody recruitment in <i>E. coli</i>	101
4.13 PMBN-PEG ₁₂ -DNP Toxicity towards <i>E. coli</i>	102
4.14 Toxicity of PMBN-PEG ₁₂ -DNP towards Stationary phase <i>E. coli</i>	103
4.15 PMBN-PEG ₁₂ -DNP Induced Mammalian Cell Toxicity	105

4.16 Potentiation of Antibiotics	107
4.17 Schematic Representation of Variety in Lipopolysaccharide Structures	109
4.18 PMBN-PEG _x -DNP mediated antibody recruitment in <i>Pseudomonas aeruginosa</i>	110
4.19 PMBN-PEG ₁₂ -DNP(Oct) Toxicity towards <i>E. coli</i>	114
4.20 Cartoon Representation of Antibody Recruitment using Pooled Human Serum	115
4.21 Antibody Recruitment from Pooled Human Serum in <i>E. coli</i>	117
 Chapter 5	
5.1 Fluorescence assay reports on Activity of PAD2 and PAD4	134
5.2 Trypsin Hydrolysis of ZRCoum	136
5.3 Calcium Dependence of PAD2 and PAD4	137
5.4 Assay Monitors PAD4 Activity in 384 – well plate	139
5.5 Assay Monitors PAD4 Activity in 384 – well plate at Room Temperature	140
5.6 Analysis of Reagent Stability	141
5.7 Time Course of PAD4 Reaction	142

5.8 Kinetics of PAD2 Reaction	143
5.9 Analysis of Trypsin Inhibition	145
5.10 Assay using Crude Cell Lysate as PAD4 Source	147
5.11 Assay Reports on PAD Inhibition	148

List of Tables

Chapter 1

1.1 Common Antibiotics Prescribed for Bacterial Infections	11
--	----

Chapter 3

3.1 List of Synthesized Vancomycin-SrtA peptide conjugates	58
--	----

3.2 List of Synthesized Vancomycin-SrtA peptide conjugates	62
--	----

Chapter 4

4.1 PMBN-PEG ₁₂ -DNP Toxicity in <i>E. coli</i> and Mammalian Cells	105
--	-----

4.2 Evidence of Synergy against <i>E. coli</i>	106
--	-----

Chapter 5

5.1 Interpretation of Z-factor	150
--------------------------------	-----

List of Reaction Schemes

Chapter 3

3.1 Synthesis of FITC Conjugated SrtA Recognition Peptides	53
3.2 Synthesis of Vancomycin-conjugated SrtA Recognition Peptides	61
3.3 Synthesis of Vancomycin-conjugated DNP-SrtA Recognition Peptides	70

Chapter 4

4.1 Synthesis of PMBN-FITC	89
4.2 Synthesis of PMBN-PEG _x -DNP Conjugates	99
4.3 Synthesis of PMBN-PEG _x -DNP Conjugates	100
4.4 Synthesis of PMBN-PEG ₁₂ -DNP(Oct)	113

Chapter 5

5.1 PAD Assay Design	129
----------------------	-----

ABSTRACT

The rapid surge in drug-resistant bacterial infections has now become one of the primary public health crises of the 21st century. In a world without effective antibiotics, modern surgical and medical procedures will become too dangerous or impossible due to the threat of untreatable bacterial infections. As discussed in Chapter 1, the emergence of antibiotic resistant bacteria threatens to render a majority of the current antimicrobial therapeutics ineffective. Every year in the United States alone, over two million people are afflicted with bacterial infections that are resistant to FDA-approved antibiotics. According to the CDC, over 20,000 of those patients died as a result of drug-resistant Gram-positive bacterial infections, such as *Streptococcus pneumoniae* (*S. pneumoniae*), *Enterococcus faecium* (*E. faecium*), and *Staphylococcus aureus* (*S. aureus*). Equally alarming is the emergence of multidrug Gram-negative pathogenic bacteria, including strains that are resistant to all currently available antibiotics. As the number of efficacious antibiotics continues to rapidly dwindle without replenishment, the possibility of entering a post-antibiotic era can become a reality. Discovery and development of drug leads against the most serious pathogenic bacteria is desperately needed to reinvigorate the antibiotic pipeline and reverse this alarming trend.

This thesis will discuss the design of two immunotherapy strategies that target bacterial cells for destruction *via* surface modeling conjugates that specifically home to bacterial cell surfaces. The Pires lab has pioneered the field of bacterial immunotherapy for the eradication of Gram-positive bacteria. In Chapter 2, we will highlight previous reports of facile bacterial surface modulation strategies that act to stimulate or attenuate the host immune system. We have extended our techniques of bacterial surface

remodeling with the goal of reactivating the host immune system to seek out and directly clear pathogenic bacteria. In Chapter 3, we set out to leverage the surface-homing properties of vancomycin to specifically tag the surface of Gram-positive *Staphylococcus aureus* with immune cell attractants. Vancomycin was conjugated to a small molecule hapten, known to effectively recruit endogenous antibodies. In combination with sortase A-mediated surface remodeling, which are house-keeping enzymes that catalyze selective and covalent modification of bacterial cell walls, we successfully demonstrated the tagging and recruitment of endogenous anti-DNP antibodies to the surface of *S. aureus*. We also showed, for the first time, *in vivo* selective targeting of *S. aureus* in live *C. elegans*, a widely used model host to understand bacterial pathogenesis and host-pathogen interactions. Together, our results pave the way for a narrow-spectrum strategy for the destruction of bacterial infections caused by *S. aureus* (drug-sensitive and -resistant) through bacterial immunotherapy.

Chapter 4 will discuss our goal is to eradicate Gram-negative superbugs by targeting problematic pathogenic bacteria for destruction by the host immune system. In this second major strategy, we report the design and development of a series of polymyxin B conjugates (a last resort antibiotic against Gram-negative pathogens), which are, to our knowledge, the first class of synthetic molecules that remodel Gram-negative bacterial cell surfaces with immune cell attractants. Given the inherent antimicrobial activity of polymyxin B, we designed agents to display dual activities against bacteria (membrane-disruption and immune activation). By leveraging the power of the immune system in clearing pathogens, this new class of molecules was shown to uniquely target Gram-negative bacteria and, additionally, potentiate existing FDA-approved antibiotics.

Additionally, in this study, the recruitment of antibodies from pooled human serum is shown, thus validating the biological relevance of this immunotherapy. We hope to establish this approach as a potential treatment option and further refine this methodology to address the clinical challenge of Gram-negative bacterial pathogens.

The last chapter of this thesis focuses on the development of a facile assay to monitor the activity and inhibition of two isoforms of the Peptidylarginine deiminases (PAD) family: PAD2 and PAD4. PADs are post-translational modifiers that catalyze the calcium-dependent conversion of arginine residues to unnatural citrulline residues in a protein substrate. The full extent of the role PADs play in normal physiology and diseased states is not yet fully understood. PADs have important roles in the formation of Neutrophil Extracellular Traps (NETs), which was a recently discovered response of the immune system against bacterial pathogens. NETs are biomolecules that encase invading pathogens, which immobilize them to assist in their clearance by the human immune system. We report on a new, fluorescence-based assay, which is readily performed under ambient conditions and is compatible with high-throughput screening platforms. Furthermore, through a collaboration with Penn State Hershey Medical Center, we utilized the assay in a high-throughput screen for potential PAD4 inhibitors.

Chapter 1

Pathogenic Bacteria

1.1 Microbes

The sheer number of the projected bacterial species on Earth can be difficult to grasp – with a total number well into the millions of individual species.¹ Bacteria are single-cell microorganisms, a few micrometers in length, that normally exist together and are characterized by a lack of a nucleus structure and membrane-bound organelles.² Due to their high adaptability to different environments, bacteria are found in even the harshest conditions on Earth. In fact, it has been reported that much of Earth's biomass is composed primarily of bacteria.³ The ability of bacteria to survive, adapt, and thrive in unusual environments is primarily driven by three features: a relatively high mutation rate, their small sizes, and a rapid binary cell division rate. The mutation rate for bacteria has been estimate at 0.003 mutations per genome per cell.⁴ . This is sharp contrast to humans, which have mutation rates of $\sim 2.5 \times 10^{-8}$ per base per generation.⁵ The increased mutation rate naturally promotes the generation of mutants within a population that possess increased fitness. Their relatively small size functions to increase the population size in any niche they occupy, providing the opportunity for favorable mutations to accumulate. Finally, a large majority of bacteria divide rapidly – with some bacteria approaching doubling times in the matter of minutes. Together, these features are extremely favorable for the rapid evolution of offspring that can adapt to new and changing environments.

Bacteria can also survive in less extreme environments such as soil, plants, ambient temperate water, and other modern-life surfaces. These are the same environments that

are occupied by humans. Not coincidentally, humans and bacteria cross paths through our co-existence. But our relationship goes beyond a co- and -independent existence. In many ways, humans (similar to most complex life on Earth) have co-evolved with bacteria. The human body represents a unique and highly dynamic environment for trillions of bacterial cells living in and on an average person.⁶ The sheer number of bacterial cells means that these microbial communities have the potential to impact human health. Commensal bacteria are harbored in many different tissues through the body, which means the host immune system has to naturally adapt to these non-self cells. An imbalance of the host immune response can lead to a number of serious health diseases. For example, a highly attenuated response may lead to uncontrolled bacteria growth, while an overly aggressive response may lead to chronic or acute inflammation.

Unlike the response to commensal bacteria, the human immune system must rapidly and efficiently attempt to eradicate pathogenic bacteria upon first exposure. In most instances, this is exactly what happens. The human immune system (both the innate and the adaptive arms) has evolved diverse and incredibly precise modes of detecting, responding, and clearing pathogens. Likewise, pathogens continue to evolve counter-measures to the defense modalities employed by human immune systems. As such, there are instances when pathogenic bacteria successfully evade the host immune response. From the initial invader, an infection often ensues that requires the intervention of therapeutic agents, such as antibiotics. For example, the notorious Gram-positive bacteria, *Staphylococcus aureus* (*S. aureus*) is known to cause a high human burden resulting in infections in various tissues of the body. *S. aureus* has long been recognized as one of the most important bacteria that cause disease in humans and the incidence of

infections have dramatically increased in the last 50 years due to the emergence of drug-resistant strains, the closed quarters associated with hospitals, and the high number of surgical procedures associated with modern medical interventions. Gaining access to the body through broken or punctured skin, *S. aureus* can cause serious infections such as bloodstream infections, pneumonia, or bone and joint infections. By readily multiplying and disrupting the normal function of healthy cells within a host organism, pathogenic bacteria will progress to a diseased state. If left untreated, the infection can rapidly escalate to become life-threatening.

1.2 Antibiotic Treatment for Bacterial Infections

Alexander Fleming's 1928 discovery and 1942 clinical use of penicillin, started the Golden Age of antibiotics and marked the foundation for the treatment of infectious diseases.⁷ Within a decade after World War II, several additional classes of important antibiotics were making it to clinical settings for the treatment of infections caused by all major types of bacteria. A majority of antibiotics being discovered during this era and since are natural products – molecules synthesized and extracted from living organisms. In fact, most of these antibiotics were produced by bacteria in an effort to reduce competing bacterial populations with the goal of gaining a competitive advantage in a world of limited resources. In a way, modern human medicine has been beneficiaries of the constant battle for space and resources on the part of environmental microbes. Over the course of millions of years, microbes have evolved extremely potent and small molecule drugs that target neighboring bacterial populations. As we harnessed these agents for our own use, it is clear today that these small antimicrobial molecules

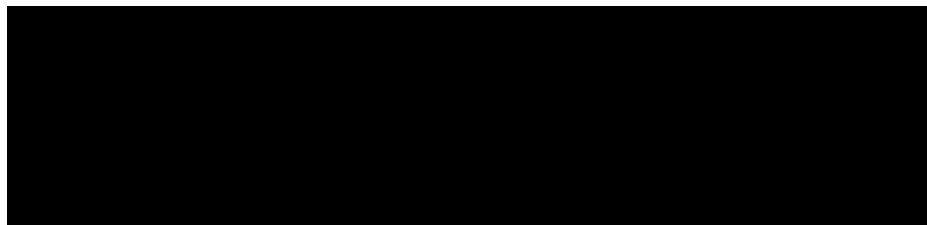
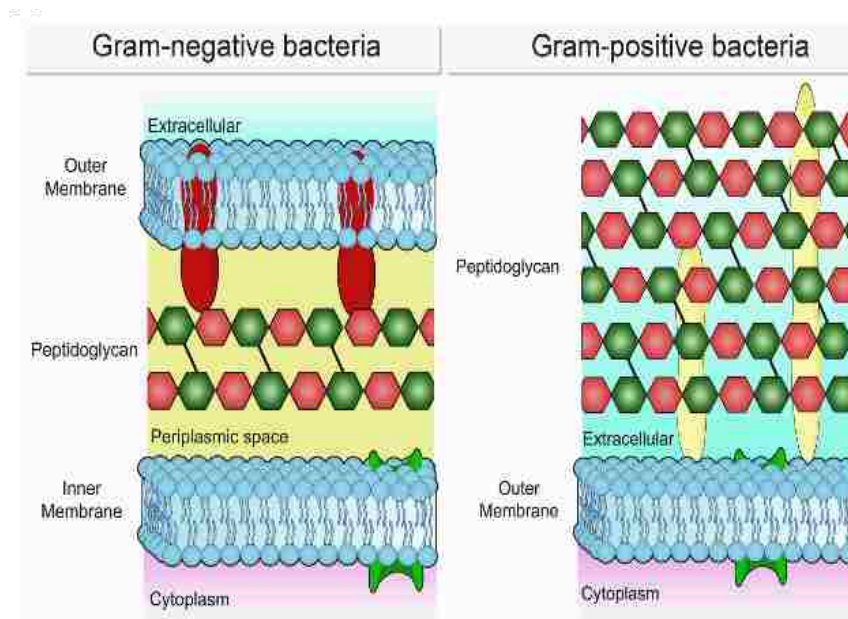
revolutionized the field of modern medicine. For several decades following the discovery of antibiotics, deaths associated with bacterial infections plummeted. Most modern households were well stocked with an arsenal of potent antibiotics in a myriad of products including soaps, detergents, cosmetic creams, toothpaste, and primary care products. Most important, the advent of invasive surgeries and cancer therapies previously deemed too precarious due to risk of infection became routine procedures in the medical setting and led to a dramatic increase in the quality of life. It is no coincidence that since the introduction of antibiotics into the clinics, the average life expectancy has increased by nearly three decades.⁸

Most antibiotics target specific biological processes in bacteria. If the disruption to this process is severe enough, the agent will result in bacterial death. Within the naturally existing bacterial warfare, a series of antibiotics have been previously cataloged against a large majority of pathogenic bacteria that infect human beings.⁹ Effective antibiotics work by inhibiting vital cellular processes that bacteria require in order to survive, such as DNA replication, protein synthesis, and cell wall biosynthesis. Of these classes, inhibitors against cell wall biosynthesis represent the largest and most widely subscribed class of antibiotics owing to their lack of human counterparts. Eukaryotic cells do not possess a structural unit similar to cell walls, opening the door to several potential drug targets within the cell wall biosynthetic pathway.¹⁰

Bacterial cell surfaces are heterogeneous mixtures comprised of lipids, proteins, and glycans. These complex molecular structures are responsible for providing bacteria with structural support and mediating interactions with its environment.¹¹ Due to its role in maintaining bacterial viability, bacterial cell walls have been the primary target for some

of the first antibacterial agents discovered. Differences in architecture of these molecular structures also form the basis for the classification of bacteria into two main categories: Gram-positive and Gram-negative. Gram-positive bacteria contain a single lipid bilayer and a thick layer of peptidoglycan, comprised of multiple layers of glycan strands that are cross-linked by oligopeptides.¹² The Gram-positive designation refers to the ability of these cells to retain the Gram stain via the peptidoglycan scaffold, which becomes readily visible under light microscopy. Conversely, bacteria that are unable to retain the Gram stain are Gram-negative bacteria and are referred to as diderms, containing two lipid bilayers separated by a thin layer of peptidoglycan¹³ (Figure 1.1). In other words, the additional outer membrane found in Gram-negative organisms function to reduce permeation and accumulation of the Gram stain. Consistently, Gram-negative bacterial species are more difficult to kill due to the protective nature of the outer lipid membrane, which effectively prevent the facile passage of most antibiotics.

There are two major categories that separate the mechanisms of antibiotics, namely bactericidal and bacteriostatic agents. A bactericidal antibiotic interferes with crucial processes, leading to effective cell death. A large number of FDA-approved antibiotics that act as bactericides happen to target the peptidoglycan building blocks necessary for cell wall synthesis (Table 1.1).¹⁴ Currently, β -lactam antibiotics represent more than half of the antibiotics that are used in clinical settings.



β -lactam antibiotics effectively block cell wall crosslinking by covalently modifying a critical serine residue at the active side of cell-anchored transpeptidases, which reduces peptidoglycan integrity and causes cell death. Glycopeptides, such as vancomycin, arrest peptidoglycan synthesis by binding to and sequestering lipid II precursor molecules. Lipid II molecules are responsible for translocating monomeric peptidoglycan building blocks from the cytosolic space, where it is biosynthesized, to the mature peptidoglycan scaffold. By blocking the delivery of monomeric peptidoglycan building blocks from the cytosol to the growing scaffold on the bacterial cell surface, cell wall biosynthesis comes to a halt. Antibiotics targeting bacterial DNA replication and repair enzymes also fall in

the bactericidal category. These agents operate by inhibiting enzymes, such as topoisomerases and DNA gyrase, which are vital processes for the maintenance and growth of bacterial cells. Fluoroquinolones are considered a broad-spectrum agents that are effective against both Gram-negative and -positive bacteria, antibiotic within this class.

Bacteriostatic antibiotics are different from bactericidal antibiotics in that these agents shut down active bacterial growth but do not cause cell death. Antibiotics in this class take advantage of non-eukaryotic structural characteristics of ribosomal subunits and other factors involved with initiation, elongation, and termination in bacterial protein synthesis. FDA-approved antibiotics in this class include tetracyclines and aminoglycosides, which target different parts of the ribosome machinery to effectively terminate protein synthesis. For example, clindamycin is commonly prescribed for the treatment of *S. aureus*.

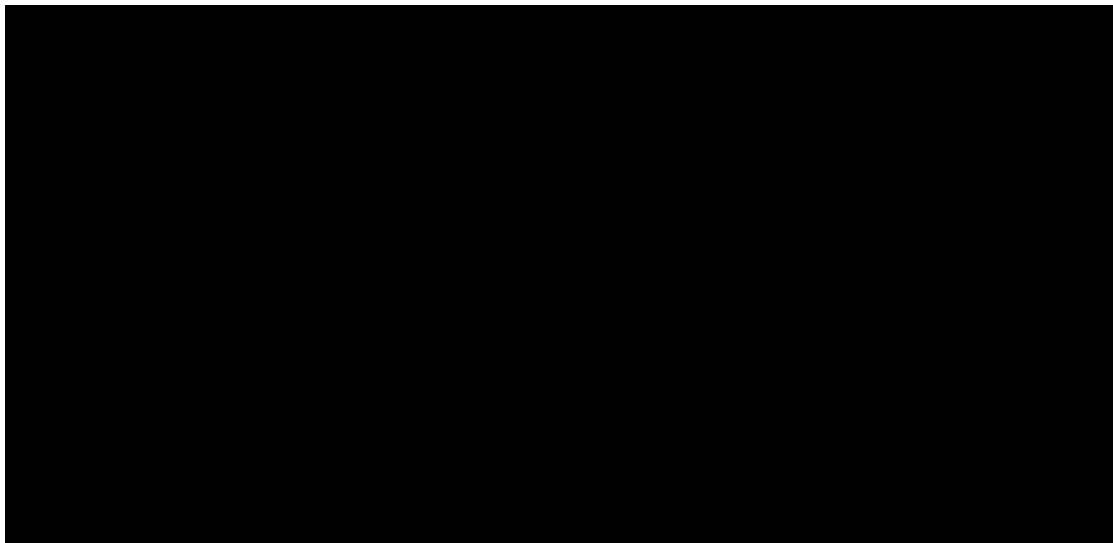
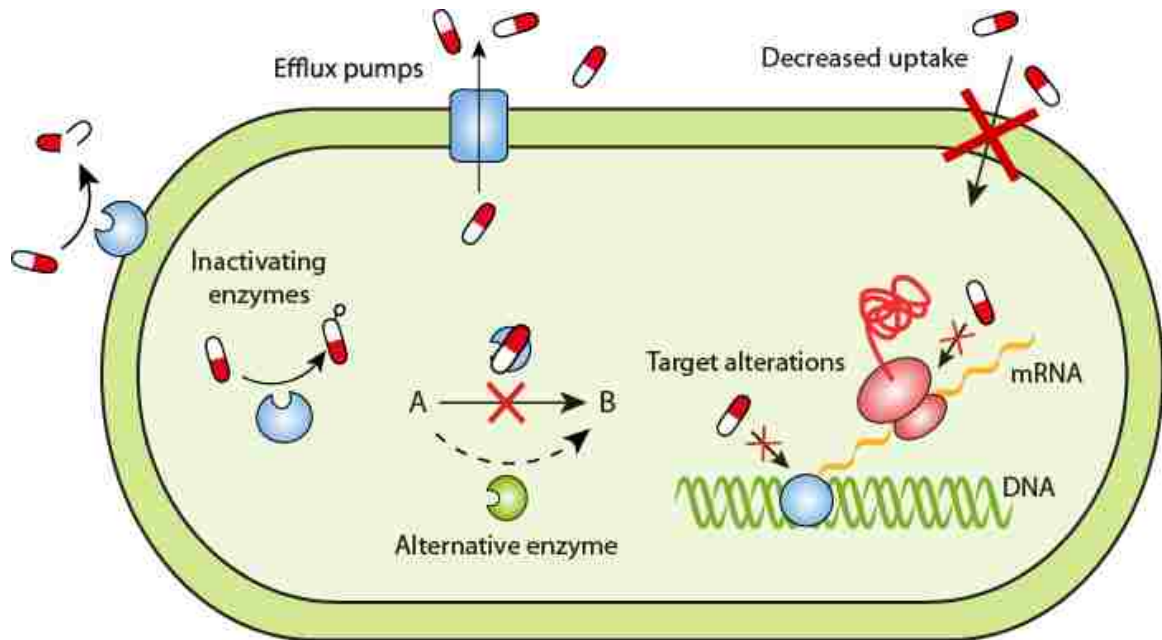
Classification	Antibiotic Example	Bacteriostatic/ Bactericidal	Mechanism of Action	Target Bacteria
β-Lactam	Penicillin / Amoxicillin	Bactericidal	Inhibit cell wall synthesis	Gram-positive
Glycopeptides	Vancomycin			
Lincosamides	Clindamycin	Bacteriostatic	Inhibit protein synthesis	
Sulfonamides	Trimethoprim-Sulfamethoxazole	Bacteriostatic	Inhibit nucleic acid synthesis	Broad Spectrum
Tetracyclines	Doxycyclin		Inhibit protein synthesis	
Fluroquinolones	Ciprofloxacin / Levofloxacin	Bactericidal	Inhibit DNA replication	
Cephalosporins	Cefclidin (4 th generation)	Bactericidal	Inhibit cell wall synthesis	
Carbapenems	Miropenam			
Aminoglycosides	Streptomycin	Bactericidal	Inhibit protein synthesis	Gram-negative
Monobactams	Aztreonam		Inhibit cell wall synthesis	
Polypeptides	Polymyxin B / Colistin		Disrupt outer membrane integrity	

Table 1.1 Common Antibiotics Prescribed for Bacterial Infections.

For many decades, the number of new antibiotics introduced into the clinics easily outpaced the emergence of resistant strains. Although the discovery and use of antibiotics was thought to signal the end of infectious diseases, the overuse and misuse of antibiotics has led to the emergence of bacterial strains that are resistant to several if not all approved antibiotics.

1.3 Mechanisms of Antibiotic Resistance in Bacteria

Over 60 years of antibiotic use has led to a precarious new reality – a scenario in which pathogenic bacteria have taken the upper hand and our ability to fight bacterial infections has been heavily eroded. This new era was brought on by decades of antibiotic use and misuse. Yet, in many ways, resistance to antibiotics is nothing new and not purely a human-mediated effect. Given the source of most antibiotics in use today – natural products from bacteria – bacteria have been evolving mechanisms of resistance slowly over millions of years.¹⁵ Bacteria have been fighting off natural “predators” since their first widespread existence on Earth. The rapid growth rates and promiscuous gene swapping by bacteria form the basis for rapid evolution and propagation of favorable phenotypes.¹⁶ In combination with the exposure to antibiotics, there is a clear and strong selective pressure on the heterogeneous population of bacteria, leading to the rapid elimination of the susceptible members and leaving the few resistant members to replicate and flourish.¹⁷



While natural evolution outside of human hosts has previously, and will continue to, shape the resistance profile of bacteria, human beings have played a major role in accelerating this process. A steady increase in frequency of drug resistant bacterial strains have been reported since the beginning of the Golden Era for virtually all major classes of antibiotics. The overuse and misuse of antibiotics are two major reasons for the

emergence of drug resistant strains. Overuse of antibiotics typically refers to the use in farm animals, which can account for a large percentage of antibiotics produced on a yearly basis*. Misuse of antibiotics mostly refers to the prescription of antibiotics for viral infections and incomplete use of the entire course of antibiotics that are prescribed. When administration of a course of antibiotics is not followed according to recommendations, it can lead to incomplete clearance of pathogens from the system. The remaining bacteria typically have acquired mutations that can be passed on to future generations. Moreover, the genetic information that encoded the superior phenotype can be additionally passed onto other bacteria as it is spread back out to the natural environment. Drug resistance is a phenomenon that is observed in virtually all known bacteria that can occur in an inter- and intra-species modalities. A single mode of drug evasion can be enough to endow bacteria with a drug-resistant phenotype. Yet, it is now clear that bacteria can acquire several genes that confer competitive advantages against antibiotics, making these strains exceedingly dangerous.¹⁸ These bacteria are known as multidrug-resistant (MDR), extremely drug-resistant (XDR) or pandrug-resistant (PDR) bacteria.¹⁹ These are all designations that refer to bacteria that can cause infections that are mostly untreatable.

Bacteria possess diverse and incredibly efficient methods to avoid the toxic actions of antibiotics. Drug modification or degradation, efflux pumps, decreased permeation of drugs, and drug target alteration are the most common mechanism used by bacteria to circumvent antibiotics (Figure 1.2).^{20, 16, 21} An effective and widely employed resistance mechanism used by bacteria involves the reduction in access of antibiotic to its molecular target, which can result in insufficient concentration to impart its intended

biological response (Figure 1.2). This can be an inherent resistance mechanism as in the case for vancomycin against Gram-negative pathogens. Vancomycin associates tightly with the peptidoglycan precursor molecules, lipid II. Pools of lipid II are found primarily on the cytoplasmic membrane of bacteria around the sites of cell division and growth. Both Gram-positive and Gram-negative bacteria possess peptidoglycan, and, in theory, both should be equally sensitive to the actions of vancomycin. However, the outer membrane layer found on the surface of Gram-negative bacteria severely restricts accumulation of vancomycin within the periplasmic space (site of lipid II in Gram-negative bacteria), thus preventing access to its molecular target. Vancomycin cannot overcome this limitation, and, therefore, is only effective as a stand-alone antibiotic against Gram-positive bacterial infections.

Another widely observed mechanism used by bacteria use to circumvent the actions of antibiotics occurs *via* the structural alteration of the molecular target of that particular drug (Figure 1.2). A mutation at the genetic levels results in a protein target with an altered primary sequence (a replacement of an amino acid). Protein changes that result in lower binding to the antibiotic will give that particular bacterial cell a selective advantage. Alternatively, a similar drug-resistant phenotype can be selected whereby the primary sequence of the target protein remains unchanged. For example, ribosomal protection proteins protect ribosomes from the action of antibiotics by directly interacting with the ribosome and changing their shape or conformation. The change in the ribosome shape prevents an antibiotic from binding and interfering with protein synthesis.²²

Drug modification or degradation by an inactivating enzyme is another prevalent, and highly effective, mechanism of resistance against β -lactam antibiotics (Figure 1.2). β -

lactam antibiotics work by structurally mimicking the dipeptide D-Alanyl-D-Alanine, which the terminal group found on the stem peptide of bacterial peptidoglycan, and effectively inactivating Penicillin Binding Proteins (PBPs). PBPs are responsible for crosslinking adjacent stem peptides within the peptidoglycan scaffold, thus increasing the strength and stiffness of this critical cellular matrix. This crosslinking step is crucial to the viability of bacterial cells and its disruption is lethal to the cells. The crosslinking reaction carried out by PBPs is initiated at the D-Alanyl-D-Alanine terminal end of the peptidoglycan. The strained β -lactam bond and the proper mimicry of D-Alanyl-D-Alanine by these antibiotics results in a covalent capture of the active site of PBPs. Consequently, PBPs modified with β -lactam cease to crosslink the peptidoglycan scaffold and cell death follows.

Bacteria resistant to β -lactam antibiotics respond to the presence of these drugs by releasing high levels of β -lactamase proteins into the surrounding media. β -lactamases enzymatically hydrolyze the β -lactam bond, which renders these drugs poor mimics of D-Alanyl-D-Alanine and unable to covalently capture PBPs.²³ The use of β -lactamase inhibitors in combination with a β -lactam antibiotic has previously proven effective at treating these β -lactam-resistant bacteria.²⁴ This combination is commonly prescribed as augmentin, which is composed of clavulanic acid, a β -lactamase inhibitor, and amoxicillin. Not surprisingly, it was not long after clavulanic acid was first used in clinics before bacteria have found a way around this drug combination as well.²⁵ The short amount of time needed for bacteria to find a way around this combination of drugs highlight the ability of bacteria to gain resistance to antibiotics. In this particular instance, bacteria that survived augmentin started to shift the crosslinking function away from

PBPs to other enzymes in order to crosslink their cell walls. L,D-transpeptidases, which are normally used to perform a separate task in bacterial cells and are structurally distinct from PBPs, are inherently insensitive to β -lactam agents.^{26, 27, 28, 29, 30} Therefore, cells that transferred the crosslinking function to L,D-transpeptidases were able to grow and proliferate in the presence of high levels of most β -lactam antibiotics.

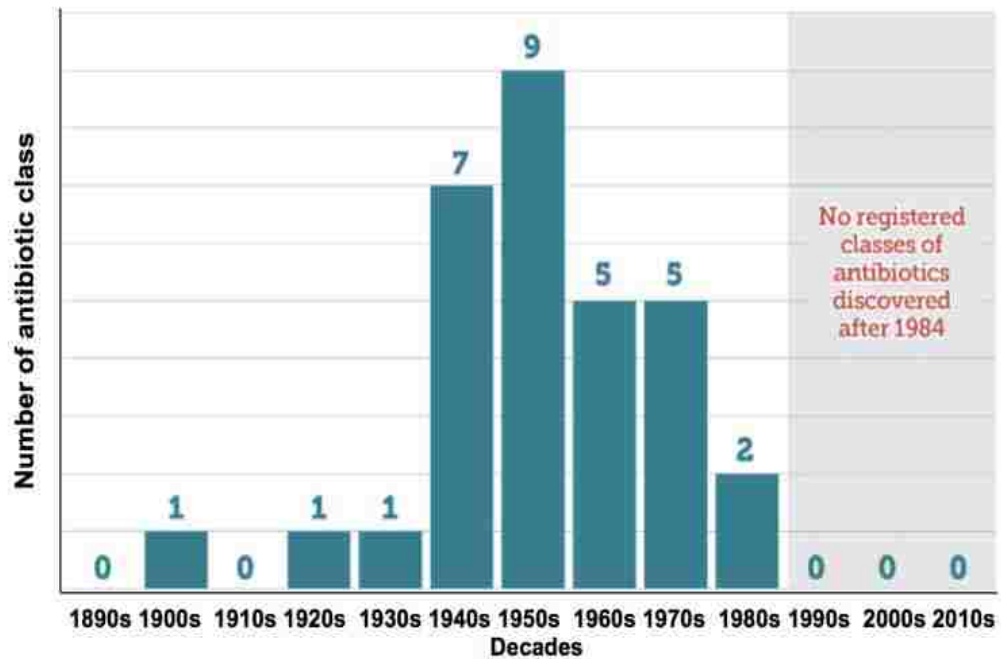
Likewise, bacteria have developed additional mechanisms to use alternative enzymes to carry out cellular processes. As a resident of the human skin, nails, and nares, *S. aureus* has the unique ability to penetrate deeper layers of host barriers. *S. aureus* have evolved three unique mechanisms to avoid the actions of two distinct classes of antibiotics. Methicillin resistant *S. aureus* (MRSA) shift the crosslinking functions necessary for cell wall growth and division to avoid inactivation by β -lactam antibiotics. Strains of MRSA express high levels of a PBP variant, PBP2a, that has inherently low affinity for β -lactam antibiotics *. This unusual PBP serves as a fully functional enzyme within the peptidoglycan biosynthetic pathway. The slower acylation of the active site serine in PBP2a forms the basis for a drug-resistant phenotype. Two additional modes of drug resistance against vancomycin in *S. aureus* exemplify the plasticity in bacterial cells in their ability to alter structural and biochemical pathways to endow new and favorable phenotypes. In the first mode, *S. aureus* avoid the actions of vancomycin by increasing the levels of D-Alanyl-D-Alanine on the peptidoglycan structure as a way of capturing vancomycin molecules away from the lipid II pool near the cell membrane.³¹ The simple expansion in the valency of dipeptides present in the mature peptidoglycan scaffold can be enough to reduce the susceptibility of vancomycin to disrupt new cell wall growth. In the second mode, *S. aureus* cells perform a wholesale alteration of their peptidoglycan

structure to include a terminal D-Lactic acid (D-Lac) in place of the terminal D-Alanine (D-Ala) residue within the stem peptide of the peptidoglycan.³² Although structurally subtle, the primary sequence change from D-Alanine to D-Lactic acid eliminates a single hydrogen bond and, consequently, results in 1000-fold weaker binding affinity to vancomycin.³³ Exposure to vancomycin triggers a shift in cell wall biosynthesis towards the intracellular production of D-Lac and D-Lac terminated building blocks. Pyruvate is converted to D-Lac and ligated onto D-Ala by the ligases to afford D-Ala-D-Lac. This unit is joined onto a tripeptide by MurF to yield the full PG pentadepsipeptide precursor, which is subsequently loaded onto the lipid carrier. Yet, production of D-Ala-D-Lac alone is insufficient to impart vancomycin resistance due to the continued cytosolic production of D-Ala-D-Ala. If available, D-Ala-D-Ala will also enter the PG biosynthetic pathway and generate vancomycin-susceptible Lipid II molecules. To ensure that primarily D-Lac terminated Lipid II molecules are assembled, a carboxypeptidase (vanX) is also encoded on the resistance plasmid. This enzyme is tasked with the proteolysis of the dipeptide D-Ala-D-Ala, thus greatly reducing the production of D-Ala terminated Lipid II molecules. Through the concerted actions of these enzymes, vancomycin resistant *S. aureus* cells continue to grow and proliferate in the presence of high concentrations of vancomycin.

Finally, it is now well established that the overexpression of membrane proteins that act as efflux pumps are, at least partly, responsible for the emergence of multi-drug-resistant bacteria.³⁴ Efflux pumps export antibiotics (along with many other small molecules) from the inside the target bacterial cells out to the extracellular space. In effect, drugs cannot accumulate to sufficiently high levels to impart their biological activity. A feature that makes these efflux pumps extremely problematic for drug design

and discovery is that they tend to exhibit a low degree of specificity therefore they recognize and pump out a myriad of structurally unrelated antibiotics with diverse mechanisms of action. A common and problematic opportunistic pathogen, *Pseudomonas aeruginosa*, exhibits low susceptibility to antibiotic treatment due to the action of multidrug efflux pumps and low permeability of the antibiotics across bacterial outer membrane.³⁵ Recent reports have shown that the combination of phenylarginine- β -naphthylamide, an efflux pump inhibitor, and cefepime (a β -lactam antibiotic), re-sensitized cefepime resistant *Pseudomonas aeruginosa* to the drug.³⁶ These promising early results demonstrate the possibility of targeting the inactivation of drug efflux pumps with the goal of potentiating known antibiotics and improving the activity of drugs currently in the pipeline.

Together, the diversity of mechanisms and the speed of resistance acquisition signify that our current stock of antibiotics will have a fairly limited utility lifespan. The continued use and misuse of antibiotics will propel us into a post-antibiotic era unless there is a re-dedication of effort and resources towards the discovery of new antibiotics. Today, drug resistant pathogenic bacteria are already responsible for thousands of deaths and billions of additional health care costs each year. Although novel antibiotics are urgently needed, no new class of antibiotics has been discovered since the 1980s (Figure 1.3). This has become a serious problem in hospitals as bacterial resistant infections continue to be on the rise despite the practice of standard precautions.



1.4 Treatment of Antibiotic Resistant Bacterial Infections

With the increasing incidences of drug resistant bacterial infections, last resort antibiotics, such as vancomycin and colistin, have now become front-line therapeutics. Even more troubling is the presence of vancomycin-resistant bacterial strains³⁷ and colistin-resistant *Escherichia coli*.^{38,39} The widespread dissemination of these pathogens may rapidly increase the cases of untreatable infections.^{40, 16} If current trends continue, modern healthcare standards will be in jeopardy. Recent estimates project that by 2050 more people will die from antimicrobial resistant infections than from all forms of cancer combined.⁴¹

While the lack of new antibiotics being introduced into clinical settings needs to be addressed from a medical, government, and training level, there are a number of promising avenues being currently pursued. One example of a class of potential antibiotics that are effective against antibiotic-resistant bacteria focuses on derivatization of current antibiotics. For example, the Boger group at Scripps Research Institute has a long history of designing and synthesizing vancomycin derivatives that have improved activities compared to the parent drug.^{42, 43} In order to try and regain the lost binding affinity of vancomycin against D-Lac displaying drug resistant strains, a series of vancomycin analogues was synthesized with modifications focused on improving the binding to D-Ala-D-Lac strands. Their successful vancomycin displayed a 40-fold increase in affinity for D-Ala-D-Lac. Most importantly, the derivative also was effective against vancomycin-resistant *Enterococcus faecalis* (VRE) (MIC = 31 µg/mL).⁴³

Some potential methods to expand the antibacterial therapy repertoire target non-direct killing modalities. A promising strategy is aimed at inhibiting the ability of bacteria to communicate with one another.⁴⁴ Bacteria use small diffusible molecules to distribute information about population density in a process termed quorum sensing. Quorum sensing has been proposed to play a role in bacterial pathogenicity. Communication between pathogenic bacteria can potentially provide a mechanism to minimize host immune responses by delaying the production of tissue-damaging virulence factors until sufficient bacteria have accumulated and the cells, in sync, are prepared to overwhelm host defense mechanisms to establish a robust infection. Therefore, the inhibition of these molecules may result in decreased colonization and virulence.

Although not approved in the United States, bacteriophage therapy has had remarkable success in Europe for antibiotic-resistant bacterial infections. Bacteriophages, commonly called phages, are viruses that infect bacteria but not mammalian cells.⁴⁵ After penetrating the bacterial surface, phages will hijack bacterial DNA, and then replicate themselves within the bacteria until the cell bursts – depending on the lifecycle of the bacteriophage. Cocktails of phage viruses matched against pathogenic bacteria of interest can effectively cure a bacterial infection in the human body with remarkable accuracy, taking out only the infiltrators.⁴⁶

Recently, the World Health Organization (WHO) assembled a list of pathogens desperately needing new therapies. At the top of the list are three drug-resistant Gram-negative bacteria followed by vancomycin-resistant *E. faecium* and MRSA (Figure 1.4). This thesis presents a novel non-direct killing method of combatting pathogenic bacteria by use of bacterial immunotherapy, specifically targeting MRSA and Gram-negative pathogenic bacteria.

WHO PRIORITY PATHOGENS LIST FOR R&D OF NEW ANTIBIOTICS

Priority 1: CRITICAL

Acinetobacter baumannii, carbapenem-resistant

Pseudomonas aeruginosa, carbapenem-resistant

Enterobacteriaceae, carbapenem-resistant, 3rd generation cephalosporin-resistant

Priority 2: HIGH

Enterococcus faecium, vancomycin-resistant

Staphylococcus aureus, methicillin-resistant, vancomycin intermediate and resistant

Helicobacter pylori, clarithromycin-resistant

Campylobacter, fluoroquinolone-resistant

Salmonella spp., fluoroquinolone-resistant

Neisseria gonorrhoeae, 3rd generation cephalosporin-resistant, fluoroquinolone-resistant

Priority 3: MEDIUM

Streptococcus pneumoniae, penicillin-non-susceptible

Haemophilus influenzae, ampicillin-resistant

Shigella spp., fluoroquinolone-resistant

1.5 REFERENCES

1. Microbiology by numbers. *Nat Rev Micro* **2011**, 9 (9), 628-628.
2. Whitman, W. B.; Coleman, D. C.; Wiebe, W. J., Prokaryotes: The unseen majority. *Proceedings of the National Academy of Sciences* **1998**, 95 (12), 6578-6583.
3. Kallmeyer, J.; Pockalny, R.; Adhikari, R. R.; Smith, D. C.; D'Hondt, S., Global distribution of microbial abundance and biomass in subseafloor sediment. *Proceedings of the National Academy of Sciences* **2012**, 109 (40), 16213-16216.
4. Drake, J. W.; Charlesworth, B.; Charlesworth, D.; Crow, J. F., Rates of Spontaneous Mutation. *Genetics* **1998**, 148 (4), 1667-1686.
5. Nachman, M. W.; Crowell, S. L., Estimate of the mutation rate per nucleotide in humans. *Genetics* **2000**, 156 (1), 297-304.
6. Spor, A.; Koren, O.; Ley, R., Unravelling the effects of the environment and host genotype on the gut microbiome. *Nat Rev Microbiol* **2011**, 9 (4), 279-90.
7. Estee Torok, E. M., Fiona Cooke, *Oxford Handbook of Infectious Diseases and Microbiology*. Oxford University Press: Oxford, New York, 2009.
8. Ventola, C. L., The Antibiotic Resistance Crisis: Part 1: Causes and Threats. *Pharmacy and Therapeutics* **2015**, 40 (4), 277-283.
9. Kohanski, M. A. D., D. J.; Collins, J. J., How Antibiotics Kill Bacteria: from targets to networks. *Nature Reviews Microbiology* **2010**, 8, 423-435.
10. Walsh, C., Molecular mechanisms that confer antibacterial drug resistance. *Nature* **2000**, 406 (6797), 775-781.
11. Silhavy, T. J.; Kahne, D.; Walker, S., The bacterial cell envelope. *Cold Spring Harb Perspect Biol* **2010**, 2 (5), a000414.
12. van Heijenoort, J., Recent advances in the formation of the bacterial peptidoglycan monomer unit. *Nat Prod Rep* **2001**, 18 (5), 503-19.
13. Glauert, A. M.; Thornley, M. J., The topography of the bacterial cell wall. *Annu Rev Microbiol* **1969**, 23, 159-98.
14. Oka, T.; Hashizume, K.; Fujita, H., Inhibition of peptidoglycan transpeptidase by beta-lactam antibiotics: structure-activity relationships. *J Antibiot (Tokyo)* **1980**, 33 (11), 1357-62.
15. Cox, G. W., G. D. , Intrinsic antibiotic resistance: mechanisms, origins, challenges and solutions. *Int J Med Microbiol* **2013**, 303 ((6-7)), 287-92.
16. Levy, S. B.; Marshall, B., Antibacterial resistance worldwide: causes, challenges and responses. *Nat Med* **2004**.
17. Spellberg, B., *Rising Plague: the global threat from deadly bacteria and our dwindling arsenal to fight them*. Prometheus Books: Amherst, New York 14228-2119, 2009.
18. Blair, J. M. A.; Webber, M. A.; Baylay, A. J.; Ogbolu, D. O.; Piddock, L. J. V., Molecular mechanisms of antibiotic resistance. *Nat Rev Micro* **2015**, 13 (1), 42-51.
19. Magiorakos, A. P.; Srinivasan, A.; Carey, R. B.; Carmeli, Y.; Falagas, M. E.; Giske, C. G.; Harbarth, S.; Hindler, J. F.; Kahlmeter, G.; Olsson-Liljequist, B.; Paterson, D. L.; Rice, L. B.; Stelling, J.; Struelens, M. J.; Vatopoulos, A.; Weber, J. T.; Monnet, D. L., Multidrug-resistant, extensively drug-resistant and pandrug-

- resistant bacteria: an international expert proposal for interim standard definitions for acquired resistance. *Clinical Microbiology and Infection* **2012**, *18* (3), 268-281.
20. Spratt, B., Resistance to antibiotics mediated by target alterations. *Science* **1994**, *264* (5157), 388-393.
 21. Nikaido, H., Multidrug efflux pumps of gram-negative bacteria. *Journal of Bacteriology* **1996**, *178* (20), 5853-5859.
 22. Livermore, D. M., Linezolid in vitro : mechanism and antibacterial spectrum. *Journal of Antimicrobial Chemotherapy* **2003**, *51* (suppl_2), ii9-ii16.
 23. Majiduddin, F. K.; Materon, I. C.; Palzkill, T. G., Molecular analysis of beta-lactamase structure and function. *International Journal of Medical Microbiology* **2002**, *292* (2), 127-137.
 24. Drawz, S. M.; Bonomo, R. A., Three Decades of β -Lactamase Inhibitors. *Clinical Microbiology Reviews* **2010**, *23* (1), 160-201.
 25. Jesús, O.; José, C.; Edurne, L.; Óscar, C.; Silvia, G.-C.; María, P.-V.; Abajo, F. J. d., Increased Amoxicillin–Clavulanic Acid Resistance in *Escherichia coli* Blood Isolates, Spain. *Emerging Infectious Disease journal* **2008**, *14* (8), 1259.
 26. Biarrotte-Sorin, S.; Hugonnet, J. E.; Delfosse, V.; Mainardi, J. L.; Gutmann, L.; Arthur, M.; Mayer, C., Crystal structure of a novel beta-lactam-insensitive peptidoglycan transpeptidase. *J Mol Biol* **2006**, *359* (3), 533-8.
 27. Magnet, S.; Arbeloa, A.; Mainardi, J. L.; Hugonnet, J. E.; Fourgeaud, M.; Dubost, L.; Marie, A.; Delfosse, V.; Mayer, C.; Rice, L. B.; Arthur, M., Specificity of L,D-transpeptidases from gram-positive bacteria producing different peptidoglycan chemotypes. *J Biol Chem* **2007**, *282* (18), 13151-9.
 28. Mainardi, J. L.; Morel, V.; Fourgeaud, M.; Cremniter, J.; Blanot, D.; Legrand, R.; Frehel, C.; Arthur, M.; Van Heijenoort, J.; Gutmann, L., Balance between two transpeptidation mechanisms determines the expression of beta-lactam resistance in *Enterococcus faecium*. *J Biol Chem* **2002**, *277* (39), 35801-7.
 29. Mainardi, J. L.; Villet, R.; Bugg, T. D.; Mayer, C.; Arthur, M., Evolution of peptidoglycan biosynthesis under the selective pressure of antibiotics in Gram-positive bacteria. *FEMS Microbiol Rev* **2008**, *32* (2), 386-408.
 30. Lavollay, M.; Arthur, M.; Fourgeaud, M.; Dubost, L.; Marie, A.; Veziris, N.; Blanot, D.; Gutmann, L.; Mainardi, J. L., The peptidoglycan of stationary-phase *Mycobacterium tuberculosis* predominantly contains cross-links generated by L,D-transpeptidation. *J Bacteriol* **2008**, *190* (12), 4360-6.
 31. Pereira, P. M.; Filipe, S. R.; Tomasz, A.; Pinho, M. G., Fluorescence Ratio Imaging Microscopy Shows Decreased Access of Vancomycin to Cell Wall Synthetic Sites in Vancomycin-Resistant *Staphylococcus aureus*. *Antimicrobial Agents and Chemotherapy* **2007**, *51* (10), 3627-3633.
 32. Lowy, F. D., Antimicrobial resistance: the example of *Staphylococcus aureus*. *Journal of Clinical Investigation* **2003**, *111* (9), 1265-1273.
 33. (a) Bugg, T. D.; Dutka-Malen, S.; Arthur, M.; Courvalin, P.; Walsh, C. T., Identification of vancomycin resistance protein VanA as a D-alanine:D-alanine ligase of altered substrate specificity. *Biochemistry* **1991**, *30* (8), 2017-21; (b) Arthur, M.; Molinas, C.; Bugg, T. D.; Wright, G. D.; Walsh, C. T.; Courvalin, P.,

- Evidence for in vivo incorporation of D-lactate into peptidoglycan precursors of vancomycin-resistant enterococci. *Antimicrob Agents Chemother* **1992**, *36* (4), 867-9; (c) Hubbard, B. K.; Walsh, C. T., Vancomycin assembly: nature's way. *Angew Chem Int Ed Engl* **2003**, *42* (7), 730-65; (d) Kahne, D.; Leimkuhler, C.; Lu, W.; Walsh, C., Glycopeptide and lipoglycopeptide antibiotics. *Chem Rev* **2005**, *105* (2), 425-48.
34. Yasufuku, T.; Shigemura, K.; Shirakawa, T.; Matsumoto, M.; Nakano, Y.; Tanaka, K.; Arakawa, S.; Kinoshita, S.; Kawabata, M.; Fujisawa, M., Correlation of Overexpression of Efflux Pump Genes with Antibiotic Resistance in Escherichia coli Strains Clinically Isolated from Urinary Tract Infection Patients. *Journal of Clinical Microbiology* **2011**, *49* (1), 189-194.
 35. Poole, K., Efflux-mediated multiresistance in Gram-negative bacteria. *Clin Microbiol Infect* **2004**, *10* (1), 12-26.
 36. Coban, A. Y.; Tanriverdi Cayci, Y.; Erturan, Z.; Durupinar, B., Effects of Efflux Pump Inhibitors Phenyl-Arginine- β -Naphthylamide and 1-(1-Naphthylmethyl)-Piperazine on the Antimicrobial susceptibility of Pseudomonas aeruginosa Isolates from Cystic Fibrosis Patients. *Journal of Chemotherapy* **2009**, *21* (5), 592-594.
 37. Chavers, L. S.; Moser, S. A.; Benjamin, W. H.; Banks, S. E.; Steinhauer, J. R.; Smith, A. M.; Johnson, C. N.; Funkhouser, E.; Chavers, L. P.; Stamm, A. M.; Waites, K. B., Vancomycin-resistant enterococci: 15 years and counting. *Journal of Hospital Infection* **2003**, *53* (3), 159-171.
 38. Liu, Y.-Y.; Wang, Y.; Walsh, T. R.; Yi, L.-X.; Zhang, R.; Spencer, J.; Doi, Y.; Tian, G.; Dong, B.; Huang, X.; Yu, L.-F.; Gu, D.; Ren, H.; Chen, X.; Lv, L.; He, D.; Zhou, H.; Liang, Z.; Liu, J.-H.; Shen, J., Emergence of plasmid-mediated colistin resistance mechanism MCR-1 in animals and human beings in China: a microbiological and molecular biological study. *The Lancet Infectious Diseases* *16* (2), 161-168.
 39. McGann, P.; Snesrud, E.; Maybank, R.; Corey, B.; Ong, A. C.; Clifford, R.; Hinkle, M.; Whitman, T.; Lesho, E.; Schaecher, K. E., Escherichia coli Harboring mcr-1 and blaCTX-M on a Novel IncF Plasmid: First report of mcr-1 in the USA. *Antimicrobial Agents and Chemotherapy* **2016**.
 40. Boucher, H. W.; Talbot, G. H.; Bradley, J. S.; Edwards, J. E.; Gilbert, D.; Rice, L. B.; Scheld, M.; Spellberg, B.; Bartlett, J., Bad bugs, no drugs: no ESKAPE! An update from the Infectious Diseases Society of America. *Clin Infect Dis* **2009**, *48* (1), 1-12.
 41. Walsh, F., Superbugs to kill 'more than cancer' by 2050. **2014**.
 42. James, R. C.; Pierce, J. G.; Okano, A.; Xie, J.; Boger, D. L., Redesign of Glycopeptide Antibiotics: Back to the Future. *ACS Chemical Biology* **2012**, *7* (5), 797-804.
 43. Okano, A.; Nakayama, A.; Wu, K.; Lindsey, E. A.; Schammel, A. W.; Feng, Y.; Collins, K. C.; Boger, D. L., Total Syntheses and Initial Evaluation of $[\Psi[C(=S)NH]Tpg4]$ vancomycin, $[\Psi[C(=NH)NH]Tpg4]$ vancomycin, $[\Psi[CH_2NH]Tpg4]$ vancomycin, and Their (4-Chlorobiphenyl)methyl Derivatives: Synergistic Binding Pocket and Peripheral Modifications for the Glycopeptide

- Antibiotics. *Journal of the American Chemical Society* **2015**, *137* (10), 3693-3704.
44. Kalia, V. C., Quorum sensing inhibitors: An overview. *Biotechnology Advances* **2013**, *31* (2), 224-245.
 45. Sulakvelidze, A.; Alavidze, Z.; Morris, J. G., Bacteriophage Therapy. *Antimicrobial Agents and Chemotherapy* **2001**, *45* (3), 649-659.
 46. Abedon, S. T.; Kuhl, S. J.; Blasdel, B. G.; Kutter, E. M., Phage treatment of human infections. *Bacteriophage* **2011**, *1* (2), 66-85.

Chapter 2

Bacterial Immunotherapy

2.1 Introduction

The threat of antibiotic-resistant strains urgently calls for the development of novel multi-pronged approaches, including improved stewardship of known antibiotics, in the development of effective vaccines or alternative strategies to treat bacterial infections. Agents that circumvent antibiotic resistance by targeting pathogens for host immune clearance have the potential to selectively stimulate protective immune responses as a treatment option for bacterial infections.¹

Of the many systems in the body, the human immune system is one of the most important. Composed of a myriad of cellular mechanisms this complex network works as a defensive biological response to dangerous pathogens. The immune system recognizes potentially harmful substances, such as viruses, bacteria, and fungi, and sequentially acts to neutralize these foreign invaders. An effective immune system will successfully clear infectious material while sparing healthy human cells. Yet, the immune system's ability to neutralize destructive offenders is not limited to foreign organisms. It can also offer support in the clearance of distorted cells, such as cancerous cells. In this case, elimination is carried out by tumor-specific T cells, immune cells developed specifically to target and attack cancer cells. However, cancerous cells have done well at evading the host immune system.² To achieve evasion, tumors use powerful adaptations to disrupt equilibrium and suppress the immune system, such as manipulation of checkpoint pathways.³ When this manipulation occurs, checkpoint pathways like CTLA-4 or PD-1 are activated to release a negative signal down-regulating the immune system and

promoting self-tolerance by suppressing T cell inflammatory activity. This host immune evasion upsets the delicate balance of the immune response, potentially leading to dire repercussions and serious health implications. Similarly, pathogenic bacteria have also evolved to thwart clearance by the immune system. When evasion is extremely successful, further medical intervention is required, in the means of antibiotic delivery or surgery to remove the untreatable infection.

The external surface of bacterial pathogens presents many diverse antigenic targets for the host immune system. As the central interface between host and pathogen, recognition of the exposed surface by the immune systems provides the host a key signature to initiate microbial clearance. It also affords the pathogen significant opportunity to present mimics of host immune modulators, alter host immune responses, express adhesins or receptor ligands to anchor the pathogen to host surfaces, and to present invasins or fusion proteins to mediate uptake into host cells.^{4, 5}

A major difficulty for bacterial pathogens is hiding this complex surface of proteins and carbohydrates from immune surveillance and TLR recognition yet exposing key molecules, such as adhesins and invasins. A common mechanism of masking bacterial surfaces is to express a carbohydrate capsule. This mechanism is used by most extracellular bacterial pathogens that circulate systemically within the body. For example, *Streptococcus pneumoniae* relies extensively on its capsule to prevent antibody and complement deposition on its surface, thereby avoiding opsonization and phagocytic clearance.⁶

Bacterial pathogens, especially Gram-negative pathogens, have developed secretion systems to export virulence factors across the bacterial membranes and either into the supernatant or directly into host cells. Secretion of virulence factors such as toxins and immune modulators is a major use of these secretion systems.^{7, 8} In Gram negative pathogens, both type III secretion systems (T3SS) and type IV secretion systems (T4SS) can insert various molecules directly into host cells, including toxins, mechanisms to paralyze phagocytosis, and many diverse effectors that alter immune functions to enhance immune evasion.

2.2 Bacteria and the Human Host

In the last few years, we have learned that humans share a complicated and intricate co-existence with bacteria living in and on our bodies. The sheer number of bacteria cells means that these microbial communities have the potential to impact human health. There exist two types of bacteria, probiotic and pathogenic bacteria. Probiotics, like *Lactobacillus*, are beneficial to our health, primarily aiding in a healthy digestive system.⁹ Unlike the response to commensal bacteria, the human immune system must rapidly and efficiently attempt to eradicate pathogenic bacteria upon exposure. An imbalance of the host immune response can lead to a number of serious health implications. An overly aggressive response may lead to chronic or acute inflammation, whereas a highly attenuated response may lead to uncontrolled bacteria growth.

In the case of the latter, uncontrolled bacteria growth may also be due to evasion of the host immune system. As discussed in the previous section, bacterial pathogens have mechanisms in place in order to thwart clearance by the immune system. Therefore, in

response to threat, researchers have developed bacterial immunotherapies that operate by provoking a selective native immune response against evading pathogenic bacteria. Treatment of microbial infections using this novel methodology possesses two main benefits. First, the immune system has evolved to combat pathogenic bacteria. In fact, the innate human immune system is constantly detecting, engaging, and destroying pathogenic bacteria. As stated, it is only when the homeostatic balance between the host immune system and the pathogenic bacteria is compromised that a bacterial infection ensues. Secondly, by targeting the immune system of the host rather than the bacteria, the propensity for bacteria to evolve resistance via selective pressure is potentially reduced.¹ It is due to these two clear advantages that immunomodulatory drugs provide great potential as future antimicrobial therapeutics.

2.3 Bacterial Immunotherapy

Unfortunately, immuno-agents against bacterial infections have lagged behind traditional antibiotics despite the tremendous clinical success of immunotherapy in other disease areas.¹⁰ This is best illustrated in the field of cancer therapy. Cancer immunotherapeutics attack cancer cells by mounting or enhancing a selective immune response against the tumor cells. Immuno-oncology has resulted in unprecedented patient responses.¹⁰ Most significantly, more robust and sustained anti-cancer responses have been observed when compared to traditional cancer chemotherapeutics.^{11, 12, 13, 14} Research groups have been working towards applying guiding principles from immuno-oncology to design molecules that target pathogenic bacteria.^{15, 16, 17, 18} These strategies act to stimulate or attenuate the host immune system in a manner that is advantageous to

clearance of infection. By exploiting an emerging chemical understanding of complex biological systems, future efforts to rationally modulate human immunological functions have the potential to augment our ability to prevent, diagnose, and treat human disease. In this field, one of the most utilized methods of synthetically tagging bacteria for host immune clearance is the employment of antibody-recruiting small molecules (ARMs).

2.3.1 Antibody-Recruiting Small Molecules (ARMs) for Bacteria Targeting

To date, the display of antibody-recruiting small molecules (ARMs) on targets such as cancer cells, viruses, and bacteria has demonstrated high potential for stimulating the host immune system.¹⁹ Bacteria eradication by the immune system relies on surface “tagging” by antibodies. As such, synthetic ARMs are comprised of a target binding domain (surface of bacteria) and an antibody binding domain. Simultaneous association of ARMs with antibodies and surface-exposed targets results in the formation of ternary complexes, which can elicit antibody dependent immune effector responses. Two potent arms of the native immune system that can potentially lead to bacterial killing based on opsonization are antibody-dependent cellular cytotoxicity (ADCC) and complement-dependent cytotoxicity (CDC) (Figure 2.1).

In the latter, the recruitment of antibodies induces a complement-dependent cytotoxic (CDC) response, in which protein aggregates are formed in target membrane. This protein aggregate, known as the membrane attack complex (MAC), is responsible for lysing the target cell by forming pores in the membrane of the cell.²⁰ This response does not rely on other immune cells, although the innate immune system is made up of

phagocytic cells (polymorphonuclear neutrophils, monocytes, macrophages), cells that release inflammatory mediator, and natural killer cells. This mechanism is generally thought to be utilized in the eradication of Gram-negative bacteria.

The other mechanism, in which the immune system facilitates immune-mediated cytotoxicity, is through the recruitment of these aforementioned effector immune cells. In these types of immune responses, antibodies opsonizing the surface of target cells are recognized by effector immune cells. In the case of antibody-dependent cellular phagocytosis (ADCP), macrophages and neutrophils recognize opsonized bacterial surfaces and phagocytose target cells.²¹ Conversely, recognition of the antibody Fc region by natural killer cells results in immune cell release of proteins such as perforin, which subsequently destroy the target through lysis. This mechanism of immunity is antibody-dependent cellular cytotoxicity (ADCC).^{22, 23}

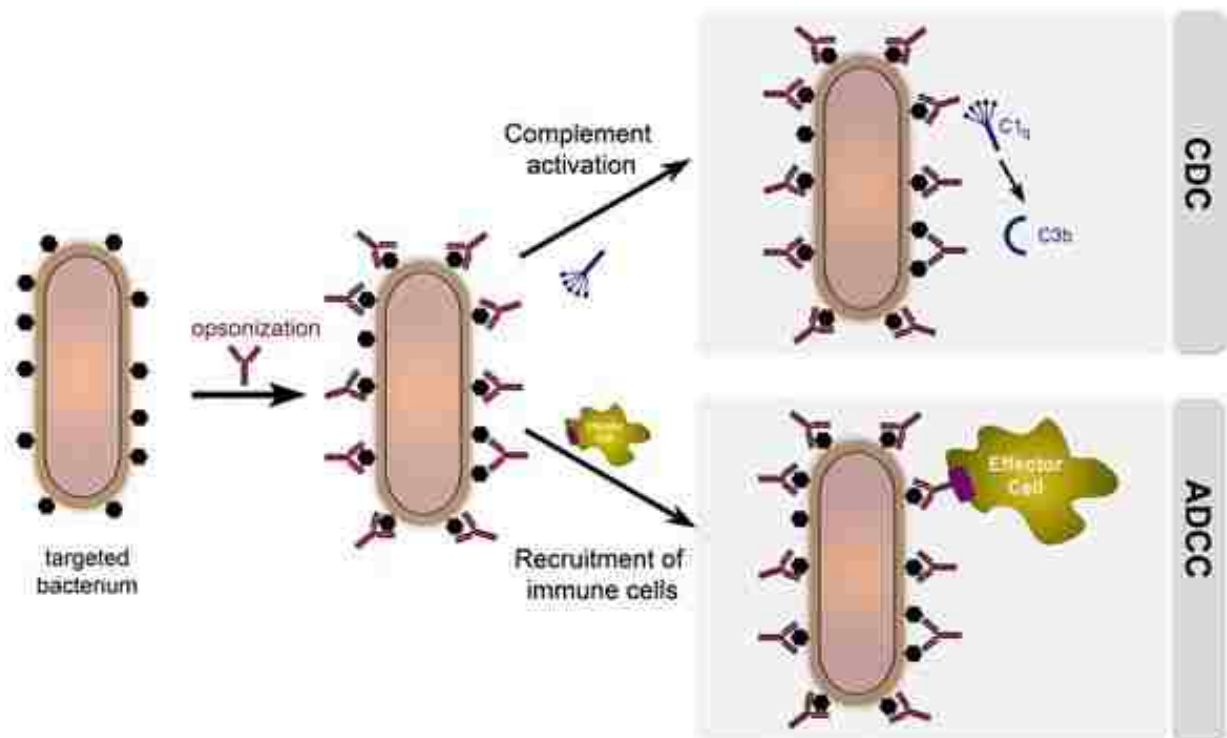


Figure 2.1 Primary Modes of Pathogen Clearance based on Immunomodulators.

Immunotherapy with antibodies has taken the leading role in this development aided by the virtually unlimited supply of purified human mAbs, which are among the immune system's most effective weapon against bacterial pathogens. Upon antigen labeling of target cell surfaces, these adaptive antibodies can bind and neutralize bacterial toxins, facilitate an immune response, and improve recognition and binding by phagocytic cells thereby increasing the phagocytic killing efficiency. In using this strategy for therapeutic purposes, antigens that bind endogenous antibodies are more appealing as they forgo the need for vaccination.

Few antigens are known to be recognized by endogenous antibodies. The first and most prominently utilized endogenous ARM is the carbohydrate galactosyl-(1-3) galactose (α -Gal) (Figure 2.2). With estimations of up to 8% of anti- α -Gal antibodies found circulating in the human blood stream, this trisaccharide epitope has produced robust immune responses used in developing cancer and HIV treatments.^{24, 25, 26,} ²⁷Another carbohydrate-based antigen is L-rhamnose (Figure 2.2). Through extensive analysis of human sera samples derived from subjects of diverse ethnicities, ages, and gender, antibodies which bind L-rhamnose were found in greater concentrations in a higher proportion of people than the previously mentioned α -Gal.²⁸ Recently L-rhamnose was used to label tumor cells and demonstrated its ability to inhibit tumor growth in vivo.²⁹ Lastly, DNP is also known to recruit endogenous antibodies (Figure 2.2). Although antibodies for the previous two epitopes mentioned, have origins linked to bacteria, the presence of anti-DNP antibodies remains debated.^{30, 31} It is known that 1% of all antibodies circulating within the human blood stream will bind to DNP haptens.^{32,} ^{33, 34} Due to its chemical structure, constructing ARMs displaying the DNP epitope is facile in comparison to the previously mention carbohydrate antigens. The use of DNP conjugated ARMs has previously been used to elicit immunomodulation responses that have targeted human immunodeficiency virus (HIV), lung cancer, prostate cancer, and colon adenocarcinoma.^{35, 36, 37}

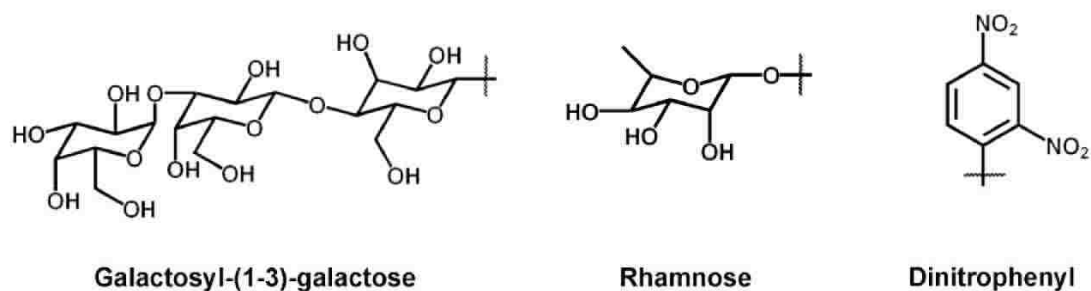


Figure 2.2 Chemical Structures of Antigens Capable of Recruiting Endogenous Antibodies. Galactosyl-(1-3) galactose, rhamnose, and dinitrophenyl are known to be epitopes or haptens for endogenous antibodies.

A variety of ARM-based antibacterial strategies have been evaluated. The first example was reported by the Bednarski laboratory in 1992. They employed a rationally designed, bifunctional molecule capable of directing anti-avidin antibodies to *E. coli*.^{38, 39} The target of interest was a mannose sugar receptor expressed on the pili of *Escherichia coli* (*E.coli*). Biotin was conjugated to the C-glycoside of mannose, a known ligand for bacterial mannose receptors, and this construct was shown to recruit anti-avidin IgG antibodies to the surface of *E. coli* in a manner dependent on the presence of conjugate, avidin, and antibodies. Furthermore, the researchers demonstrated that complexes between avidin, antibody, and ARM could mediate complement- and macrophage-dependent cytotoxicity.

More recently, in 2003 and 2006, Whitesides and co-workers developed ARMs that target pathogenic bacteria by utilizing the potent antibiotic vancomycin.^{40, 41} Constructing vancomycin- fluorescein polyvalent polymers allowed for the targeting of the surface of several Gram-positive bacteria, including *S. aureus*, *S. epidermidis*, and *S. pneumoniae*).

The polymeric vancomycin was used to target the site of new peptidoglycan and the fluorescein moiety promoted the recruitment of anti-fluorescein antibodies to the surface of various Gram-positive bacteria. Using fluorescence microscopy and flow cytometry, the authors demonstrated that the antibody-recruiting polymer could mediate phagocytosis of opsonized bacteria in the presence of anti-fluorescein antibodies.

Each of these previous studies demonstrates the feasibility of stimulating the host immune system as an effective strategy to thwart off pathogenic bacterial infections. However, these methods suffer drawbacks such as vaccination, low bioavailability, or indirect antigen cell surface labeling. The antigens utilized, biotin and fluorescein, would not be suitable for inducing an immune response without prior immunization. To mitigate this shortcoming, the hapten utilized should ideally recruit endogenous host antibodies to the bacterial surface.

In 2014, the Pires laboratory pioneered the use of a direct targeting agent, where bacterial cell surfaces were selectively modified with antigens that recruit endogenous antibodies to eliminate the need for vaccination. Since then they have pioneered the field of bacteria immunotherapy utilizing haptens recognized by endogenous antibodies.^{15, 16, 17} In their novel immunomodulation strategy, D-amino acid Antibody Recruitment Therapy (DART), they developed a series of D-amino acid derivatives that selectively modified bacterial cell surfaces with small molecule haptens. Synthetic D-amino acids were metabolically incorporated as cell wall building blocks, which led to cell surface presentation of unnatural sidechains modified with haptens. They showed that the presence of DNP-conjugated D-amino acids led to extensive peptidoglycan remodeling and triggered the recruitment of endogenous antibodies (existing antibodies in human

serum) and induced phagocytosis by macrophages. In a second generation form of DART, they showed the ability of PBP transpeptidases to incorporate D-amino acids possessing diverse C-terminus modifications. Through this study, it was observed that exogenous D-amino carboxamide variants are more readily incorporated into the peptidoglycan than the natural carboxylic acid containing D-amino acid substrate. They show that that DNP-conjugated D-amino carboxamides elicited a greater immune response in *B. subtilis* and *E. faecalis*.¹⁶

Poignantly, the use of employing antibodies to treat infections has long ago been established. Using antibodies to treat infections became a reality in the late 1800's when a German physiologist, Emil von Behring, developed serum therapies against diphtheria and tetanus.⁴² He found that he could transfer serum from infected horses to ill patients stricken with the disease. The antitoxins, as he coined them, from the horse serum targeted the disease in the patients and triggered a robust immune response. Stricken patients were healed and Von Behring later won the first Nobel Prize in medicine for employing antitoxins (antibodies, as we call them today) in 1901. Afterward, passive serum therapy was the preferred method in treating not only diphtheria and tetanus, but also scarlet fever and meningitis.⁴³ As we are well aware of today, the use of the antiserum was particularly effective against pathogens, capable of evading the immune system. With the advent of antibiotic therapy, serum therapy faded into background. However, Von Behring's discovery may be making its second debut as a life-saving remedy.

In this thesis, the development of an immunotherapy strategy to specifically target *Staphylococcus aureus* and the challenging Gram-negative pathogenic bacteria is discussed. By utilizing derivatives of antibiotics, which naturally home to the bacteria surface, bacterial cell surfaces were selectively modified with antigens that recruit endogenous antibodies. The antibody recruitment molecules were designed to afford high levels of bioavailability and selectively modulate bacterial surfaces in a direct manner to reduce off target immune responses effecting host cells. In *Staphylococcus aureus*, we report on the selective and covalent modification of the bacterial cell wall primed for the recruitment of endogenous antibodies. We also show, for the first time, *in vivo* selective targeting of *S. aureus*. In developing an immunotherapy strategy for Gram-negative bacteria, we describe the first class of synthetic molecules that remodel Gram-negative bacterial cell surfaces with immune cell attractants. The results of this thesis demonstrate a viable treatment option to address the clinical challenge of *Staphylococcus aureus* and Gram-negative bacterial pathogens.

2.4 REFERENCES

1. Hancock, R. E. W.; Nijnik, A.; Philpott, D. J., Modulating immunity as a therapy for bacterial infections. *Nat Rev Micro* **2012**, *10* (4), 243-254.
2. Vinay, D. S.; Ryan, E. P.; Pawelec, G.; Talib, W. H.; Stagg, J.; Elkord, E.; Lichtor, T.; Decker, W. K.; Whelan, R. L.; Kumara, H. M. C. S.; Signori, E.; Honoki, K.; Georgakilas, A. G.; Amin, A.; Helferich, W. G.; Boosani, C. S.; Guha, G.; Ciriolo, M. R.; Chen, S.; Mohammed, S. I.; Azmi, A. S.; Keith, W. N.; Bilsland, A.; Bhakta, D.; Halicka, D.; Fujii, H.; Aquilano, K.; Ashraf, S. S.; Nowsheen, S.; Yang, X.; Choi, B. K.; Kwon, B. S., Immune evasion in cancer: Mechanistic basis and therapeutic strategies. *Seminars in Cancer Biology* **2015**, *35*, Supplement, S185-S198.
3. Francisco, L. M.; Sage, P. T.; Sharpe, A. H., The PD-1 pathway in tolerance and autoimmunity. *Immunological Reviews* **2010**, *236* (1), 219-242.
4. Berne, C.; Ducret, A.; Hardy, G. G.; Brun, Y. V., Adhesins involved in attachment to abiotic surfaces by Gram-negative bacteria. *Microbiology spectrum* **2015**, *3* (4), 10.1128/microbiolspec.MB-0018-2015.
5. Kaparakis-Liaskos, M.; Ferrero, R. L., Immune modulation by bacterial outer membrane vesicles. *Nat Rev Immunol* **2015**, *15* (6), 375-387.
6. Hyams, C.; Camberlein, E.; Cohen, J. M.; Bax, K.; Brown, J. S., The Streptococcus pneumoniae Capsule Inhibits Complement Activity and Neutrophil Phagocytosis by Multiple Mechanisms. *Infection and Immunity* **2010**, *78* (2), 704-715.
7. Christie, P. J.; Atmakuri, K.; Krishnamoorthy, V.; Jakubowski, S.; Cascales, E., Biogenesis, architecture, and function of bacterial type IV secretion systems. In *Annual Review of Microbiology*, 2005; Vol. 59, pp 451-485.
8. Morgan, B. P.; Marchbank, K. J.; Longhi, M. P.; Harris, C. L.; Gallimore, A. M., Complement: Central to innate immunity and bridging to adaptive responses. *Immunology Letters* **2005**, *97* (2 SPEC. ISS.), 171-179.
9. Kim, H. S.; Gilliland, S. E., *Lactobacillus acidophilus* as a Dietary Adjunct for Milk to Aid Lactose Digestion in Humans¹. *Journal of Dairy Science* **66** (5), 959-966.
10. Nathan, C., Fresh approaches to anti-infective therapies. *Sci Transl Med* **2012**, *4* (140), 140sr2.
11. Rosenberg, S. A.; Yang, J. C.; Restifo, N. P., Cancer immunotherapy: moving beyond current vaccines. *Nat Med* **2004**, *10* (9), 909-15.
12. Grupp, S. A.; Kalos, M.; Barrett, D.; Aplenc, R.; Porter, D. L.; Rheingold, S. R.; Teachey, D. T.; Chew, A.; Hauck, B.; Wright, J. F.; Milone, M. C.; Levine, B. L.; June, C. H., Chimeric antigen receptor-modified T cells for acute lymphoid leukemia. *N Engl J Med* **2013**, *368* (16), 1509-18.
13. Khalil, D. N.; Smith, E. L.; Brentjens, R. J.; Wolchok, J. D., The future of cancer treatment: immunomodulation, CARs and combination immunotherapy. *Nat Rev Clin Oncol* **2016**, *13* (6), 394.
14. Morgensztern, D.; Herbst, R. S., Nivolumab and Pembrolizumab for Non-Small Cell Lung Cancer. *Clin Cancer Res* **2016**, *22* (15), 3713-7.

15. Fura, J. M.; Sabulski, M. J.; Pires, M. M., D-amino acid mediated recruitment of endogenous antibodies to bacterial surfaces. *ACS Chem Biol* **2014**, *9* (7), 1480-9.
16. Fura, J. M.; Pires, M. M., D-amino carboxamide-based recruitment of dinitrophenol antibodies to bacterial surfaces via peptidoglycan remodeling. *Biopolymers* **2015**, *104* (4), 351-9.
17. Fura, J. M.; Pidgeon, S. E.; Birabaharan, M.; Pires, M. M., Dipeptide-Based Metabolic Labeling of Bacterial Cells for Endogenous Antibody Recruitment. *ACS Infect Dis* **2016**, *2* (4), 302-309.
18. Pidgeon, S. E.; Fura, J. M.; Leon, W.; Birabaharan, M.; Vezenov, D.; Pires, M. M., Metabolic Profiling of Bacteria by Unnatural C-terminated D-Amino Acids. *Angew Chem Int Ed Engl* **2015**, *54* (21), 6158-62.
19. McEnaney, P. J.; Parker, C. G.; Zhang, A. X.; Spiegel, D. A., Antibody-Recruiting Molecules: An Emerging Paradigm for Engaging Immune Function in Treating Human Disease. *ACS Chemical Biology* **2012**, *7* (7), 1139-1151.
20. Podack, E. R., Molecular composition of the tubular structure of the membrane attack complex of complement. *Journal of Biological Chemistry* **1984**, *259* (13), 8641-8647.
21. Weiner, L. M.; Surana, R.; Wang, S., Antibodies and cancer therapy: versatile platforms for cancer immunotherapy. *Nature reviews. Immunology* **2010**, *10* (5), 317-327.
22. Smyth, M. J.; Cretney, E.; Kelly, J. M.; Westwood, J. A.; Street, S. E. A.; Yagita, H.; Takeda, K.; Dommelen, S. L. H. v.; Degli-Esposti, M. A.; Hayakawa, Y., Activation of NK cell cytotoxicity. *Molecular Immunology* **2005**, *42* (4), 501-510.
23. Nimmerjahn, F.; Ravetch, J. V., Fc[gamma] receptors as regulators of immune responses. *Nat Rev Immunol* **2008**, *8* (1), 34-47.
24. Owen, R. M.; Carlson, C. B.; Xu, J.; Mowery, P.; Fasella, E.; Kiessling, L. L., Bifunctional Ligands that Target Cells Displaying the $\alpha\beta 3$ Integrin. *ChemBioChem* **2007**, *8* (1), 68-82.
25. Naicker, K. P.; Li, H.; Heredia, A.; Song, H.; Wang, L.-X., Design and synthesis of [small alpha]Gal-conjugated peptide T20 as novel antiviral agent for HIV-immunotargeting. *Organic & Biomolecular Chemistry* **2004**, *2* (5), 660-664.
26. Perdomo, M. F.; Levi, M.; Sällberg, M.; Vahlne, A., Neutralization of HIV-1 by redirection of natural antibodies. *Proceedings of the National Academy of Sciences* **2008**, *105* (34), 12515-12520.
27. Carlson, C. B.; Mowery, P.; Owen, R. M.; Dykhuizen, E. C.; Kiessling, L. L., Selective Tumor Cell Targeting Using Low-Affinity, Multivalent Interactions. *ACS Chemical Biology* **2007**, *2* (2), 119-127.
28. Sheridan, R. T. C.; Hudon, J.; Hank, J. A.; Sondel, P. M.; Kiessling, L. L., Rhamnose Glycoconjugates for the Recruitment of Endogenous Anti-Carbohydrate Antibodies to Tumor Cells. *ChemBioChem* **2014**, *15* (10), 1393-1398.
29. Li, X.; Rao, X.; Cai, L.; Liu, X.; Wang, H.; Wu, W.; Zhu, C.; Chen, M.; Wang, P. G.; Yi, W., Targeting Tumor Cells by Natural Anti-Carbohydrate Antibodies Using Rhamnose-Functionalized Liposomes. *ACS Chemical Biology* **2016**, *11* (5), 1205-1209.

30. Jin, Y.; Xin, Y.; Zhang, W.; Ma, Y., Mycobacterium tuberculosis Rv1302 and Mycobacterium smegmatis MSMEG_4947 have WecA function and MSMEG_4947 is required for the growth of M. smegmatis. *FEMS Microbiology Letters* **2010**, *310* (1), 54-61.
31. Galili, U.; Clark, M. R.; Shohet, S. B.; Buehler, J.; Macher, B. A., Evolutionary relationship between the natural anti-Gal antibody and the Gal alpha 1----3Gal epitope in primates. *Proceedings of the National Academy of Sciences of the United States of America* **1987**, *84* (5), 1369-1373.
32. Karjalainen, K.; Mäkelä, O., Concentrations of three hapten-binding immunoglobulins in pooled normal human serum. *European Journal of Immunology* **1976**, *6* (2), 88-93.
33. Farah, F. S., Natural antibodies specific to the 2,4-dinitrophenyl group. *Immunology* **1973**, *25* (2), 217-226.
34. Ortega E, K. M., Larralde C., Natural DNP-binding immunoglobulins and antibody multispecificity. *Mol Immunol* **1984**, *21* (10), 883-888.
35. Murelli, R. P.; Zhang, A. X.; Michel, J.; Jorgensen, W. L.; Spiegel, D. A., Chemical Control over Immune Recognition: A Class of Antibody-Recruiting Small Molecules That Target Prostate Cancer. *Journal of the American Chemical Society* **2009**, *131* (47), 17090-17092.
36. Lu, Y.; You, F.; Vlahov, I.; Westrick, E.; Fan, M.; Low, P. S.; Leamon, C. P., Folate-Targeted Dinitrophenyl Hapten Immunotherapy: Effect of Linker Chemistry on Antitumor Activity and Allergic Potential. *Molecular Pharmaceutics* **2007**, *4* (5), 695-706.
37. Parker, C. G.; Domaoal, R. A.; Anderson, K. S.; Spiegel, D. A., An Antibody-Recruiting Small Molecule That Targets HIV gp120. *Journal of the American Chemical Society* **2009**, *131* (45), 16392-16394.
38. Bertozzi, C. R.; Bednarski, M. D., A receptor-mediated immune response using synthetic glycoconjugates. *Journal of the American Chemical Society* **1992**, *114* (14), 5543-5546.
39. Bertozzi, C. R.; Bednarski, M. D., Antibody targeting to bacterial cells using receptor-specific ligands. *Journal of the American Chemical Society* **1992**, *114* (6), 2242-2245.
40. Krishnamurthy, V. M.; Quinton, L. J.; Estroff, L. A.; Metallo, S. J.; Isaacs, J. M.; Mizgerd, J. P.; Whitesides, G. M., Promotion of opsonization by antibodies and phagocytosis of Gram-positive bacteria by a bifunctional polyacrylamide. *Biomaterials* **2006**, *27* (19), 3663-3674.
41. Metallo, S. J.; Kane, R. S.; Holmlin, R. E.; Whitesides, G. M., Using Bifunctional Polymers Presenting Vancomycin and Fluorescein Groups To Direct Anti-Fluorescein Antibodies to Self-Assembled Monolayers Presenting d-Alanine-d-Alanine Groups. *Journal of the American Chemical Society* **2003**, *125* (15), 4534-4540.
42. *Nobel Lectures, Physiology or Medicine 1901-1921*. Elsevier Publishing Company: Amsterdam, 1967.
43. Walsh, F., Superbugs to kill 'more than cancer' by 2050. **2014**.

Chapter 3

Immuno-Targeting of *Staphylococcus aureus* via Sortase A-Mediated Incorporation of Vancomycin-Antigen Complexes

3.1 ABSTRACT

As the threat of methicillin-resistant *Staphylococcus aureus* continues to loom over the power of modern medicine, new methodologies to treat bacterial infections is of paramount importance. We set out to leverage the surface-homing properties of vancomycin to specifically tag the surface of Gram-positive pathogens with immune cell attractants. Vancomycin, which accumulates preferentially at the regions of cell division/growth (concentrated pools of Lipid II molecules), target a dipeptide motif found in the cell wall of bacteria. Additionally, previous research has shown that exogenous peptides can be covalently incorporated into the peptidoglycan of *S. aureus* via the sortase A enzyme, SrtA. This chapter will discuss the development of vancomycin-conjugated SrtA-recognition peptides, which were shown to covalently modify the bacterial cell surface through sortase A-mediated surface remodeling. Initially, fluorescent handles were conjugated to the peptide-drug complexes, in order to answer fundamental questions, such as peptide recognition sequence, optimal linker length for incorporation, and potential toxicity. Using these determined conditions, the conjugated fluorophore on the peptide-drug complex was exchanged for a DNP antigen moiety to facilitate the recruitment of anti-DNP antibodies, readily found in human blood serum. The studies presented in this chapter demonstrate that the incorporation of DNP antigens within the bacterial peptidoglycan scaffold enhances the recruitment of endogenous anti-

DNP antibodies to the bacterial cell surface by nearly four-fold compared to unlabeled cells. Furthermore, we show, for the first time, the *in vivo* selective targeting of *S. aureus* in live *C. elegans*, a widely used model host to understand bacterial pathogenesis and host-pathogen interactions. In conjunction, these results pave the way for a narrow-spectrum strategy for the destruction of bacterial infections caused by *S. aureus* (drug-sensitive and -resistant) through bacterial immunotherapy.

3.2 INTRODUCTION

The cell wall of Gram-positive bacteria has served as a fruitful target for the development of antibacterial therapies for decades.¹ As discussed previously, Gram-positive bacteria are surrounded by a mesh-like scaffold of peptidoglycan, which is composed of multiple layers of N-acetylglucosamine (NAG) and N-acetylmuramic acid (NAM) glycan strands that are cross-linked by oligopeptides and provides bacteria with immense structural support.² Due to the critical role of the cell wall during cellular growth and division, molecules that interfere with the necessary enzymatic processes related to peptidoglycan synthesis have become some of the most successful antibiotic agents. Additionally, cell walls come in direct contact with the human hosts, a feature that can be exploited by the immune system in the detection and eradication of these pathogens. The remodeling of bacterial surfaces using surface-homing antibiotics holds considerable potential as a unique and targeted method to modulate the immune response by host organisms. As such, we explored the possibility of utilizing the antibiotic, vancomycin, as a means to target the surface of Gram-positive bacteria. We designed vancomycin-antigen conjugates, in order to decorate the bacterial surface with an immune stimulant. The potential as an antigen-conjugated surface displaying molecule is of great interest albeit concentration must remain below the minimal inhibitory concentration (MIC) of the bacteria. We became interested in designing a surface-remodeling method that would (1) increase the number of DNP epitopes against pathogens that display reduced D-Ala-D-Ala content on mature PG scaffolds, (2) generate covalent tags onto the PG scaffold and (3) conduct as a narrow-spectrum drug.

We aimed to target *S. aureus*, and explored the possibility of combining vancomycin with a peptidic recognition motif specific to *S. aureus*. The cell wall of *S. aureus* is very diverse and plays many important roles in the establishment of various infectious diseases. As such, the bacteria have devised methods for covalently decorating their cell wall with surface proteins, which can be involved in pathogenicity. *S. aureus* lack pili or fimbrial structures and instead rely on surface protein-mediated adhesion to host cells or invasion of tissues as a strategy to escape immune defenses.³ In order to engage this strategy, this facultative anaerobe decorates its cell surface with a diverse set of virulence factors (e.g., exotoxins, exoenzymes, and adhesins) via sortase A (SrtA) mediated transpeptidation.^{4,5} Critical for gaining entry into and colonization in host tissues, SrtA transpeptidase is a surface-bound enzyme that attaches bacterial proteins onto the PG scaffold of *S. aureus* (Figure 3.1).⁶

In anchoring proteins, sortase A recognizes the short, LPXTG peptide motif (where X is any amino acid) and catalyze the acyl-transfer onto lipid II of *S. aureus*.⁴ As the PG monomeric unit from lipid II is loaded onto the existing PG scaffold, so will the anchored protein (Figure 3.1).⁷ After continued PG biosynthesis, the anchored protein will eventually be presented at the cell surface. Spiegel and coworkers have previously shown that *S. aureus* cells treated with fluorescently labeled LPXTG peptides resulted in the labeling of bacterial surfaces.⁸ Furthermore, the conjugation of fluorescein to the N-terminus of LPXTG and subsequent labeling of the bacterial surface, allowed for the recruitment of anti-FITC antibodies to *S. aureus*.⁹

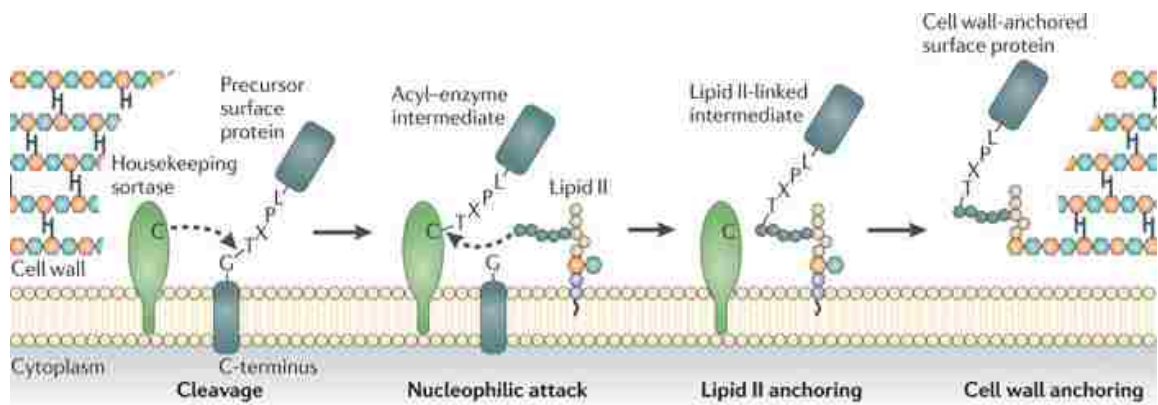


Figure 3.1 Remodeling of Bacterial Surface via Sortase A. The transpeptidase recognizes a SrtA specific peptide sequence (LPXTG). A cysteine in the active site of SrtA attacks the amide bond between the glycine and threonine residues to generate an acyl enzyme intermediate. Further reaction of this intermediate with the nucleophilic amine of a pentaglycine crosslinking oligopeptide of lipid II anchors the secreted proteins to the membrane. As the PG monomeric unit from lipid II is loaded onto the existing PG scaffold, so will the anchored protein. After additional PG biosynthesis, the anchored protein will eventually be presented at the cell surface. *Nature Reviews Microbiology* 9, 166-176 (March 2011).

Although these results highlight the potential in using SrtA-based peptide sequences to install unnatural handles on cell surfaces, the concentrations required for efficient labeling are not physiologically relevant (0.5-1 mM during overnight incubation). These high concentrations are necessary due to the nature of the transpeptidase reaction carried out by SrtA (high K_M), whereby both of its substrates are highly concentrated at the cell surface. Coinciding with the work described in this thesis, the reporting of the covalent conjugation of vancomycin to LPXTG was shown to bring the substrate peptide to its partner, lipid II, based on the ability of vancomycin to

associate with the D-Ala-D-Ala dipeptide on lipid II.¹⁰ By increasing the effective concentration of the LPXTG, efficient SrtA mediated tagging was possible at low micromolar concentrations. We set out to develop a potentially novel immunotherapy strategy by exploiting the propensity of bacteria to incorporate exogenous Srt A recognition peptides into their peptidoglycan that are conjugated to vancomycin displaying antibody-recruiting haptens (Figure 3.2). We hypothesized that a synthetic immunology approach could provide a highly efficient method for developing alternative antibiotic agents.

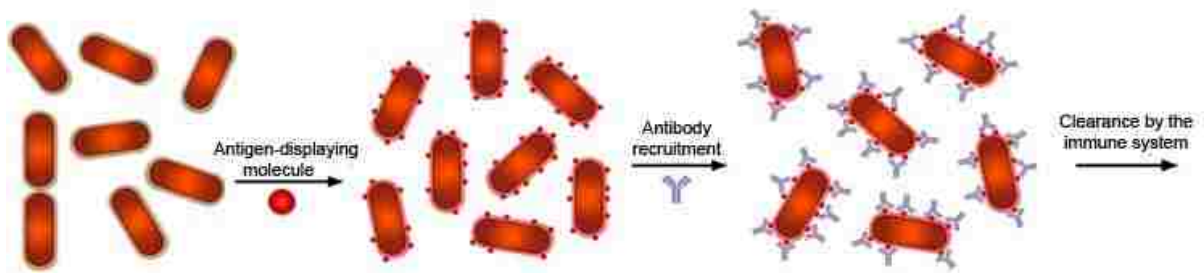


Figure 3.2 Schematic Representation of *S. aureus* Immunotherapy. *S. aureus* is incubated with sortase A recognition peptides conjugated to vancomycin-DNP. The DNP epitope is the antigen which is then covalently bound to the peptidoglycan surface of *S. aureus*. Following the labeling, the binding of anti-DNP IgG antibodies leads to the eventual clearance by the immune system.

3.3 RESULTS AND DISCUSSION

3.3.1. Fluorescent Labeling of *S. aureus* using vancomycin-BODIPY

Vancomycin, and related glycopeptides, imparts cytotoxicity by binding to the terminal D-Ala-D-Ala found on the PG stem peptide. As mentioned, the PG layer of the cell wall is rigid due to its highly cross-linked structure. As new layers of PG are synthesized, new building blocks of peptidoglycan get inserted (monomers of N-acetylmuramic acid and N-acetylglucosamine) into the membrane. Vancomycin binds to the building blocks of the peptidoglycan and prevents the transpeptidase from acting on these new formed blocks and thus prevents cross-linking of the peptidoglycan layer. By causing the peptidoglycan layer to be less rigid and more permeable, vancomycin addition eventually leads to the death of the bacteria (Figure 3.3). Due to the antibiotic's surface homing ability, we hypothesized that we could exploit the natural tendency of the antibiotic as a synthetic immunology approach.

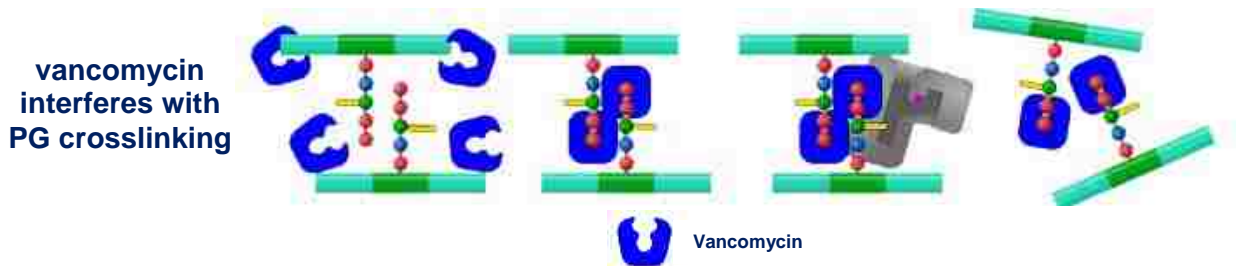
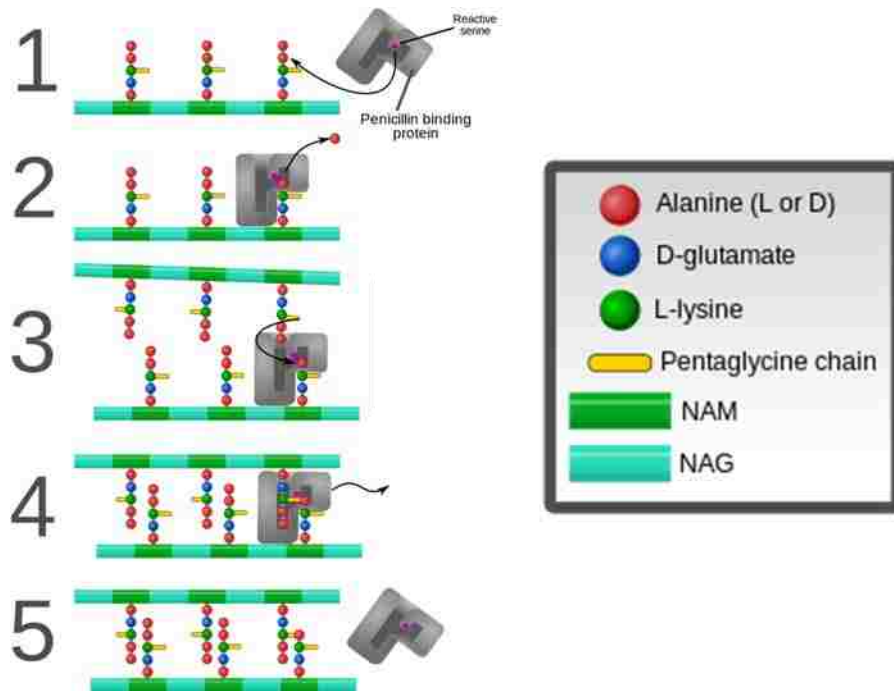


Figure 3.3 Mechanism of Vancomycin. Penicillin binding proteins (PBPs) rest on peptidoglycan and are responsible for the crosslinking between N-acetylglucosamine (NAG) and N-acetylmuramic (NAM) chains. Once vancomycin has irreversibly bound to D-Ala-D-Ala, PBPs are unable to recognize the site and connect the oligopeptide via their pentaglycine chains. (*Mcstrother, Vancomycin resistance.svg April 9, 2011*)

In assessing the binding affinity to the surface of *S. aureus*, we utilized a fluorescent vancomycin conjugate, vancomycin-BODIPY. *S. aureus* cells were incubated in medium supplemented with vancomycin-BODIPY (4 $\mu\text{g} / \text{mL}$) for 30 min at 37 °C. After allotted incubation time, cells were washed and fluorescence was quantified via flow cytometry at indicated time points (Figure 3.4). We observed a decrease in fluorescence in the first 5 min suggesting the dissociation of vancomycin-BODIPY from the surface of the bacteria. Due to this, we explored the use of a covalent method for installing vancomycin antigen conjugates on the surface of bacteria.

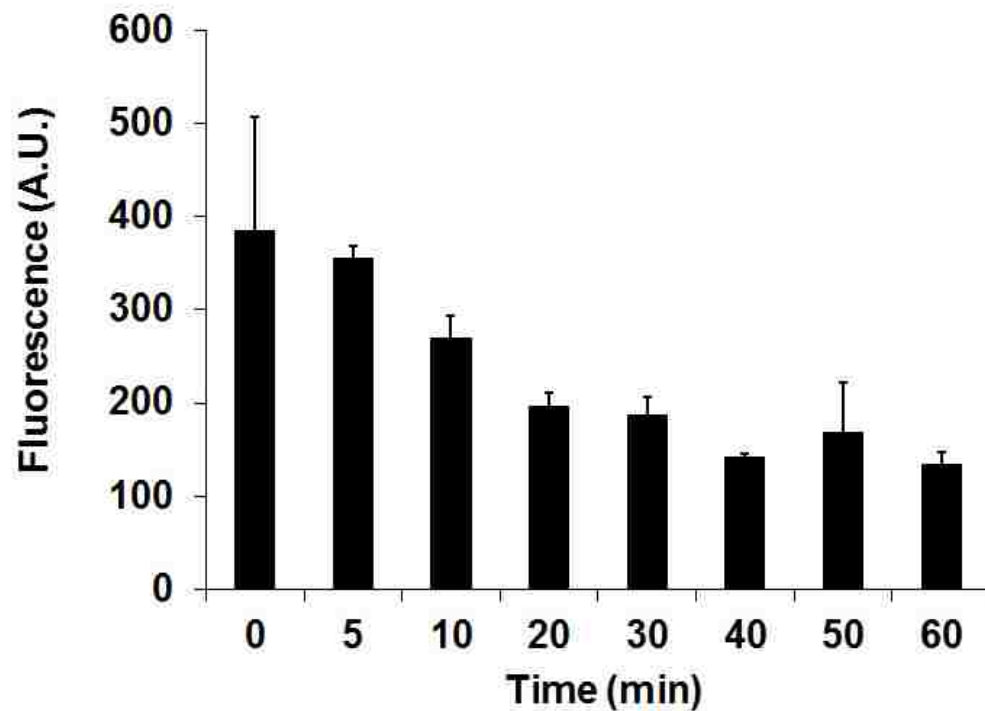
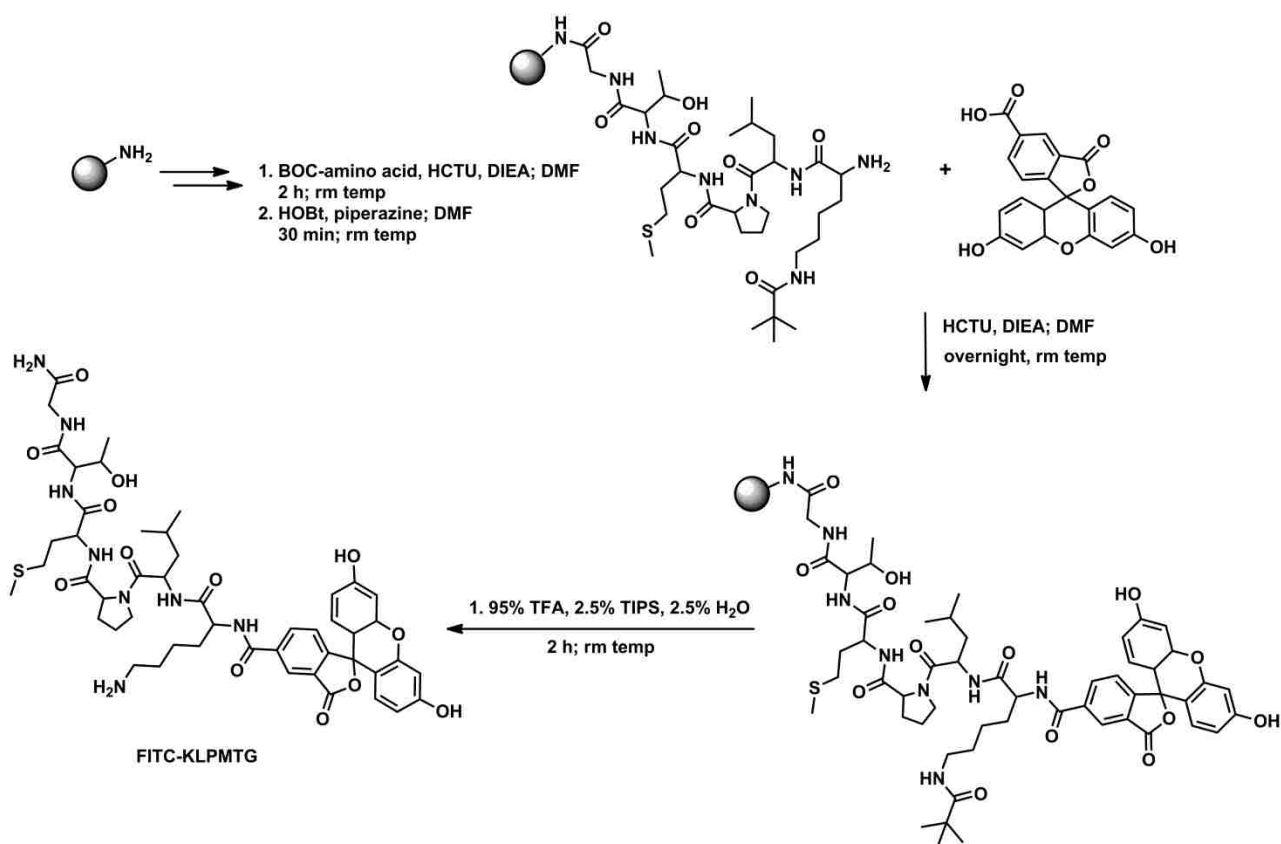


Figure 3.4 Vancomycin-BODIPY Dissociation from *S. aureus* Surface. Flow cytometry analysis of vancomycin-BODIPY-labeled *S. aureus* cells after indicated times. Data are represented as mean + SD (n = 3).

3.3.2 SrtA-mediated Incorporation in *S. aureus*

Some surface proteins require SrtA for the covalent anchorage to the peptidoglycan of Gram-positive bacteria. The enzyme recognizes secreted proteins bearing a specific sortase motif, Leu-Pro-X-Thr-Gly (LPXTG), and Leu-Pro-X-Thr-Gly/Leu-Pro-X-Thr-Ala-Ala (LPXTG/LPXTAA), for *Staphylococcus aureus* and *Streptococcus pyogenes*, respectively (where X is any amino acid). Other Gram-positive bacteria will also possess sortase enzymes, yet may have different recognition motifs¹¹ and substrate requirements.¹² Although the natural sortase substrate is the LPETG motif in *S. aureus*, the use of methionine in the central position of the pentapeptide demonstrated enhanced cell surface labeling.⁷ However, due to the role of SrtA as a housekeeping enzyme responsible for covalently modifying the peptidoglycan with proteins, the K_m of the enzyme is high.¹³ Thus, the required LPXTG-motif containing peptide concentration needed for labeling requires millimolar concentrations.

Initially, we synthesized peptides to establish the baseline values for efficient SrtA-mediated incorporation into the peptidoglycan of *S. aureus*. All fluorescently labeled SrtA recognition peptides were built via solid-phase peptide synthesis using standard Fmoc-chemistry (Scheme 3.1). We constructed two variants, FITC-KLPMTG-NH₂ and FITC-KLPETG-NH₂, and a control peptide exhibiting a scrambled SrtA sequence, FITC-KMGTL_P, employing the fluorescein (FITC) fluorophore which is compatible for solid-phase synthesis. *S. aureus* cells were incubated overnight in medium supplemented with 1 mM of FITC-KLPMTG, FITC-KLPETG or control peptide, FITC-KMGTL_P.



Scheme 3.1 Synthesis of FITC Conjugated SrtA Recognition Peptides. Peptides were synthesized using Fmoc-protected amino acids conjugated on Sieber resin. FITC fluorophore was conjugated to the N-terminus. Following conjugation, deprotection of the N-terminus of lysine and TFA cleavage from the resin afforded FITC Conjugated SrtA Recognition Peptides. Synthesis shown for FITC-KLPMTG; all peptides underwent same synthetic procedure.

The bacteria cells were washed and analyzed for the acquisition of green fluorescence from the fluorescein fluorophore. Consistent with previous reports, we observe roughly a 2-fold increase in surface labeling exposed to FITC-KLPMTG over bacteria exposed to FITC-KLPETG. Both the unlabeled bacteria and bacteria treated with the scrambled control displayed reduced fluorescence (Figure 3.5).

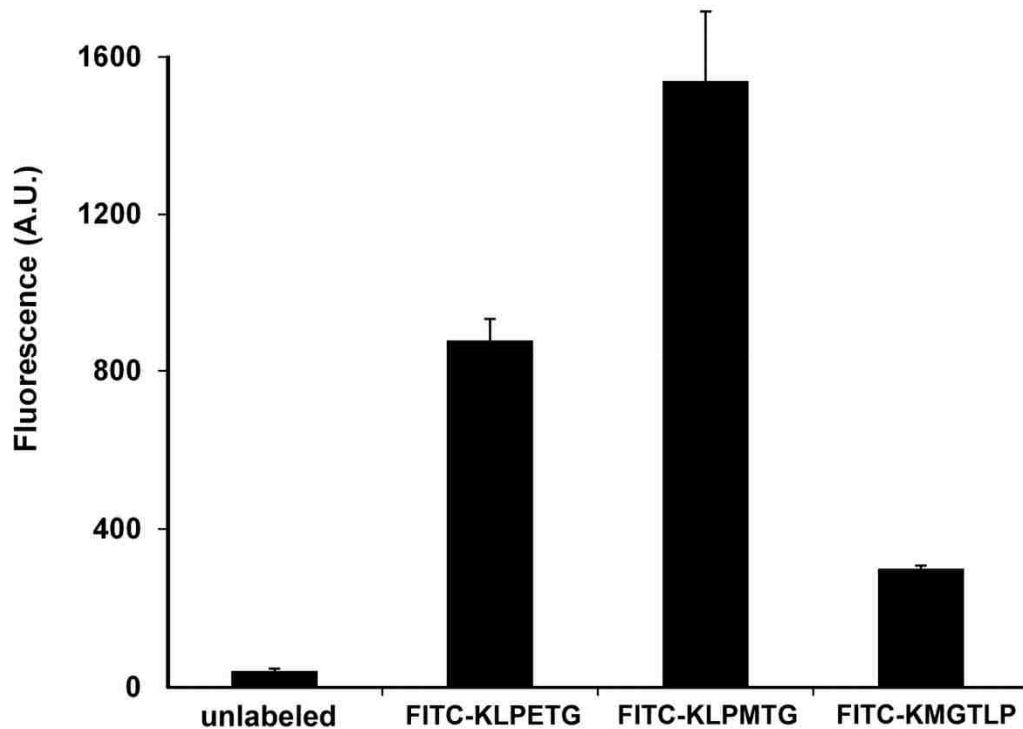


Figure 3.5 Incorporation of FITC Conjugated SrtA Recognition Peptides.

Flow cytometry analysis of *S. aureus* incubated overnight in the presence of LB alone, and LB supplemented with 1 mM of FITC-KLPETG or 1 mM of FITC-KLPMTG or 1 mM of FITC-KMGTLTLP. Data are represented as mean + SD (n = 3).

Next, we visualized the labeled *S. aureus* via fluorescence microscopy and observed a uniform fluorescence signal throughout the cell (Figure 3.6). We believe the difference in fluorescence levels in bacteria treated with different peptide sequences suggests a specific process of incorporation. In this case, we believe SrtA activity is responsible for selectively incorporating the LPMTG-containing peptide into the cell wall over the scrambled control.

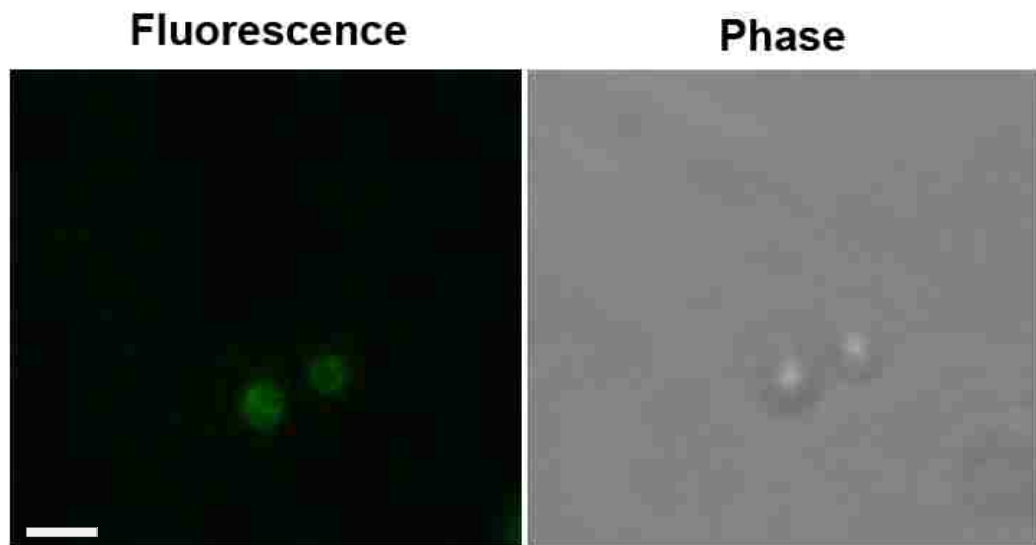


Figure 3.6 DIC and Fluorescent Microscopy Image of FITC-KLPMTG Labeled *S. aureus*. *S. aureus* were incubated in LB supplemented with 1 mM FITC-KLPMTG overnight at 37 °C. Cells were washed and imaged. Scale bar represents 1 μ m.

3.3.3 Vancomycin-conjugated SrtA Recognition Peptide Incorporation in *S. aureus*

Next, we constructed fluorescent peptides consisting of the LPMTG motif and the antibiotic, vancomycin. In particular, we varied the linker between the LPMTG and vancomycin to establish the optimum linker length (Figure 3.7). The spacer between these two units should be long enough to accommodate the binding of the D-Ala-D-Ala by vancomycin and the docking of the LPMTG onto the SrtA active site.

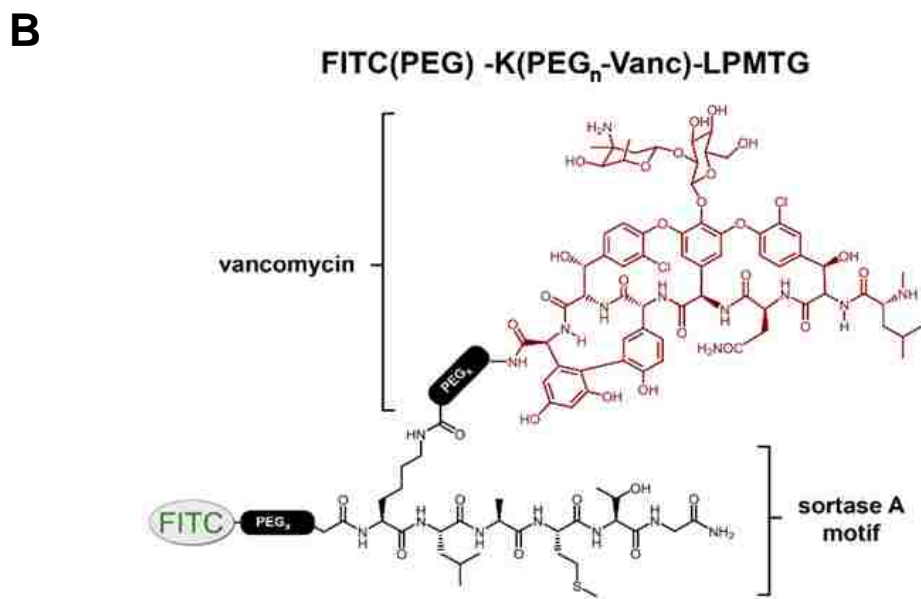
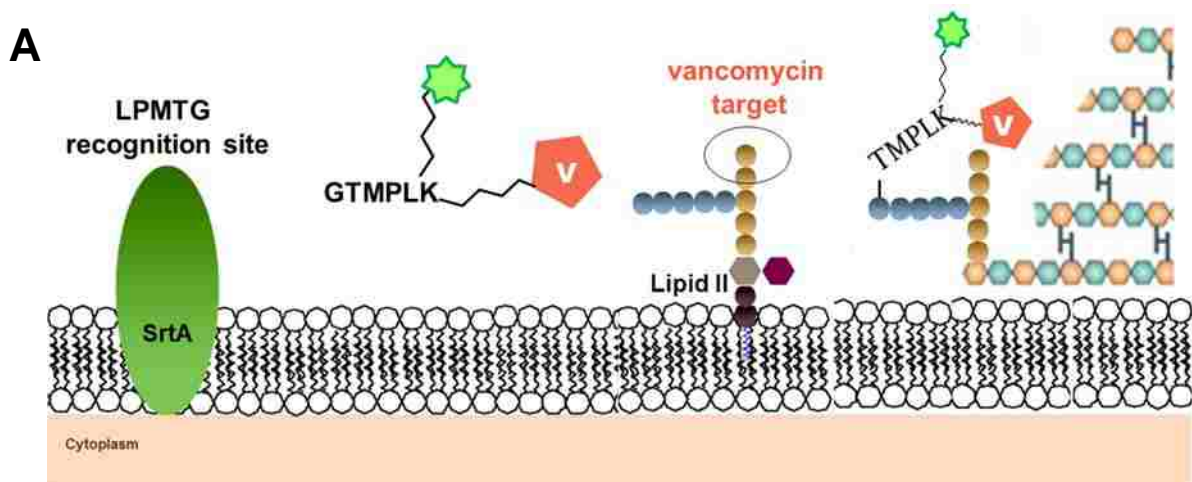


Figure 3.7 Cartoon representation of SrtA incorporation of Vancomycin-peptide conjugates. (A) Scheme depicting the anchoring of sortase A peptides onto PG. The presence of vancomycin positions the conjugate at the site of the sortase A enzyme. Due to this the effective concentration of the sortase A peptide substrate increases causing swift incorporation and transfer onto Lipid II. (B) Structure of sortase-vancomycin conjugates.

In the absence of structural data, we sought to empirically establish the optimum tether by evaluating a small panel of poly ethylene glycol (PEG) spacers. The high flexibility and solubility of PEG should be ideal for the bridging of LPMTG with vancomycin. We constructed several peptides with this backbone, FITC(PEG)-K(PEG_n-Vanc)-LPMTG, where n = 0, 1, 2, 3 (Table 3.1). We anticipated building this panel of peptides completely on solid support. However, vancomycin is deglycosylated in the presence of trifluoroacetic acid, eliminating the vancosamine and vancosaminyl-*O*-glucose sugars.^{14,15}

Compound :	PEG Linker :	Abbreviation :
FITC(PEG)-KLPMTG	0	FITC-PEG0
FITC(PEG)-K(PEG)-LPMTG	1	FITC-PEG1
FITC(PEG)-K(PEG₂)-LPMTG	2	FITC-PEG2
FITC(PEG)-K(PEG₃)-LPMTG	3	FITC-PEG3

FITC(PEG)-K(Vanc)LPMTG	0	FITC-PEG0Vanc
FITC(PEG)-K(PEG-Vanc)-LPMTG	1	FITC-PEG1Vanc
FITC(PEG)-K(PEG₂-Vanc)-LPMTG	2	FITC-PEG2Vanc
FITC(PEG)-K(PEG₃-Vanc)-LPMTG	3	FITC-PEG3Vanc

Table 3.1 List of Synthesized Vancomycin-SrtA peptide conjugates.

To confirm, we dissolved vancomycin in 95% TFA and obtained a HPLC trace (Figure 3.8). We overlaid the trace with the traces of pure vancomycin and pure vancomycin aglycon (vancomycin without the sugars). As seen in the trace, even pure vancomycin is susceptible to the 0.1% TFA added in the HPLC solvents. Therefore, the series of constructs were built using a combination of solid and solution phase chemistries and purified using 0.001% TFA HPLC solvents, due to the high sensitivity of vancomycin towards acidic conditions.

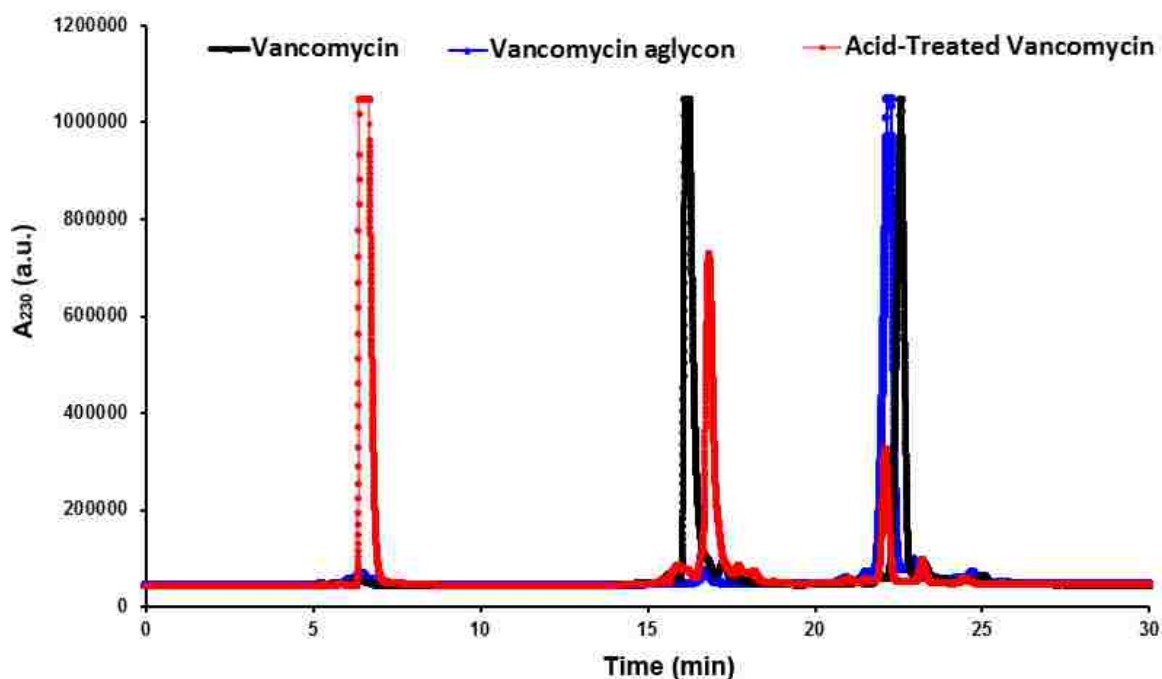
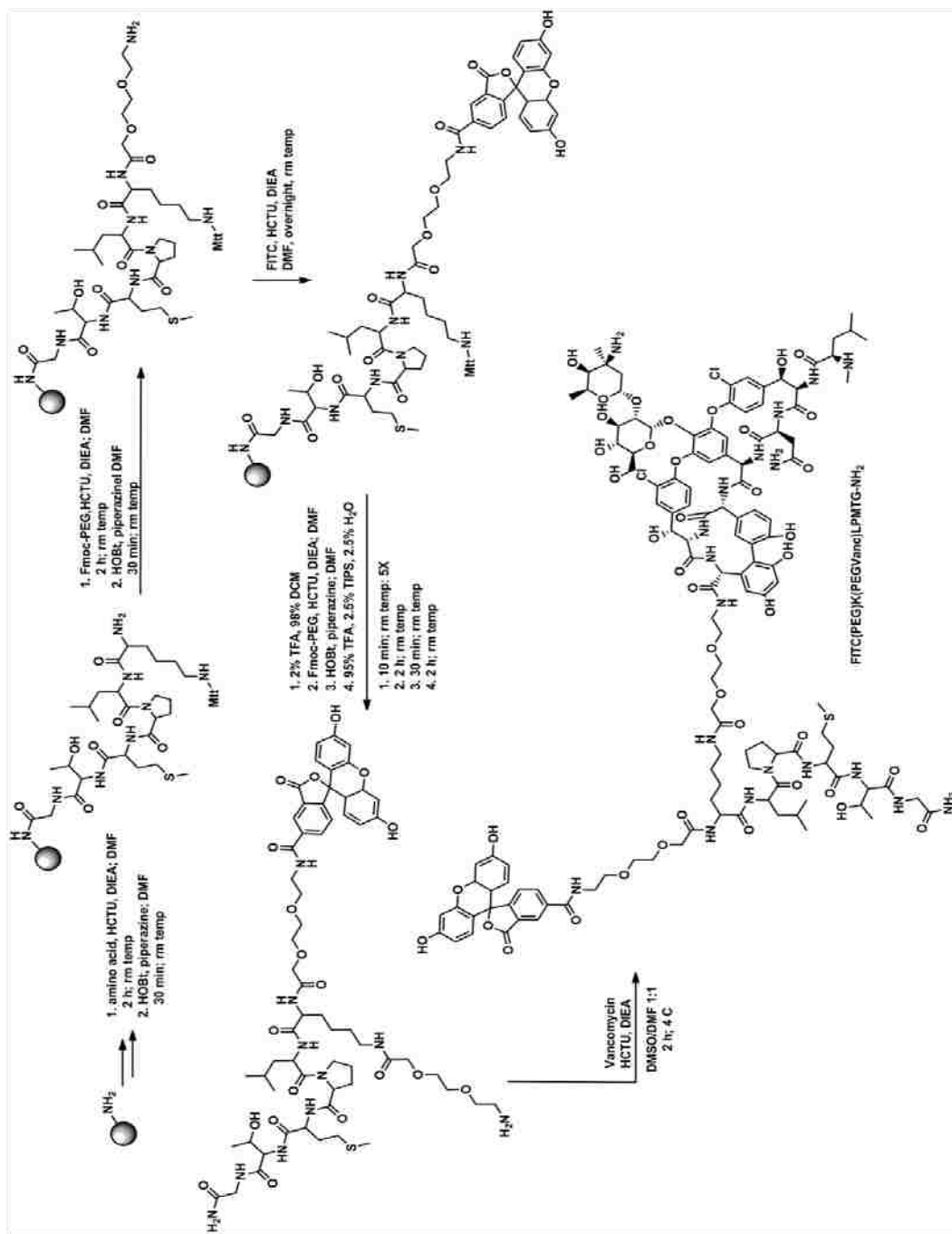


Figure 3.8 Vancomycin Acid Susceptibility. Vancomycin treated with 95% TFA (red trace) displays three peaks in the HPLC trace, depicting the vancomycin peak (center), the sugars (left) and the vancomycin aglycon (right). Vancomycin (black trace) is susceptible to HPLC acidic solvents displaying the vancomycin aglycon peak (right).

Vancomycin was coupled to the primary amine of PEG linker or directly to the lysine side chain, resulting in the final constructs (Scheme 3.2). All compounds were purified via reverse phase high performance liquid chromatography (RP-HPLC). Masses were confirmed using either electrospray ionization mass spectrometry (ESI-MS) or matrix assisted laser desorption/ionization time of flight mass spectrometry (MALDI-TOF MS).

S. aureus was incubated overnight in medium supplemented with 5 μ M of each construct. The bacteria cells were washed and analyzed by flow cytometry. We observed a 30-fold increase in fluorescence for bacteria exposed to FITC-PEG0Vanc and FITC-PEG1Vanc over unlabeled bacteria (Figure 3.9). This increase is attributed to the presence of vancomycin. The peptides not conjugated to vancomycin displayed very little to no fluorescence, indicating that vancomycin is needed to position the peptide near SrtA at the cell membrane. Lipid II, the target of vancomycin, is anchored on the cell membrane and is the recipient of the sortase cargo. We observed a loss in fluorescence for the peptides with a longer linker between the sortase A motif and vancomycin. This indicates length dependence between the motif and the antibiotic. The low levels of fluorescence associated with these samples may have resulted from nonspecific binding of the peptide construct to the bacterial surface or from low levels of intracellular accumulation.



Scheme 3.2 Synthesis of Vancomycin-conjugated SrTA Recognition Peptides. Peptides were synthesized using Fmoc-protected amino acids conjugated on Sieber resin. The selective deprotection of the amino side chain of lysine and coupling of Fmoc-protected PEG units was performed. After purification, the peptide was coupled to vancomycin to afford vancomycin-conjugated SrTA recognition peptide. Synthesis shown for FITC-PEG1Vanc; all peptides underwent same synthetic procedure.

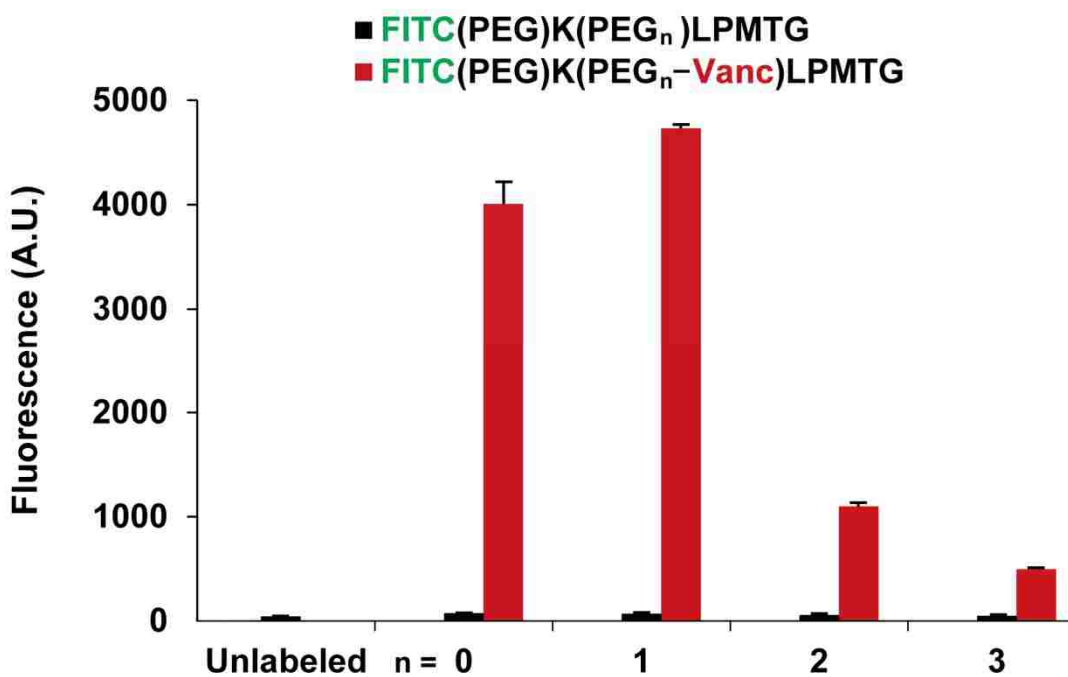


Figure 3.9 Vancomycin-conjugated SrtA Recognition Peptide Incorporation in *S. aureus*. Flow cytometry analysis of *S. aureus* cells incubated overnight in LB supplemented with panel of fluorescent conjugates at 5 μ M. Data are represented as mean + SD (n = 3).

Next, we probed the distance between the sequence motif and the fluorophore. We constructed another peptide incorporating an additional PEG group before the FITC fluorophore (Table 3.2).

Compound :	PEG Linker :	Abbreviation :
FITC(PEG ₂)-K(PEG)LPMTG	1	FITC-2PEG1
FITC(PEG ₂)-K(PEG-Vanc)-LPMTG	2	FITC-2PEG1Vanc

Table 3.2 List of Synthesized Vancomycin-SrtA peptide conjugates.

Incubating *S. aureus* with 5 μ M of FITC-PEG1Vanc or FITC-2PEG1Vanc overnight led to a 2.5 – fold increase in fluorescence for the FITC-2PEG1Vanc treated bacteria over the FITC-PEG1Vanc treated bacteria (Figure 3.10). Thus, the addition of the spacers before the fluorophore handles seems to aid in incorporation efficiency.

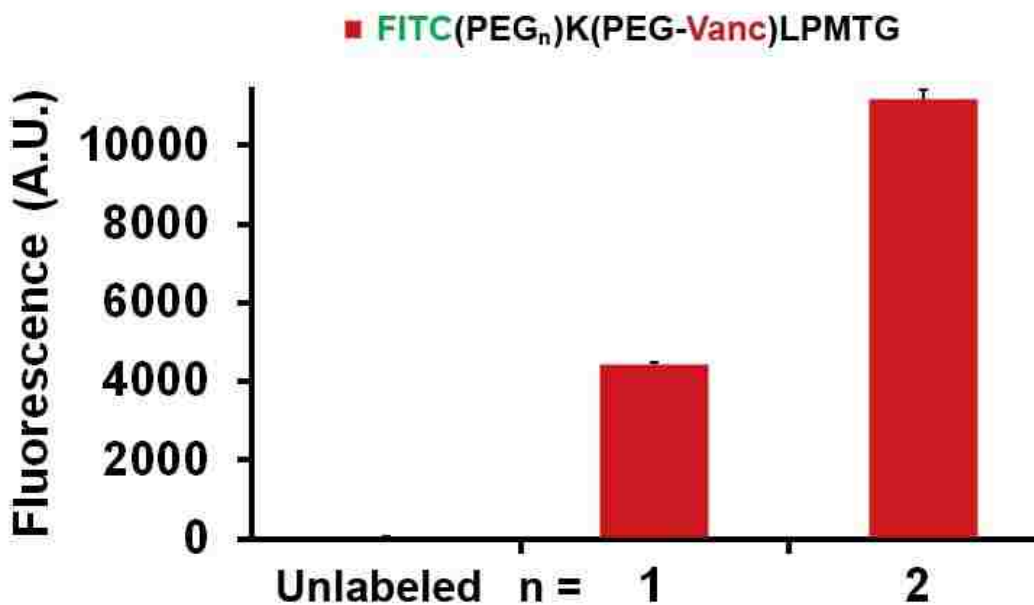


Figure 3.10 Vancomycin-conjugated SrtA Recognition Peptide Incorporation in *S. aureus*. Flow cytometry analysis of *S. aureus* cells incubated overnight in LB supplemented with panel of fluorescent conjugates at 5 μ M. Data are represented as mean + SD (n = 3).

We believe this incorporation suggests a specific process of incorporation by Srt A, and therefore, should only label Gram – positive bacteria where Srt A is heavily expressed. To test this, we incubated 2PEG1Vanc with several different bacteria of varying Srt A expression levels. After overnight incubation, the bacteria were washed and fluorescence was quantified via flow cytometry. As evident from the fluorescence levels, 2PEG1Vanc is incorporated into *S. aureus* to the greatest extent (Figure 3.11).

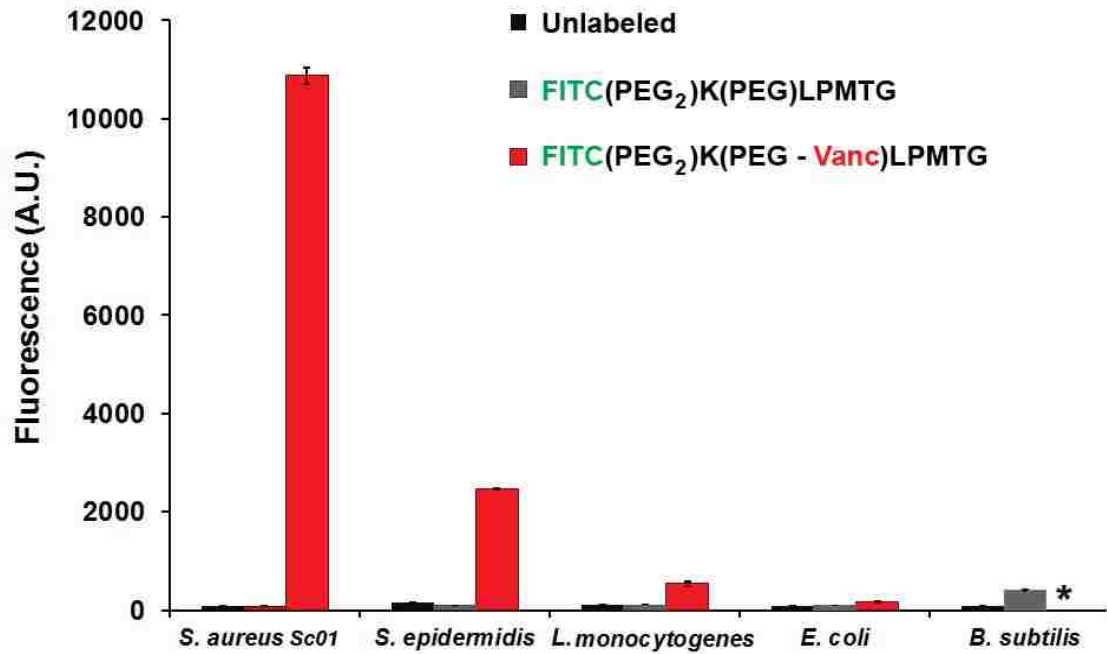


Figure 3.11 Vancomycin-conjugated SrtA Recognition Peptide Incorporation in Various Bacterial Strains. Flow cytometry analysis of bacterial cells incubated overnight in LB supplemented with FITC-2PEG1 or FITC-2PEG1Vanc at 5 μ M. Data are represented as mean + SD (n = 3).

As expected, the Gram-negative *E. coli* failed to incorporate the construct. *Listeria monocytogenes* displayed low incorporation levels, as the bacteria boasts a high expression of sortase B over sortase A.¹⁶ *S. epidermidis* rely on Srt A-mediated covalent modification and non-covalent interactions with surface polymers such as teichoic acids to decorated their cell surface.^{17,18} As such, *S. epidermidis* displayed the second highest fluorescence levels, depicting mild incorporation. Lastly, *B. subtilis* failed to grow under the pressure of 5 μ M FITC-2PEG1Vanc. This is due to the high toxicity of vancomycin towards *B. subtilis*. As seen in Figure 3.12, the minimal inhibitory concentration (MIC) of vancomycin is 0.39 μ g / mL (0.27 μ M) in *B. subtilis*.

Toxicity of Vancomycin in Gram-positive Bacteria

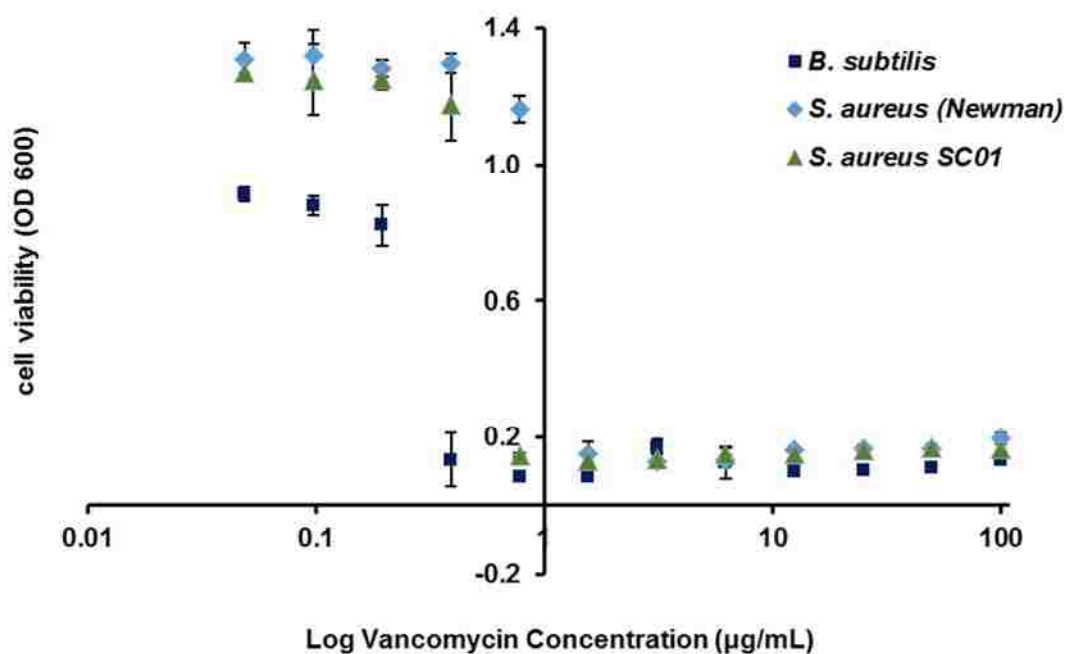


Figure 3.12 Toxicity of Vancomycin in Gram-positive Bacteria. MIC determinations were performed in cation-adjusted Mueller-Hinton Broth (CaMHB). The MIC was defined as the lowest vancomycin concentration at which visible growth was inhibited following 18 h incubation at 37 °C. Data are represented as mean + SD (n = 3).

As this data shows selective labeling of *S. aureus*, it favorably compliments the use of the construct as a recruitment tool for the host immune system. Moreover, the increased length between the fluorophore and the rest of construct favorably compliments antibody recruitment to the bacterial cell surface since the antigen location requires exposure to the extracellular space. In order to use this technique for antibody recruitment, we want to ensure that the peptide becomes incorporated throughout the peptidoglycan not just at the site of the target of vancomycin. Vancomycin accumulates preferentially at the regions of cell division/growth (concentrated pools of Lipid II molecules). If that is the case, then only dividing cells would be labeled with the peptide

since there is an accumulation of Lipid II during bacterial growth. If vancomycin is solely present to bring the peptide closer to sortase A and then the enzyme incorporates it into the peptidoglycan, as we assume, then the peptide should be uniform through-out the peptidoglycan surface of the bacteria. Using confocal microscopy, cells were imaged during two different growth phases: exponential and stationary phase. *S. aureus* (OD 6.0) was incubated with fluorescently-labeled 2PEG1Vanc for 15 min and 4 h. After allotted time, cells were washed, fixed and analyzed via fluorescence microscopy. We observed septal fluorescence and fluorescence of the bacterial surface after the 15 min incubation time (Figure 3.13, top). This is attributed to high concentration of Lipid II during the growth phase. However, after 4 h the fluorescence can be seen through-out the surface, consistent with SrtA incorporation of the fluorescent construct into the peptidoglycan (Figure 3.13, bottom). These results demonstrate the selectivity for *S. aureus* and the uniform display of the construct over the surface of the bacteria. In exploiting this selectivity, we sought to conjugate an epitope to the peptide, in order to potentially generate a narrow-spectrum immuno-therapy technique for *S. aureus*.

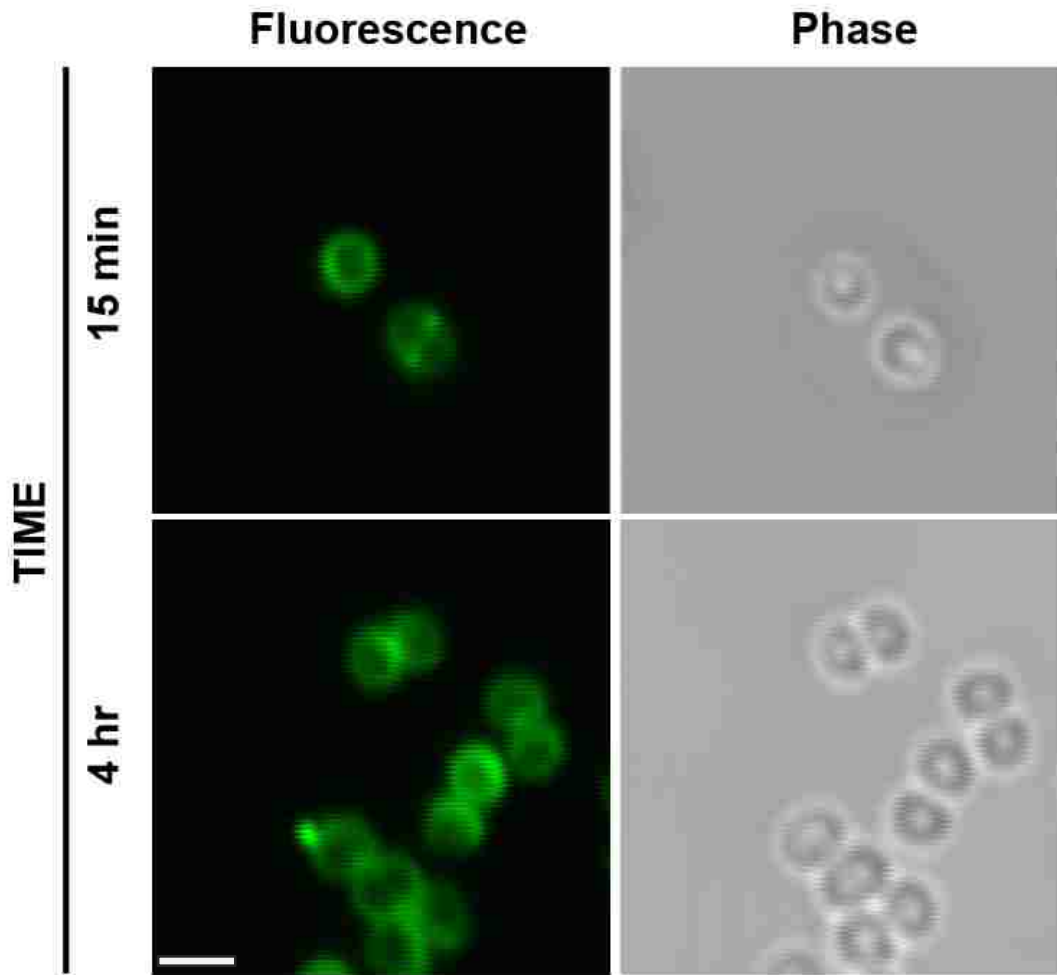


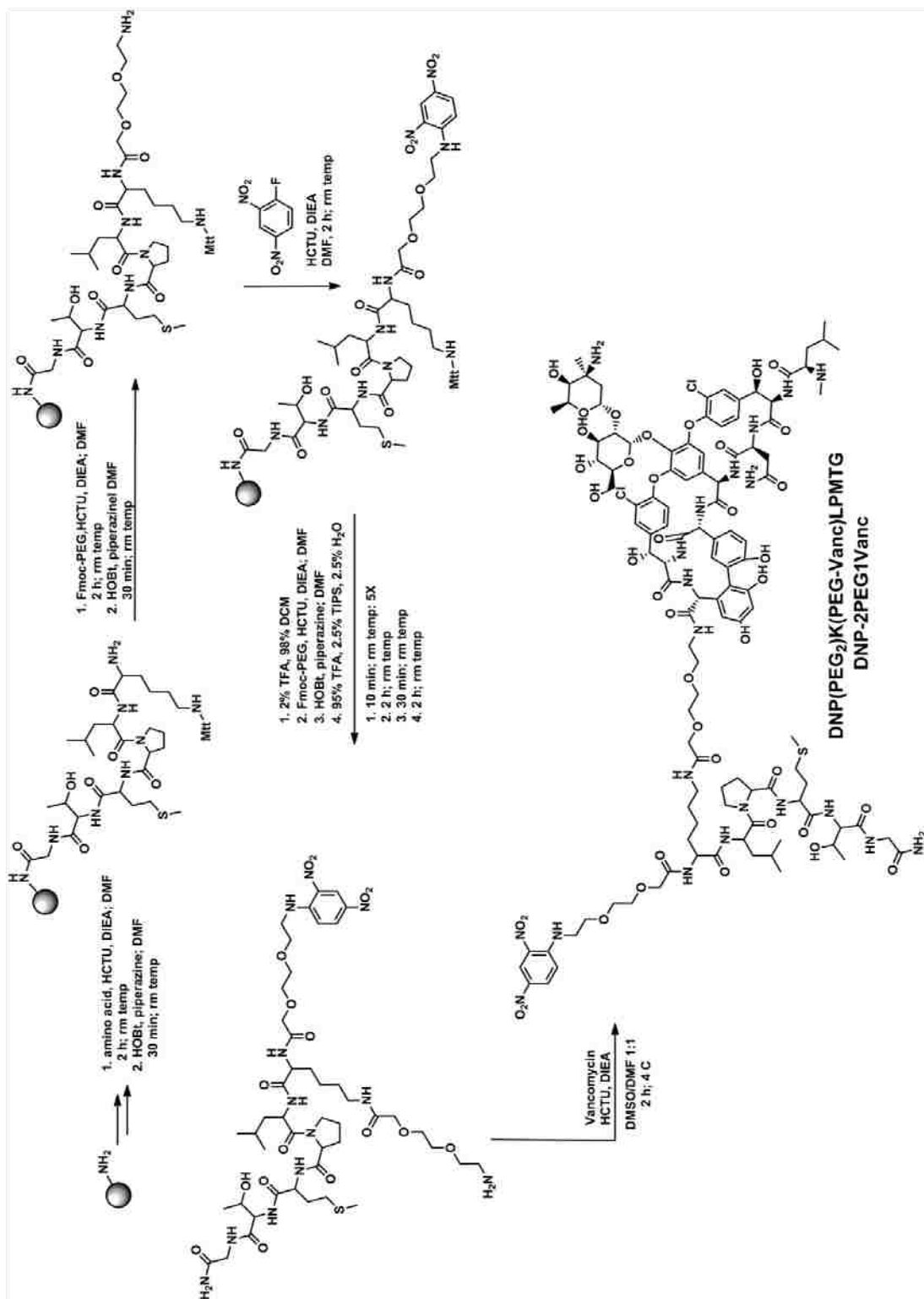
Figure 3.13 DIC and Fluorescent Microscopy Image of FITC-2PEG1Vanc Labeled *S. aureus*. Log phase *S. aureus* were incubated in LB supplemented with 5 μ M FITC-2PEG1Vanc for 15 min (top) or 4 h (bottom) at 37 °C. Cells were washed and imaged. Scale bar represents 1 μ m.

3.3.4 DNP-Conjugate Mediated Opsonization of *S. aureus*

The effectiveness of these constructs as an antibody recruitment facilitator was assessed by replacing the fluorophore with an immune stimulant epitope. To accomplish this, we utilized 2,4-dinitrophenol (DNP), chosen for the relatively high concentration of anti-DNP antibodies in human serum.¹⁹ Minding the length requirements determined in the previous labeling studies, we synthesized a DNP- displaying construct (Scheme 3.3).

We synthesized, DNP(PEG₂)K(PEG-Vanc)LPMTG (DNP-2PEG1Vanc), with the anticipation that SrtA would be able to recognize and incorporate it into the peptidoglycan, as with the FITC-labeled peptides. For this set of experiments, we utilized a mutant strain of *S. aureus* (Wood strain), in which endogenous protein A is knocked out. Protein A, a surface protein anchored to the cell surface by SrtA, binds to the Fc terminus of mammalian immunoglobulins in a nonimmune fashion, causing decoration of the staphylococcal surface with antibody.^{20,21} Protein A is the bacteria's defense against the immune system. For our experiments since the recruitment efficiency is quantified by fluorescence the presence of protein A would increase background fluorescence by binding to the fluorescent anti-DNP antibodies. The Wood strain was utilized in order to clearly show proof-of-concept for antibody recruitment to *S. aureus*. Additionally, we hypothesized that teichoic acid-based polyanionic polymers (wall teichoic acid and lipoteichoic acid) contained within the cell wall of *S. aureus* may serve to hinder the permeation and binding of anti-DNP antibodies to the modified peptidoglycan.^{22, 23,24} By growing the bacteria overnight in the presence of DNP-2PEG1Vanc and tunicamycin, a known wall teichoic acid inhibitor, cell surface antibody binding was greatly increased

compared to FITC-conjugated anti-DNP binding observed in previous experiments. The recruitment capability of the peptide constructs was quantified by fluorescence of FITC-labeled anti-DNP on the surface of the bacteria. We observed nearly a 15-fold increase for *S. aureus* labeled with the vancomycin-conjugated peptide over *S. aureus* labeled with the non-vancomycin conjugated peptide (Figure 3.14).



Scheme 3.3 Synthesis of Vancomycin-conjugated DNP-SrtA Recognition Peptides. Peptides were synthesized using Fmoc-protected amino acids conjugated on Sieber resin. The selective deprotection of the amino side chain of lysine and coupling of Fmoc-protected PEG units was performed. After purification, the peptide was coupled to vancomycin to afford DNP-2PEG1Vanc.

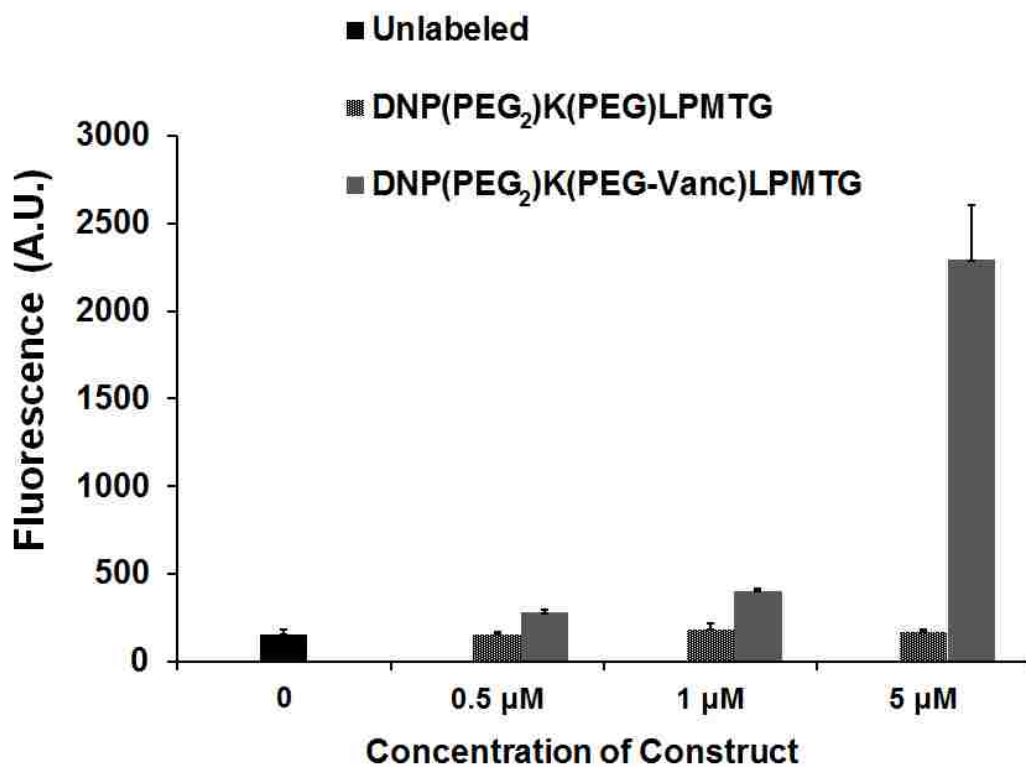


Figure 3.14 Antibody Recruitment to the Surface of *S. aureus*-Wood Strain. Cells were incubated overnight in LB supplemented with indicated concentration of specified DNP-conjugate followed by incubation with anti-DNP antibodies. Data are represented as mean + SD (n = 3).

In order to emulate a more biological representation, we sought to recruit antibodies to the surface of methicillin-resistant *S. aureus*. In order to eliminate the IgG binding contribution of protein A, we blocked the surface of the bacteria with polyclonal IgG prior to FITC-labeled anti-DNP addition. We observed a 3-fold increase for *S. aureus* treated with the vancomycin-conjugated peptide over unlabeled *S. aureus* (Figure 3.15).

Also, it is worth noting that even at 10 times the recruitment concentration (50 μM) of DNP-2PEG1Vanc, we observed marginal bacterial growth inhibition (Figure 3.16).

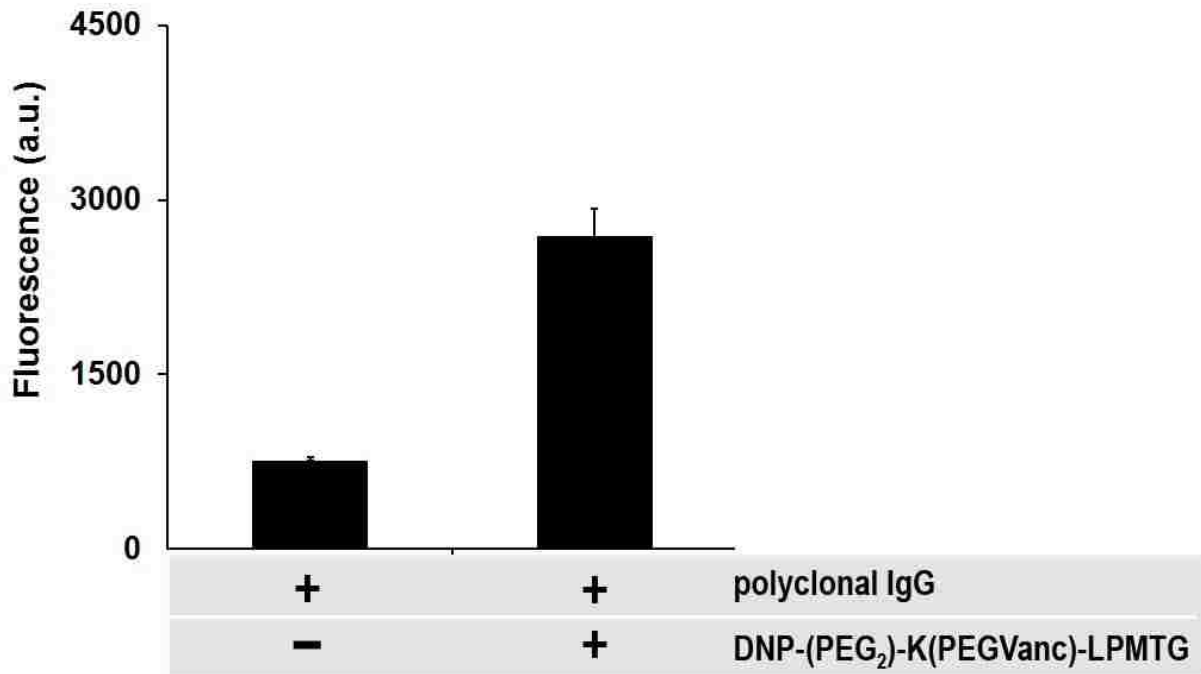


Figure 3.15 Antibody Recruitment to the Surface of *S. aureus* Sc01. Cells were incubated overnight in LB supplemented with 5 μM of DNP-2PEG1Vanc followed by incubation with polyclonal IgG. After washings, cells were incubated with anti-DNP antibodies. Data are represented as mean + SD ($n = 3$).

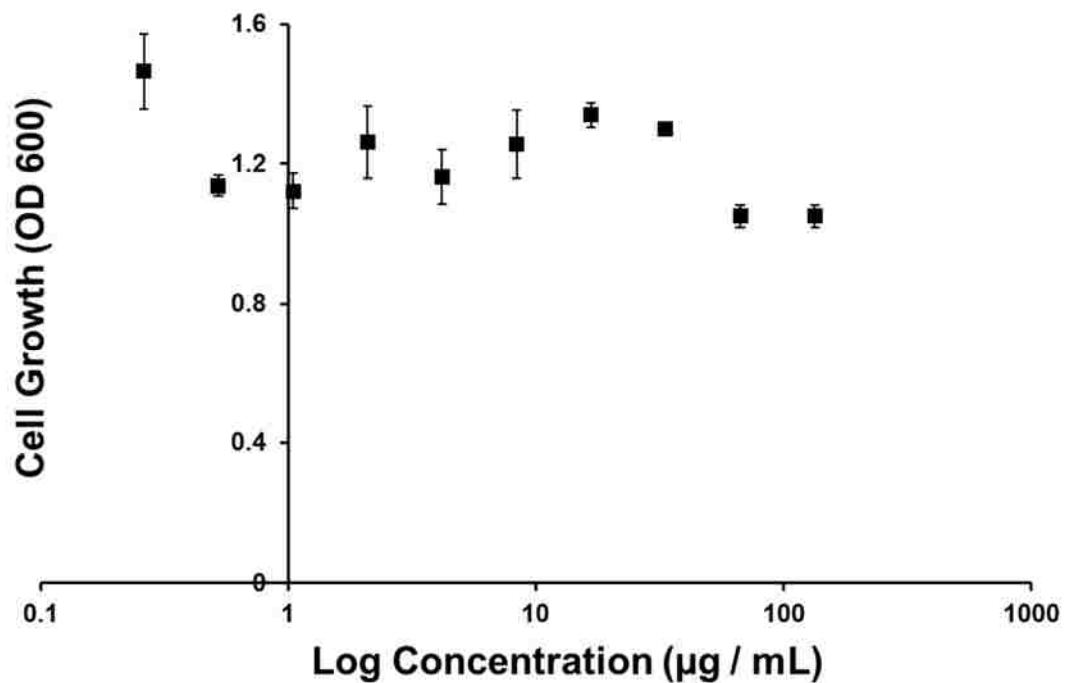


Figure 3.16 DNP-2PEG1Vanc Toxicity towards *S. aureus* Sc01. *S. aureus* Sc01 cells were incubated with varying concentrations of DNP-2PEG1Vanc for 18 h at 37 °C. Bacterial viability was evaluated by measuring the absorbance at 600 nm. Data are represented as mean + SD (n = 3).

In addition to antibody recruitment ability, we set out to assess the toxicity of DNP-2PEG1Vanc against host mammalian cells. One of the major possible advantages of using this peptide construct to target bacteria derives from the fact that it relies upon the enzymatic incorporation at the surface of the cell. No mammalian enzymes are known to exist and accept –LPXTG substrates, potentially giving this strategy high selectivity. Therefore, it is anticipated that in a living organism, administered SrtA substrates would be preferentially utilized by bacteria.

To evaluate the toxicity of DNP-2PEG1Vanc, HEK293 cells were incubated in the presence of varying concentrations of construct for 24 h and analyzed by standard viability assays (Figure 3.17). At all concentrations examined, we observed no significant loss of viability, thus highlighting an important feasibility consideration of our strategy.

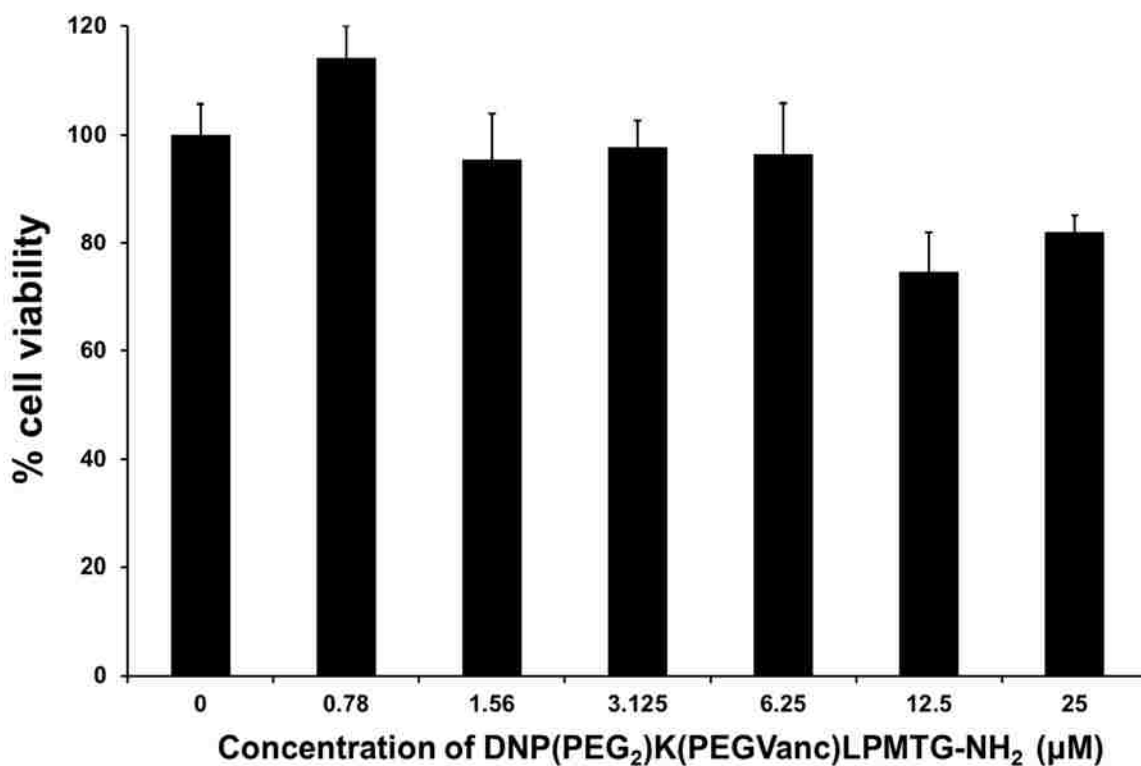


Figure 3.17 Induced Mammalian Toxicity. HEK293 cells were incubated for 24 hours in the absence or the presence of increasing concentrations of construct. Cellular viability was evaluated with MTT by measuring absorbance at 580 nm. Data are represented as mean + SD (n = 3).

3.3.5 *In vivo* Labeling of *S. aureus* Sc01 in *C. elegans*

We anticipate that this strategy can be a worthwhile model to apply synthetic immunology in *in vivo* models in the future. To test this feasibility, we first sought to determine if our lead compound, FITC-(PEG₂)K(PEG-Vanc)LPMTG, can label *S. aureus* Sc01 *in vivo*. In pursuing live labeling, we chose the model organism, *Caenorhabditis elegans* (*C. elegans*).

On the day of experiments, *C. elegans* were washed with M9 buffer and incubated with 10% LB broth and 10% *S. aureus* Sc01 in M9 buffer at room temperature for 4 h. After washing the *C. elegans* with M9 buffer, they were resuspended in M9 buffer supplemented with 10% LB broth and either 50 μ M FITC-(PEG₂)K(PEG-Vanc)LPMTG (FITC-2PEG1Vanc) or 50 μ M FITC(PEG₂)K(PEG)LPMTG (FITC-2PEG1) and incubated for an additional 30 min at room temperature. The *C. elegans* were harvested, washed, resuspended in 10 mM sodium azide and analyzed by confocal microscopy. Remarkably, we observed *in vivo* labeling of *S. aureus* Sc01 in *C. elegans* treated with FITC-2PEG1Vanc (Figure 3.18). We observed no bacterial labeling with treatment of FITC-2PEG1. To our knowledge, this is the first SrtA mediated labeling of methicillin-resistant *S. aureus* in *C. elegans*.

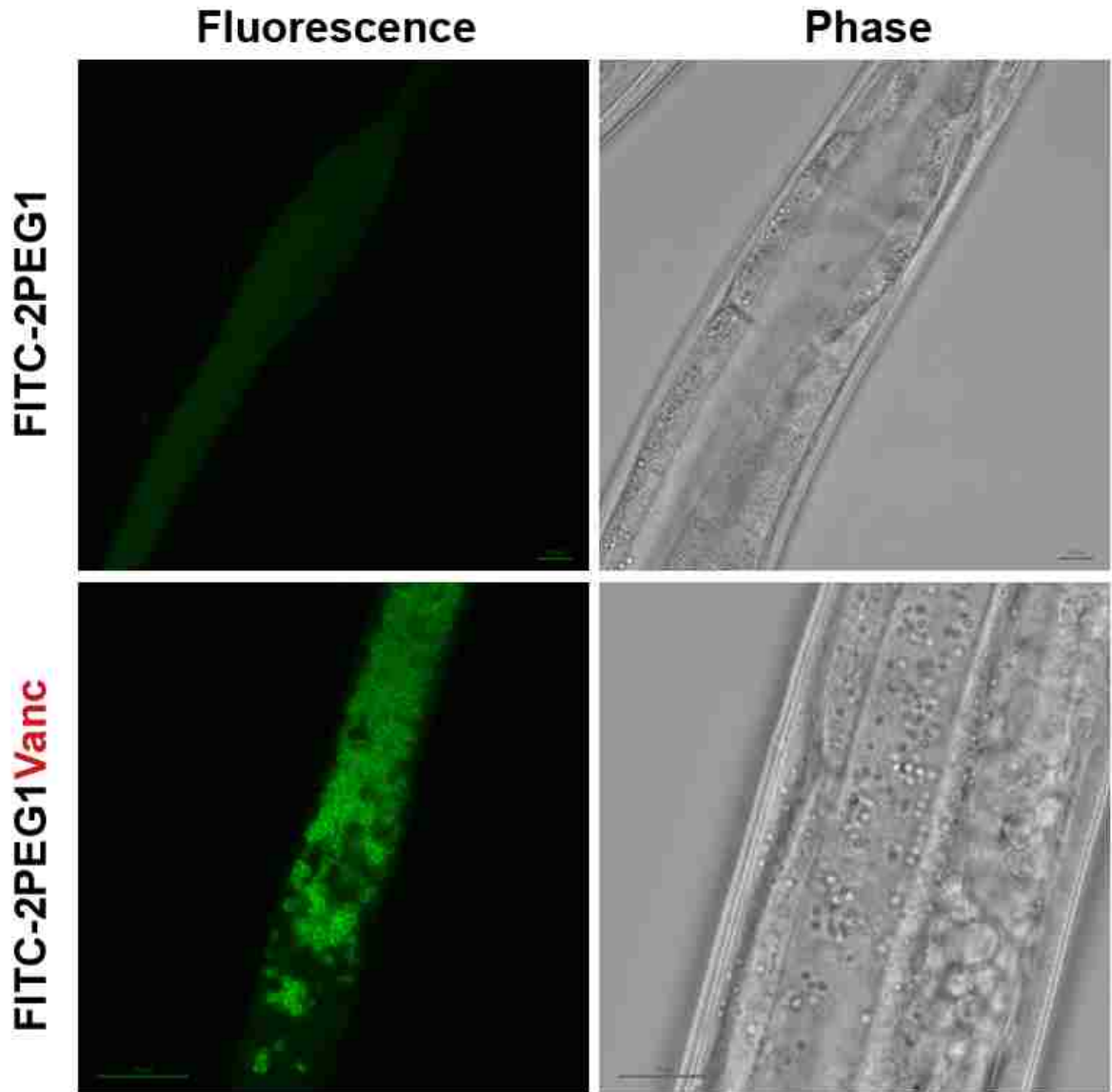


Figure 3.18 *in vivo* Labeling of *S. aureus* Sc01 in *C. elegans*. Confocal microscopy images of *S. aureus* Sc01 in *C. elegans*. *C. elegans* were infected with bacteria for 4 h at room temperature. *C. elegans* were washed to remove any bacteria not ingested. *C. elegans* were subsequently incubated with 50 μ M of either FITC-2PEG1Vanc or FITC-2PEG1 for 30 min at room temperature. After washing and treatment with 10 mM sodium azide, *C. elegans* were imaged with confocal microscopy. Scale bars = 10 μ m.

3.3.6 SrtB-mediated Incorporation in *L. monocytogenes*

Lastly, we explored whether the use of specific sortase incorporation could be expanded to other sortases present in other bacteria. Whereas SrtA acts on most of the proteins in the peptidoglycan fraction, sortase B (SrtB) appears to target minor amounts of surface polypeptides. Motifs recognized by SrtB are defined by the consensus sequence, -NXZTN, where X can be any amino acid and Z typically lends to a charged amino acid.¹⁶ Noteworthy, the sorting motif recognized by SrtB has been experimentally tested only with the surface protein IsdC involved in iron acquisition. IsdC of *S. aureus* and *Bacillus anthracis* are recognized by SrtB at NPQTN and NPKTG motifs, respectively.^{25, 26} Differences in sequence motif are dependent on the organism/substrate with the aforementioned exceptions, experimental data supporting the recognition of other sorting motifs are lacking.

Listeria monocytogenes, a ubiquitous food-borne Gram-positive bacterium, interacts with host cells through a number of surface proteins to induce pathogenesis of listeriosis. *L. monocytogenes* contains and utilizes both, SrtA and SrtB. Mariscotti et al. reported elegant work in identifying the motifs recognized by SrtB of *L. monocytogenes* and unveiled the unique capacity of *L. monocytogenes* SrtB for recognizing a sorting motif lacking the invariant proline at position (2), exemplified by sequence, -NAKTN.¹⁶

We constructed a FITC-conjugated SrtB recognition peptide and incubated *L. monocytogenes* overnight in medium supplemented with FITC(PEG)NAKTN. After analysis, we observed approximately a 30-fold increase in surface labeling in bacteria exposed to 1 mM FITC(PEG)NAKTN over unlabeled bacteria (Figure 3.20).

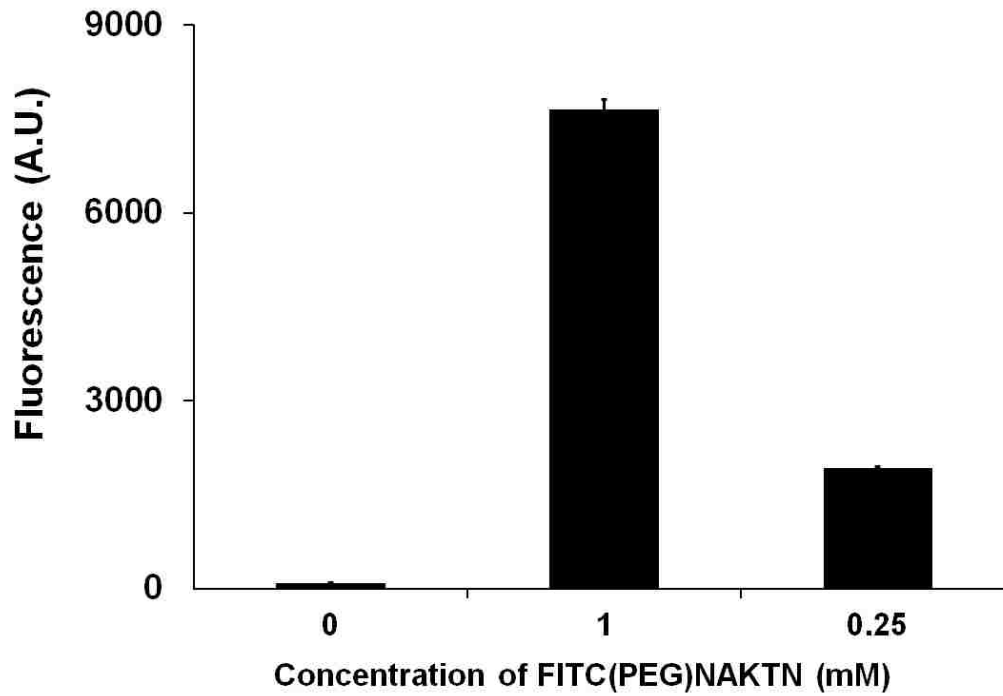


Figure 3.19 SrtB-mediated Fluorescent Peptide Incorporation in *Listeria monocytogenes*. Flow cytometry analysis of *L. monocytogenes* cells incubated overnight in LB supplemented with FITC(PEG)NAKTN at designated concentrations. Data are represented as mean + SD, (n = 3).

From this data, we anticipate that selective tagging of *L. monocytogenes* through SrtB mediated incorporation can be utilized as another bacterial immunotherapy technique.

3.4 CONCLUSION

The utilization of immunomodulatory strategies for combating pathogenic bacterial infections represents an attractive alternative to traditional antibiotic therapeutics. In this strategy, we show specific and selective targeting of methicillin-resistant *S. aureus* for clearance by the host immune system. This technique exploits the SrtA mediated incorporation of vancomycin-conjugated peptides. We show that a panel of fluorescently labeled vancomycin-conjugated SrtA recognition peptides is readily incorporated into the peptidoglycan of *S. aureus* within 15 min of treatment. From these studies, we empirically observed peptidoglycan incorporation dependent on peptide linker length. We hypothesize that this length restriction arises from the distance between the sortase A enzyme and the vancomycin binding site, Lipid II. We identified that FITC-(PEG₂)K(PEG-Vanc)LPMTG is the optimal construct for efficient selective incorporation into the cell wall *S. aureus*, while achieving minimal incorporation in *S. epidermidis*, and achieving marginal to no incorporation in *L. monocytogenes*, *E. coli*, and *B. subtilis*.

We show that DNP(PEG₂)K(PEG-Vanc)LPMTG is readily incorporated into the peptidoglycan and permits the recruitment of anti-DNP antibodies to the cell surface of methicillin-sensitive *S. aureus* and methicillin-resistant *S. aureus*. Furthermore, we show, for the first time, the successful SrtA mediated labeling of methicillin-resistant *S. aureus* in *C. elegans*.

Through these studies, we illustrate a strategy that has the potential to be an effective therapy against bacterial infections caused by *S. aureus*. We anticipate that the unique metabolic labeling process of this strategy may reduce the potential for the emergence of resistance. *S. aureus* bacteria rely on SrtA to metabolically incorporate

almost 20 different sortase substrates, necessary for cellular evasion, colonization, and consequently, pathogenicity. By employing this essential method of incorporation, the chance of rapid bacterial resistance is not expected. Moreover, the use of SrtA mediated incorporation significantly limits this strategy to *S. aureus*, making this an appealing platform for narrow-spectrum bacterial immunotherapy.

3.5 REFERENCES

1. Oka, T.; Hashizume, K.; Fujita, H., Inhibition of peptidoglycan transpeptidase by beta-lactam antibiotics: structure-activity relationships. *J Antibiot (Tokyo)* **1980**, *33* (11), 1357-62.
2. van Heijenoort, J., Recent advances in the formation of the bacterial peptidoglycan monomer unit. *Nat Prod Rep* **2001**, *18* (5), 503-19.
3. Marraffini, L. A.; DeDent, A. C.; Schneewind, O., Sortases and the Art of Anchoring Proteins to the Envelopes of Gram-Positive Bacteria. *Microbiology and Molecular Biology Reviews* **2006**, *70* (1), 192-221.
4. Marraffini, L. A.; Dedent, A. C.; Schneewind, O., Sortases and the art of anchoring proteins to the envelopes of gram-positive bacteria. *Microbiol Mol Biol Rev* **2006**, *70* (1), 192-221.
5. Foster, T. J.; Höök, M., Surface protein adhesins of Staphylococcus aureus. *Trends in Microbiology* **1998**, *6* (12), 484-488.
6. Hendrickx, A. P.; Budzik, J. M.; Oh, S. Y.; Schneewind, O., Architects at the bacterial surface - sortases and the assembly of pili with isopeptide bonds. *Nat Rev Microbiol* **2011**, *9* (3), 166-76.
7. Kruger, R. G.; Otvos, B.; Frankel, B. A.; Bentley, M.; Dostal, P.; McCafferty, D. G., Analysis of the substrate specificity of the Staphylococcus aureus sortase transpeptidase SrtA. *Biochemistry* **2004**, *43* (6), 1541-51.
8. Nelson, J. W.; Chamesian, A. G.; McEnaney, P. J.; Murelli, R. P.; Kazmiercak, B. I.; Spiegel, D. A., A Biosynthetic Strategy for Re-engineering the Staphylococcus aureus Cell Wall with Non-native Small Molecules. *ACS Chemical Biology* **2010**, *5* (12), 1147-1155.
9. Gautam, S.; Kim, T.; Lester, E.; Deep, D.; Spiegel, D. A., Wall teichoic acids prevent antibody binding to epitopes within the cell wall of Staphylococcus aureus. *ACS Chemical Biology* **2016**, *11* (1), 25-30.
10. Hansenova Manaskova, S.; Nazmi, K.; van 't Hof, W.; van Belkum, A.; Martin, N. I.; Bikker, F. J.; van Wamel, W. J.; Veerman, E. C., Staphylococcus aureus Sortase A-Mediated Incorporation of Peptides: Effect of Peptide Modification on Incorporation. *PLoS One* **2016**, *11* (1), e0147401.
11. Boekhorst, J.; de Been, M. W. H. J.; Kleerebezem, M.; Siezen, R. J., Genome-Wide Detection and Analysis of Cell Wall-Bound Proteins with LPxTG-Like Sorting Motifs. *Journal of Bacteriology* **2005**, *187* (14), 4928-4934.
12. Pallen, M. J.; Lam, A. C.; Antonio, M.; Dunbar, K., An embarrassment of sortases; a richness of substrates? *Trends in microbiology* *9* (3), 97-101.
13. Huang, X.; Aulabaugh, A.; Ding, W.; Kapoor, B.; Alksne, L.; Tabei, K.; Ellestad, G., Kinetic Mechanism of Staphylococcus aureus Sortase SrtA. *Biochemistry* **2003**, *42* (38), 11307-11315.
14. Boger, D. L.; Miyazaki, S.; Loiseleur, O.; Beresis, R. T.; Castle, S. L.; Wu, J. H.; Jin, Q., Thermal Atropisomerism of Aglucovancomycin Derivatives: Preparation of (M,M,M)- and (P,M,M)-Aglucovancomycins. *Journal of the American Chemical Society* **1998**, *120* (35), 8920-8926.

15. Nagarajan, R.; Schabel, A. A., Selective cleavage of vancosamine, glucose, and N-methyl-leucine from vancomycin and related antibiotics. *Journal of the Chemical Society, Chemical Communications* **1988**, (19), 1306-1307.
16. Mariscotti, J. F.; Portillo, F. G.-d.; Pucciarelli, M. G., The *Listeria monocytogenes* Sortase-B Recognizes Varied Amino Acids at Position 2 of the Sorting Motif. *Journal of Biological Chemistry* **2009**, *284* (10), 6140-6146.
17. Otto, M., *Staphylococcus epidermidis* – the “accidental” pathogen. *Nature reviews. Microbiology* **2009**, *7* (8), 555-567.
18. Navarre, W. W.; Schneewind, O., Surface Proteins of Gram-Positive Bacteria and Mechanisms of Their Targeting to the Cell Wall Envelope. *Microbiology and Molecular Biology Reviews : MMBR* **1999**, *63* (1), 174-229.
19. Jakobsche, C. E.; Parker, C. G.; Tao, R. N.; Kolesnikova, M. D.; Douglass, E. F.; Spiegel, D. A., Exploring Binding and Effector Functions of Natural Human Antibodies Using Synthetic Immunomodulators. *ACS Chemical Biology* **2013**, *8* (11), 2404-2411.
20. J., D., Crystallographic refinement and atomic models of a human Fc fragment and its complex with fragment B of protein A from *Staphylococcus aureus* at 2.9- and 2.8-Å resolution. *Biochemistry* **1981**, *20* (9), 2361-70.
21. Boyle, M. D. P.; Reis, K. J., Bacterial Fc Receptors. *Nat Biotech* **1987**, *5* (7), 697-703.
22. Brown, S.; Santa Maria, J. P.; Walker, S., Wall Teichoic Acids of Gram-Positive Bacteria. *Annual review of microbiology* **2013**, *67*, 10.1146/annurev-micro-092412-155620.
23. Swoboda, J. G.; Campbell, J.; Meredith, T. C.; Walker, S., Wall Teichoic Acid Function, Biosynthesis, and Inhibition. *Chembiochem : a European journal of chemical biology* **2010**, *11* (1), 35-45.
24. Campbell, J.; Singh, A. K.; Santa Maria, J. P.; Kim, Y.; Brown, S.; Swoboda, J. G.; Mylonakis, E.; Wilkinson, B. J.; Walker, S., Synthetic lethal compound combinations reveal a fundamental connection between wall teichoic acid and peptidoglycan biosyntheses in *Staphylococcus aureus*. *ACS chemical biology* **2011**, *6* (1), 106-116.
25. Maresso, A. W.; Chapa, T. J.; Schneewind, O., Surface Protein IsdC and Sortase B Are Required for Heme-Iron Scavenging of *Bacillus anthracis*. *Journal of Bacteriology* **2006**, *188* (23), 8145-8152.
26. Mazmanian, S. K.; Ton-That, H.; Su, K.; Schneewind, O., An iron-regulated sortase anchors a class of surface protein during *Staphylococcus aureus* pathogenesis. *Proceedings of the National Academy of Sciences* **2002**, *99* (4), 2293-2298.

Chapter 4

Synthetic Immuno-Attractants against Gram-Negative Pathogens

4.1 ABSTRACT

The number of drug-resistant bacterial infections has been rapidly rising and may soon approach epidemic levels. For these reasons, there is an urgent need for novel antimicrobial modalities to be developed. The emergence of multi-resistant bacteria that are part of the ESKAPE (*Enterococcus faecium*, *Staphylococcus aureus*, *Klebsiella pneumoniae*, *Acinetobacter baumannii*, *Pseudomonas aeruginosa*, and *Enterobacter species*) group of pathogens is a particularly acute challenge to the healthcare system. ESKAPE pathogens are the leading cause of nosocomial infections worldwide. This chapter will discuss our efforts in re-engaging the immune system towards Gram-negative pathogenic bacteria *via* synthetic molecules that remodel bacterial cell surfaces with immune cell attractants. More specifically, we built conjugates composed of polymyxin B, an antibiotic that inherently homes to bacterial cells surfaces, linked to antigenic epitopes that engage endogenous antibodies. Given the inherent antimicrobial activity of polymyxin, we additionally showed that these agents display dual activities against bacteria. By leveraging the power of the immune system in clearing pathogens, this new class of molecules was shown to uniquely target Gram-negative bacteria and, additionally, potentiate existing FDA-approved antibiotics. We hope to establish this approach as a viable treatment option and further refine this methodology to address the clinical challenge of Gram-negative bacterial pathogens.

4.2 INTRODUCTION

The rapid surge in drug-resistant bacterial infections has now become one of the primary public health crises of the 21st century, consequently, driving a renewed effort to find antibiotics with unique mechanisms of action. As mentioned in Chapter 1, the World Health Organization considers Gram-negative pathogens high priority target areas. Every year in the United States alone, over two million people are afflicted with bacterial infections resistant to FDA-approved antibiotics. Most alarming is the emergence of multidrug Gram-negative pathogenic bacteria, including strains that are resistant to all currently available antibiotics.³ The four most problematic infections are caused by drug resistant *Klebsiella pneumoniae* (*K. pneumoniae*), *Acinetobacter baumannii* (*A. baumannii*), *Pseudomonas aeruginosa* (*P. aeruginosa*), and *Escherichia coli* (*E. coli*). The paucity of drugs against these pathogens means that we run the risk of entering a post-antibiotic era.

Compared to Gram-positive organisms, Gram-negative bacteria possess an outer membrane (OM) that lies to the exterior of the cytoplasmic membrane bilayer. The additional layer serves as a formidable barrier to permeation of small molecule antibiotics and larger biomacromolecules.⁴ Partly for these reasons, there are currently fewer antibiotics that are active against Gram-negative bacteria. As mentioned in Chapter 3, bacterial cell surfaces play crucial roles in the normal physiology and pathogenicity (in the case of pathogenic bacteria) of these organisms. Proteins and structural polymers at the cell surface are actively involved in bacterial adhesion, colonization, and engagement with the host immune cells.^{5,6} We envisioned a molecule that successfully targeted one of the structural polymers on the surface of Gram-negative bacteria.

We expanded on our recent finding that we can decorate the surface of Gram-negative bacteria using antibiotic conjugates that home to and associate with bacterial cell surfaces. Due to the vast surface area of bacterial cell surfaces and their exposure to the host organism, it is the principal bacterial structure recognized by the human immune system.

We reasoned that grafting immune cell attractant tags on bacterial cell surfaces would result in effective recruitment of immune cells. In the previous chapter, we had targeted the modification of bacterial peptidoglycan (PG) for the installation of antibody recruiting haptens. Although Gram-negative bacteria also have PG scaffolds and they are remodeled via synthetic cell wall analogs, the presence of the OM prevents any engagement with immune cells. Instead, we had to explore a different mode of surface modification. Gram-negative bacterial cells generally possess negatively charged surfaces due to the high abundance of lipopolysaccharide (LPS). Lipid A, an essential lipid component of LPS, is composed of a phosphorylated diglucosamine unit connected to lipid chains (Figure 4.1).

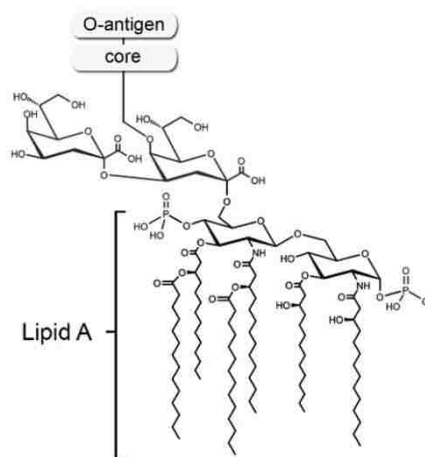


Figure 4.1 Structure of LPS.

The naturally occurring lipopeptide antibiotic, polymyxin B (PMB), is unique in the ability to associate with Lipid A with high affinity and specificity. PMBs are comprised of hydrophobic and hydrophilic domains, both of which are pivotal for their antibacterial activity. The core PMB scaffold consists of a cyclic hexapeptide linked to a

linear tripeptide with an N-terminal fatty acyl tail (Figure 4.2). Five L- α,γ -diaminobutyric acid (Dab) residues decorate the scaffold, the primary amines of which are positively

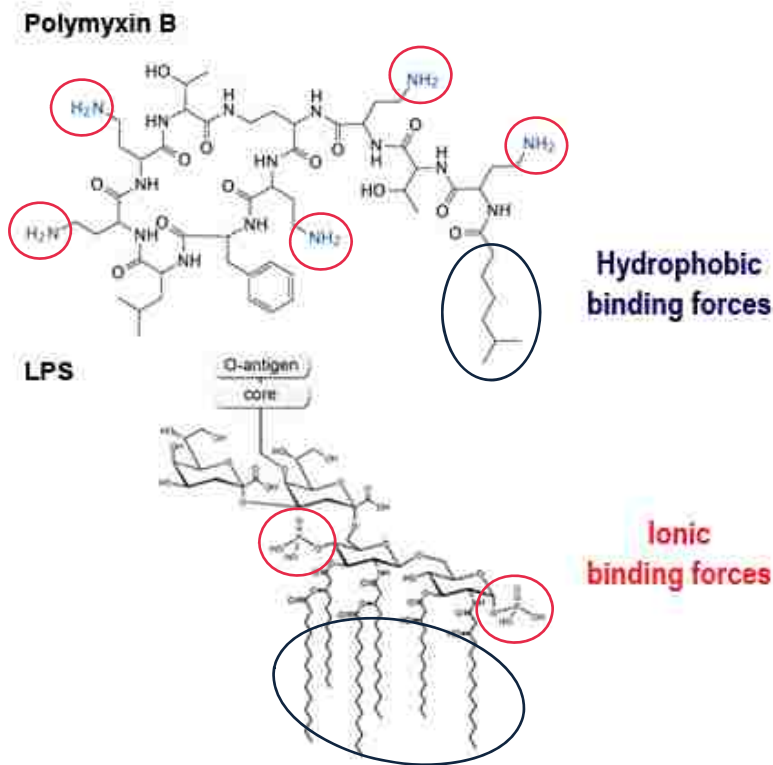


Figure 4.2 Representation of PMB and LPS Binding. Polymyxin B and LPS bind through ionic forces and strong hydrophobic forces.

charged at physiological pH (7.4). Two hydrophobic residues in positions 6 and 7 of the cyclic hexapeptide form an intermediary hydrophobic segment that breaks the succession of cationic Dab residues. Specifically, the cationic cyclic peptide binds to negatively

charged Lipid A on bacterial OMs and the aliphatic fatty acid tail anchors into the membrane (Figure 4.2).⁷ PMB is thought to impart its antibacterial activity by binding to the OM surface and destabilizing the OM layer – although the exact mechanism has yet to be fully elucidated.^{8,9} These features made PMB an attractive target for our surface remodeling strategy, as both of these structural components were integrated into our design to establish the optimum combination of inherent antimicrobial activity in synergy with immunomodulation.

Herein, we describe a strategy aimed at targeting bacterial cells for destruction via small molecule conjugates that specifically home to Gram-negative bacterial cell surfaces. By exploiting surface exposed features (e.g., Lipid A) unique to Gram-negative bacteria, we hypothesized that heterobifunctional agents composed of Polymyxin B (PMB) would lead to the specific surface presentation with epitopes that engage various components of the immune system (e.g., antibodies and primary immune cells). The use of surface homing agents that inherently possess antimicrobial activity represents a significant advance due to the potential synergism between (1) the direct bactericidal activity of the homing beacon and (2) the engagement of immune system. Combined, we showed that these agents effectively target Gram-negative pathogen in two distinct ways with minimal toxicity towards host cells.

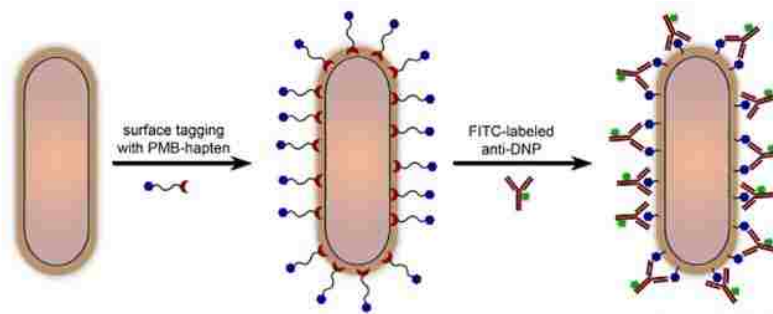


Figure 4.3 Schematic Representation of Gram-negative Bacterial Immunotherapy. Gram-negative bacteria are incubated with PMB-hapten conjugates. Following the labeling, the binding of anti-DNP IgG antibodies leads to the eventual clearance by the immune system.

4.3 RESULTS AND DISCUSSION

4.3.1 Fluorescent Labeling of *E. coli* using PMBN-FITC

In collaboration with the Regen Group, they synthesized a fragment of PMB known as PMB nonapeptide (PMBN) (Figure 4.4). PMBN is devoid of the membrane-disrupting fatty acid tail but, critically, retains the cyclic heptapeptide responsible for association to Lipid A.^{10, 11} The smaller PMBN fragment has attenuated antimicrobial activity, which can be useful in isolating the effect of surface-homing in our strategy. We tested the toxicity of PMBN to *E. coli* and determined the MIC to be 40 $\mu\text{g/mL}$.

We generated a fluorescent PMBN by coupling fluorescein to (BOC)-protected PMBN (Scheme 4.1). After purification and removal of the protecting groups, the construct was incubated overnight with *E. coli* to assess its ability to label the cell surface. *E. coli* was grown in LB supplemented with increasing concentrations of the PMBN-FITC (0 – 200 μM). The cells were harvested, washed, and analyzed via flow cytometry. By quantifying fluorescence, we observed

a roughly 30-fold increase in fluorescence for bacteria exposed to 40 μM of the construct (Figure 4.5). Concentrations of greater than 40 μM of the construct were toxic to the bacteria cells as assessed by optical density (600 nm).

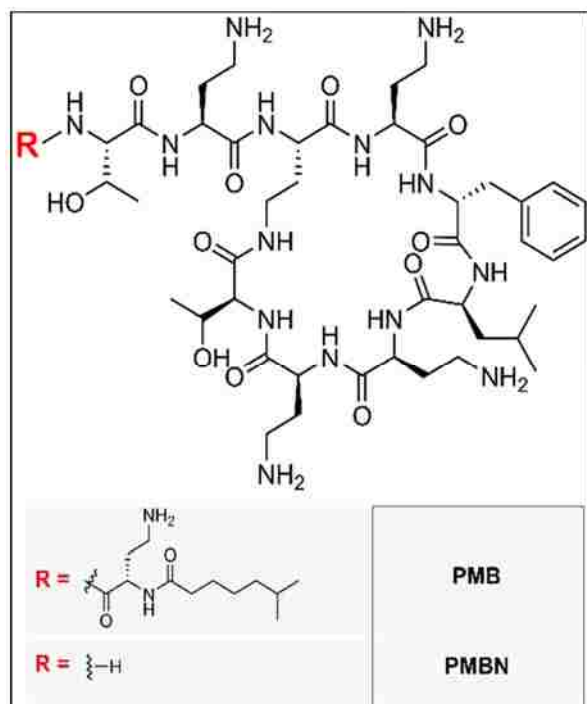
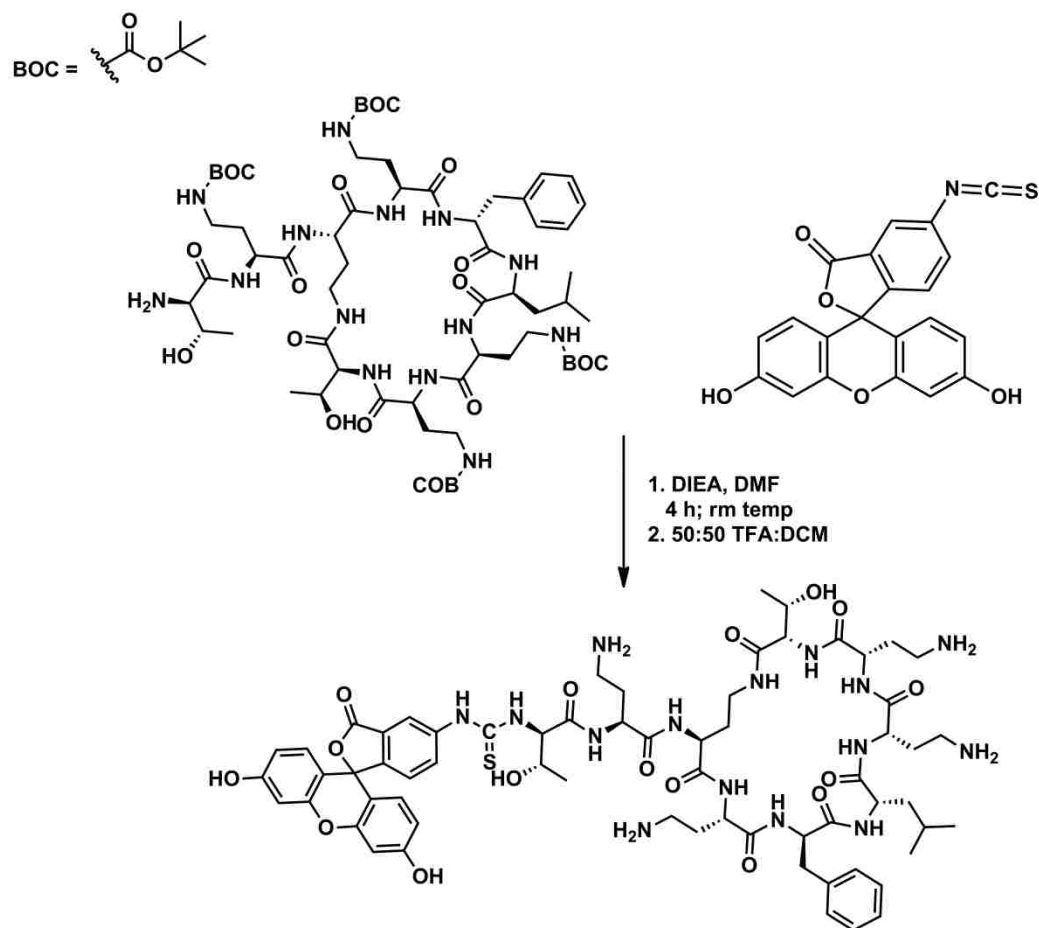


Figure 4.4 Structures of Polymyxin B and PMB-Nonapeptide (PMBN).



Scheme 4.1 Synthesis of PMBN-FITC. (BOC)-PMBN (1 eq.) was reacted with fluorescein isothiocyanate (1.5 eq.) in DMF with *N,N*-diisopropylethylamine (DIEA) (2 eq.). After acidic treatment to remove the –BOC protecting groups, the compound was purified via normal phase

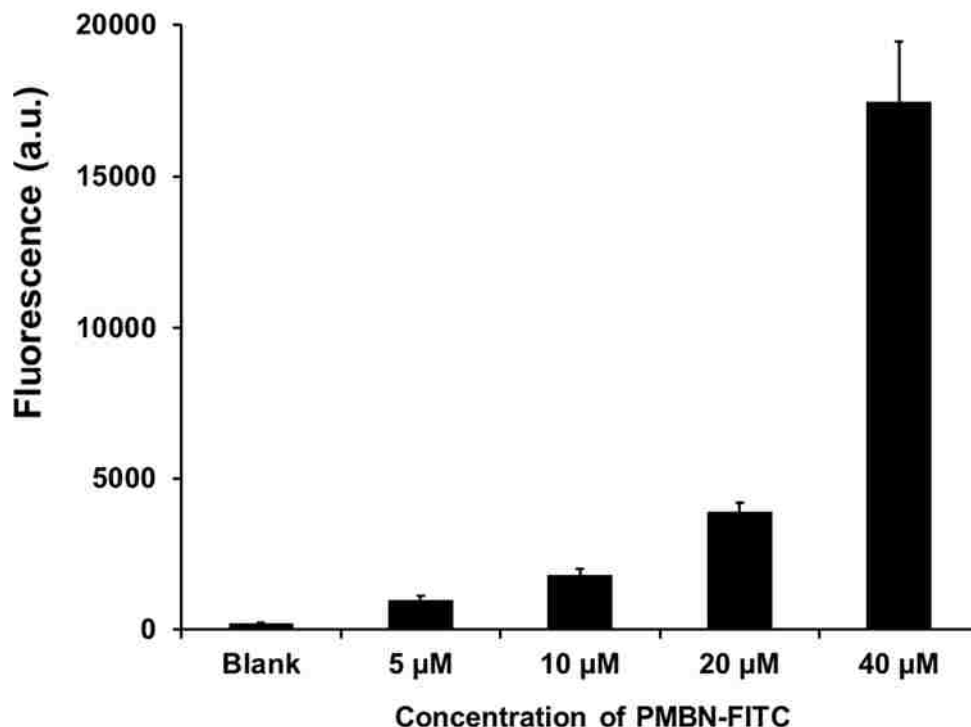


Figure 4.5 PMBN-FITC Labeling of *E. coli*. Flow cytometry analysis of *E. coli* incubated overnight in the presence of LB alone, and LB supplemented with increasing concentrations of PMBN-FITC. Data are represented as mean + SD (n = 3).

Given the nature of the interaction between PMBN and LPS on cell surfaces, which is independent of cell growth/division, we sought to establish labeling to cells in stationary phase. Bacterial cells at stationary phase display dramatically lower metabolic rates and do not undergo extensive cell growth and division.¹² A large fraction of the currently available antibiotics fail to effectively clear bacterial pathogens at stationary phase due to their reliance on processes related to cell growth and division.¹³ Therefore, developing a molecule that elicits a therapeutic effect against stationary phase bacteria would be valuable in the treatment of latent bacterial infections.

We incubated stationary phase (OD = 1.4) *E. coli* in media supplemented with 40 μ M PMBN-FITC at 37 °C. At indicated time points, the bacteria were harvested, washed, and analyzed by flow cytometry. We observed an increased in fluorescence over time, with maximum fluorescence after 2 h of incubation (Figure 4.6). After 2 h, a reduction in fluorescence is observed. This may arise from stationary phase bacteria death due to lack of nutrients.

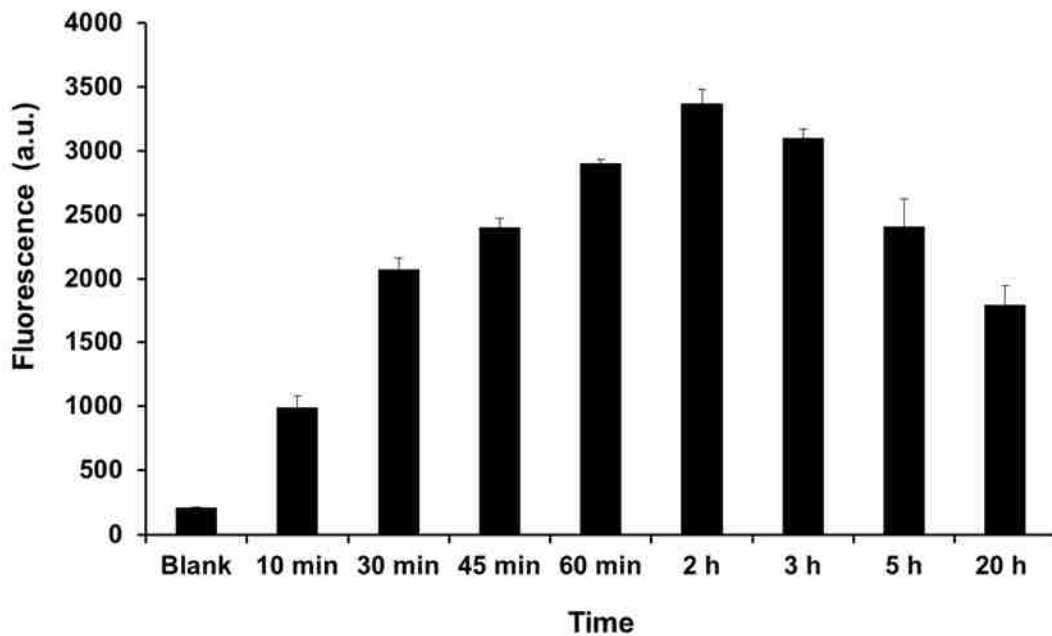


Figure 4.6 PMBN-FITC Labeling of *E. coli* over Time. Flow cytometry data of stationary phase *E. coli* incubated with 40 μ M PMBN-FITC for indicated time points in LB media. Data are represented as mean + SD (n = 3).

In further understanding how PMBN-FITC interacts with the cell surface, we sought to determine the persistence of association of the construct to the bacterial surface. Stationary phase *E. coli* was incubated with 40 μM PMBN-FITC for 2 h at 37 $^{\circ}\text{C}$. After harvesting and washing, the bacteria were resuspended in phosphate buffer saline (PBS) and the loss of fluorescence was monitored over time. We did not observe immediate dissociation of the construct from the bacterial surface (Figure 4.7).

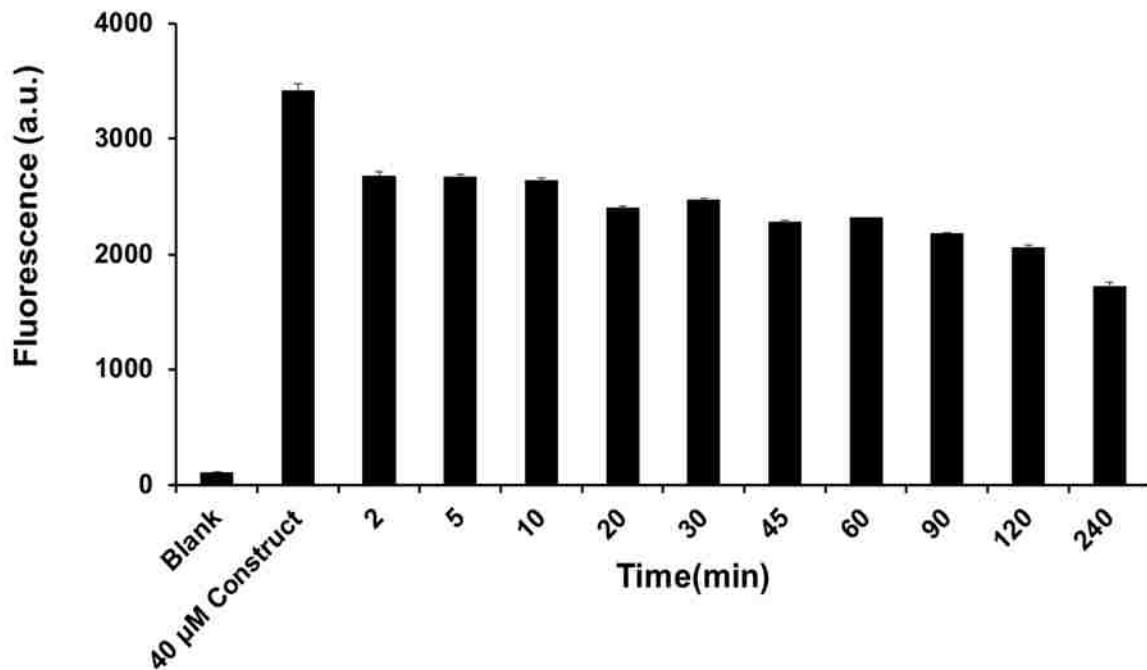


Figure 4.7 PMBN-FITC Dissociation from *E. coli* Surface. Flow cytometry data of stationary phase *E. coli* incubated with 40 μM PMBN-FITC for 2 h, then incubated in PBS for indicated time before analysis. Data are represented as mean + SD (n = 3).

Next, we explored how the addition of cations would affect the labeling ability of PMBN-FITC to the surface of the bacteria. As mentioned, polymyxin B exerts its antimicrobial activity through an electrostatic interaction of the cationic Dab residues with the negatively charged phosphate groups of lipid A of LPS. This complex formation displaces divalent cations (Ca^{2+} and Mg^{2+}) that bridge adjacent LPS molecules.^{14, 15, 16} Therefore, we expected that salt concentrated media would negatively affect the labeling efficiency of PMBN-FITC to the *E.coli* surface by competing for the negatively charged phosphate groups of lipid A.

We incubated stationary phase ($\text{OD} = 1.4$) *E. coli* in the presence of $40 \mu\text{M}$ PMBN-FITC for 2 h in medium of differing salt concentrations. We utilized Luria Broth (LB) as a control. LB is the complete growth media for *E. coli*. Mueller Hinton (MH) Broth is the broth of choice for antimicrobial susceptibility testing. It is commonly used in the micro dilution technique of assessing minimal inhibitory concentration of antibiotics and contains $11.5 \text{ mg/L Ca}^{2+}$ and 2.5 mg/L Mg^{2+} . We further supplemented Mueller Hinton (MH) Broth with additional cations, resulting in a final concentration of $21.5 \text{ mg/L Ca}^{2+}$ and $12.5 \text{ mg/L Mg}^{2+}$.

Upon fluorescent analysis, we observed the expected trend of decreased labeling efficiency with increased salt concentration (Figure 4.8). The data shows efficient PMBN-FITC labeling of *E. coli* over time when incubated with LB media. Conversely, as the concentration of calcium and magnesium increases, and the propensity for competition increases, the level of fluorescence decreases, indicating a lack of efficient labeling of the construct of the *E. coli* surface. From this data, we also observe a steady increase in fluorescence for *E. coli* incubated with the construct in LB media.

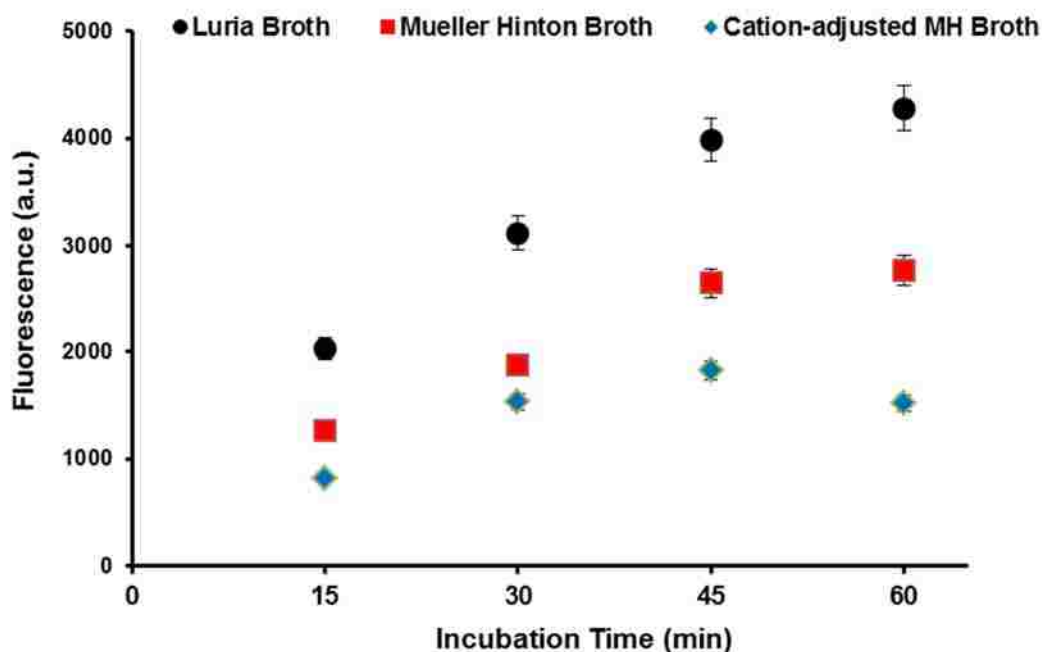


Figure 4.8 Cation Effect on PMBN-FITC Labeling of *E. coli*. Flow cytometry data of stationary phase *E. coli* incubated with 40 μ M PMBN-FITC for indicated time points in different media. Data are represented as mean + SD (n = 3).

Lastly, we visualized the labeled *E. coli* via fluorescent microscopy. We observed a uniform fluorescence signal along the cell surface (Figure 4.9). We observed heavily concentrated signal at the poles of the bacteria, a finding that is consistent with polymyxin B nonapeptide bacterial surface labeling.^{17, 18}

Taken together, we believe our modification of polymyxin B does not interrupt its ability to interact with the surface of *E. coli*. We observed PMBN-FITC labeling of the *E. coli* surface, through interaction with the negatively charged LPS. Furthermore, we show that PMBN-FITC labels stationary phase *E. coli*. As mentioned, a large fraction of the currently available antibiotics fail to effectively clear bacterial pathogens at stationary

phase due to their reliance on processes related to cell growth and division. Therefore, PMBN derivatives have heightened potential to act as an immunotherapeutic towards hard to treat bacterial infections.

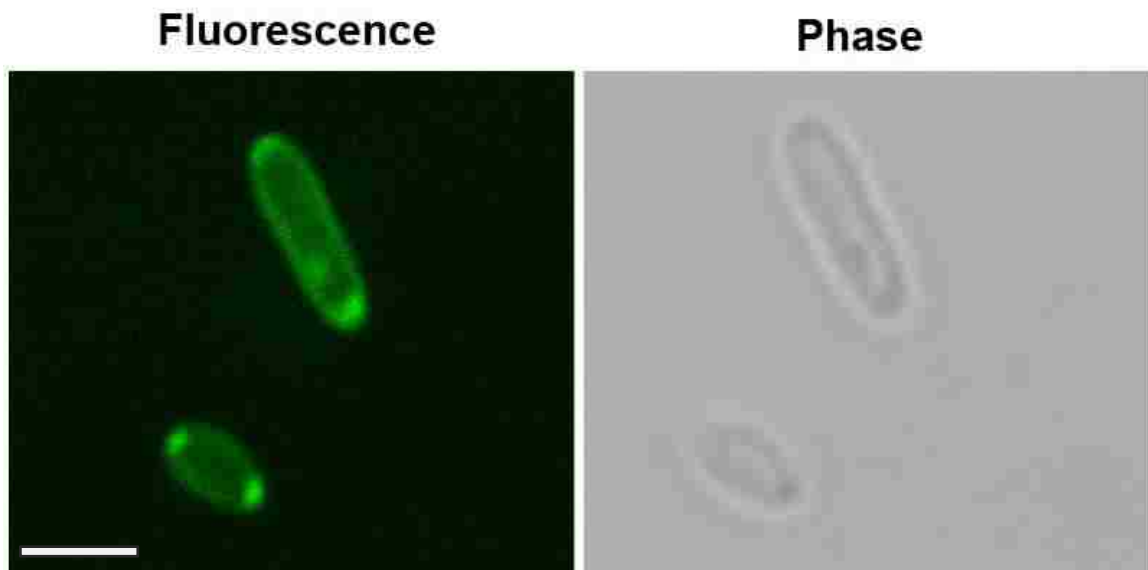


Figure 4.9 DIC and Fluorescent Microscopy Image of PMBN-FITC Labeled *E. coli*. Stationary phase *E. coli* were incubated in LB supplemented with 40 μ M PMBN-FITC for 2 h at 37 $^{\circ}$ C. Cells were washed and imaged. Scale bar represents 2

4.3.2 PMBN-DNP Mediated Opsonization of *E. coli*

The outer membrane (OM) of Gram-negative bacteria (Figure 4.10) is a unique and highly asymmetric lipid bilayer, heavily populated by proteins and other biopolymers. Composed of phospholipids in the inner leaflet and lipopolysaccharide (LPS) in the outer leaflet, the complexity and crowdedness of the OM makes it an effective barrier against the permeation of both hydrophobic and hydrophilic compounds. LPS, a complex amphiphatic molecule, consists of lipid A, a core oligosaccharide, and an O-antigen polysaccharide. The O-antigen varies in length depending to the bacteria and is comprised of oligosaccharide. It also renders additional protection from the antimicrobial action of certain antibiotics and can potentially interfere with the approach and binding of extracellular antibodies onto haptens.¹⁹

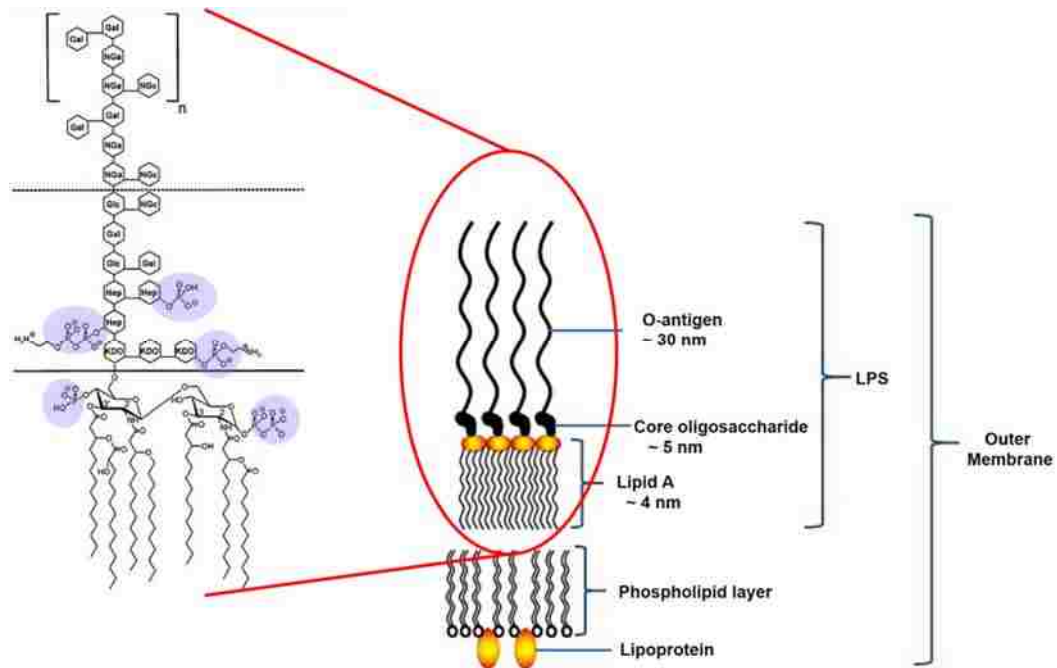


Figure 4.10 Gram-negative bacterial Outer Membrane Molecular Complexity. The LPS molecule can be divided into three main regions: Lipid A, which anchors LPS to the outer membrane, the core region, containing the majority of the functional groups, and the repeating O-antigen unit. (Left) Chemical structure of endotoxin from *E. coli* O111:B4 according to Ohno and Morrison.²

We hypothesized that the accessibility of DNP epitopes to the extracellular space could drastically effect antibody recruitment to the bacteria surface and therefore reduce immune response. Furthermore, the OMs of bacteria strains vary, in regards to the makeup of the O-antigen. We anticipated that the structure and dynamics of the conjugates would impact the interactions of PMB and LPS, exposure of DNP to the outer space, and the stability of the OMs. In designing the PMBN-DNP conjugate that could recruit endogenous antibodies, the PMBN and DNP units cannot be altered. Modification of those chemical structures can lead to poor surface homing and/or poor antibody recruitment.

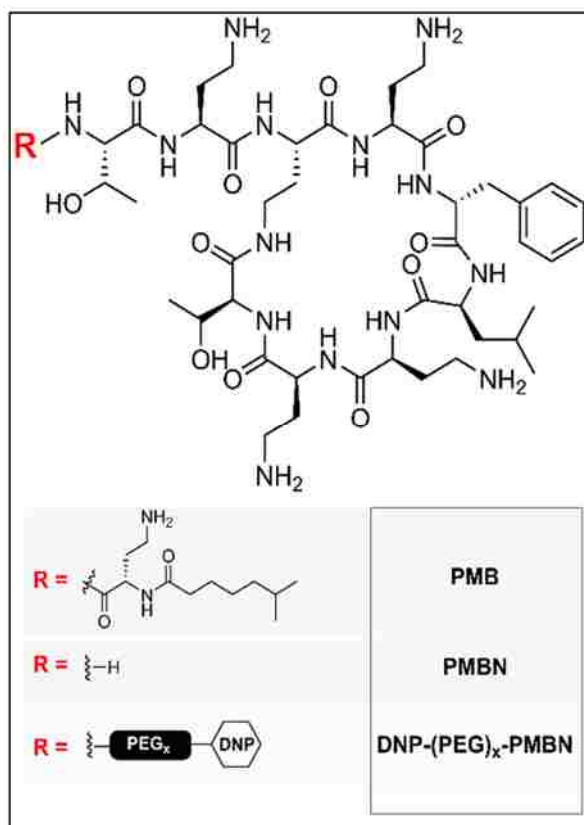
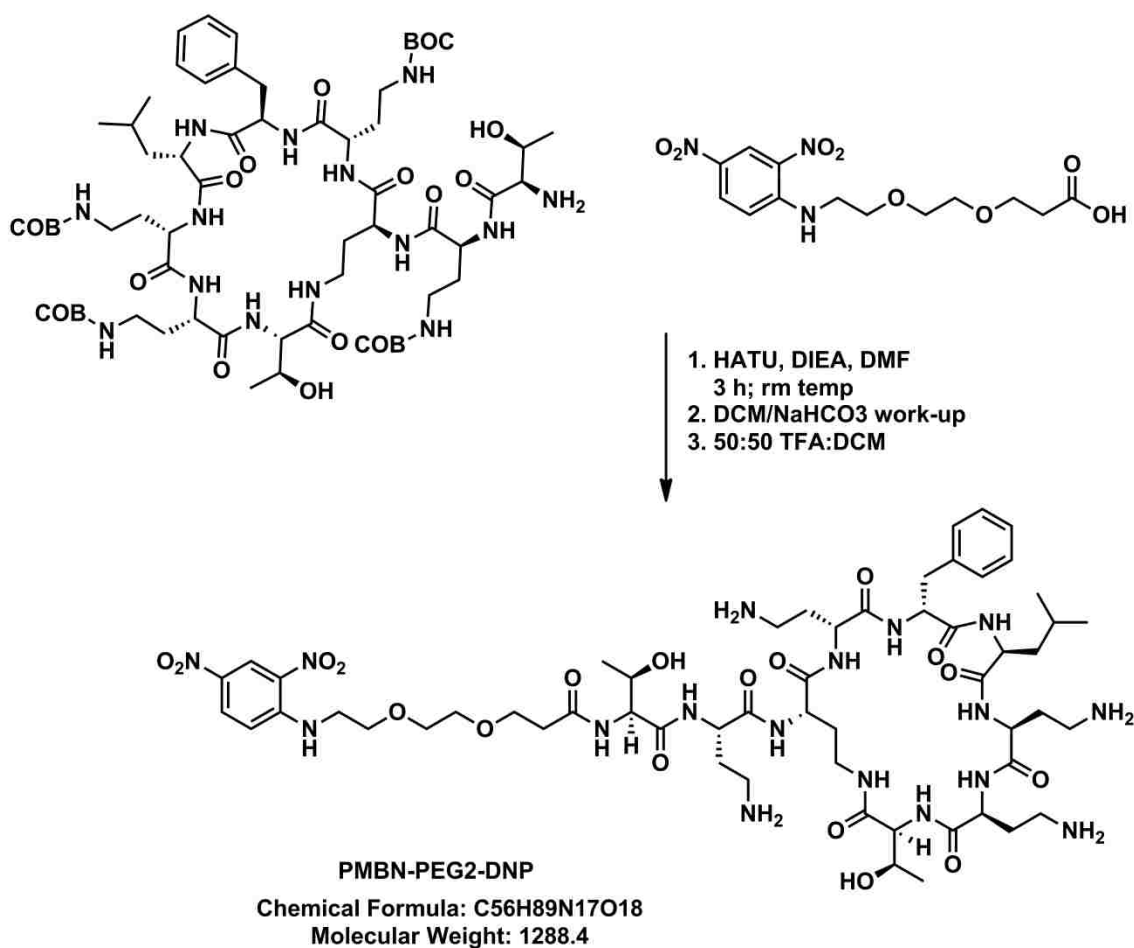
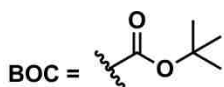


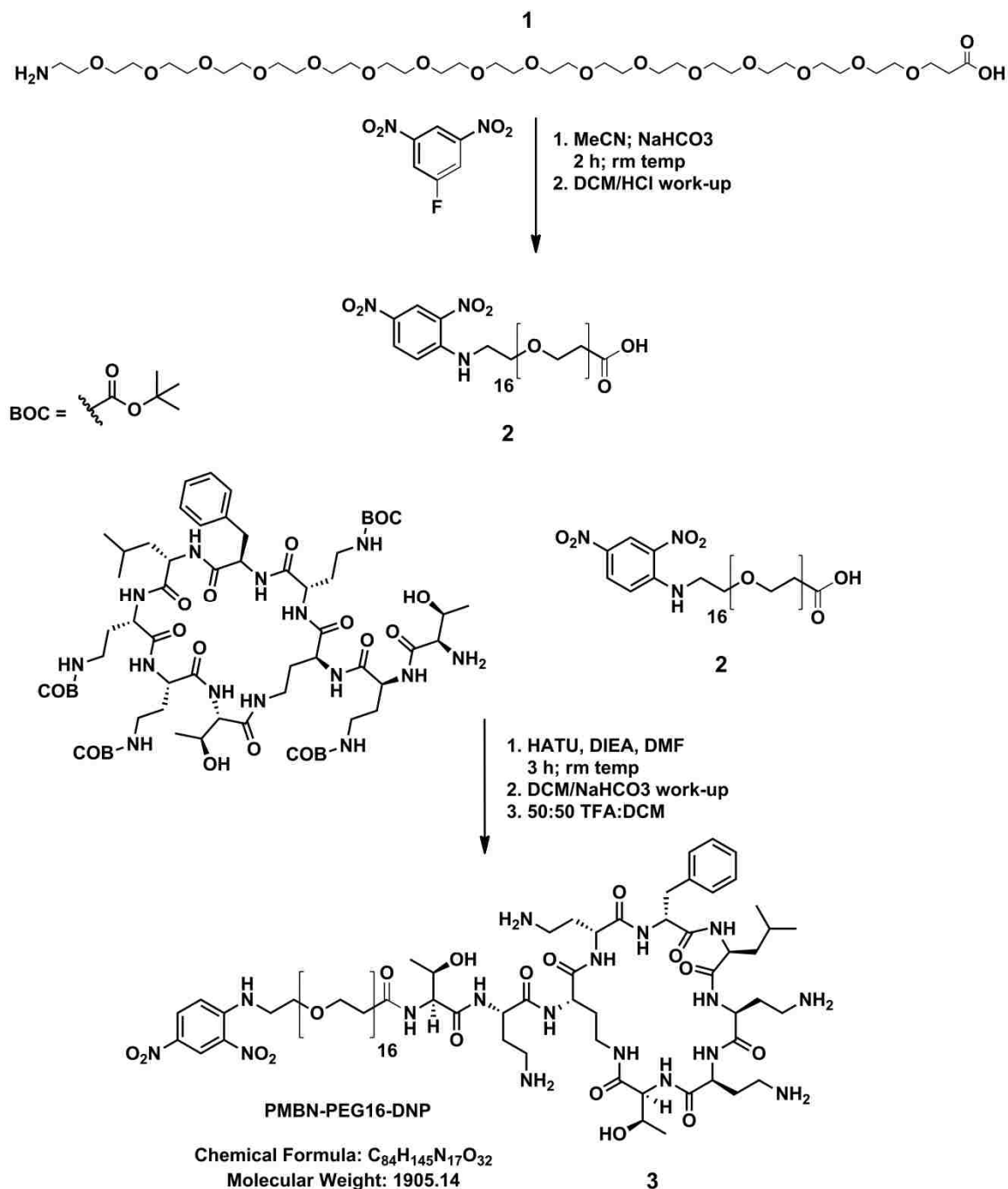
Figure 4.11 Structures of Polymyxin B and PMBN-DNP conjugates with PEG linkers.

However, the linker connecting the two units must be carefully designed to: (1) minimally disrupt the binding to LPS on bacterial cell surface (PMBN), (2) maximize DNP availability on cell surfaces, and (3) possess the proper chemo-physical properties of a drug-like molecule.

We chose the flexible spacer, polyethylene glycol (PEG), to be coupled onto the N-terminus followed by the arylation with DNP (Figure 4.11). We reasoned that the PEG spacer may play a pivotal role in determining antibody recruitment levels by improving the hapten presentation. In collaboration with the Regen Group, they synthesized a fragment of PMB known as PMB nonapeptide (PMBN) (Figure 4.11). PMBN is devoid of the membrane-disrupting fatty acid tail but, critically, retains the cyclic heptapeptide responsible for association to Lipid A.^{11, 10} The smaller PMBN fragment has attenuated antimicrobial activity, which can be useful in isolating the effect of surface-homing in our strategy. Therefore, we synthesized, purified, and characterized 7 PMBN- (PEG)₂₋₂₄-DNP conjugates, which systematically varied on the number of PEG units (Scheme 4.2, Scheme 4.3).



Scheme 4.2 Synthesis of PMBN-PEG_x-DNP Conjugates. (BOC)-PMBN (1eq.) was reacted with PEG₂-DNP (1.5eq.) in DMF with HATU (1.4eq.) and DIEA (3eq.). After reaction time, the product was extracted with DCM and the protecting groups were removed in acidic conditions. Purification on normal phase with 2% MeOH / DCM afforded conjugate, PMBN-PEG₂-DNP. Synthesis was repeated for conjugates with PEG_x (x = 4, 6, 12).



Scheme 4.3 Synthesis of PMBN-PEG_x-DNP Conjugates. Amino-PEG16-acid (1eq.) was reacted with 2, 4-dinitrofluorobenzene (5 eq.) in a mixture of MeCN and NaHCO₃ for 2 h. After extraction with DCM, the product was isolated and used without further purification. (BOC)-PMBN (1 eq.) was reacted with PEG16-DNP (1.5eq.) in DMF with HATU (1.4eq.) and DIEA (3eq.). After reaction time, the product was extracted with DCM and the protecting groups were removed in acidic conditions. Purification on normal phase with 2% MeOH / DCM afforded conjugate, PMBN-PEG₁₆-DNP. Synthesis was repeated for conjugates with PEG_x (x = 20, 24).

We continued our investigations into this immunotherapy strategy utilizing *E. coli* as the initial model organism to evaluate antibody recruitment. In this experiment, *E. coli* cells from overnight stationary phase (10^6 cells) were treated with the panel of DNP-(PEG)₂₋₂₄-PMBN agents. Following the treatment, *E. coli* cells were incubated with 0.02 $\mu\text{g}/\text{mL}$ FITC-labeled anti-DNP antibody for 1 h at 37 °C. After washing and fixing cells in 4% formaldehyde, the cells were analyzed for cellular fluorescence by flow cytometry (Figure 4.12).

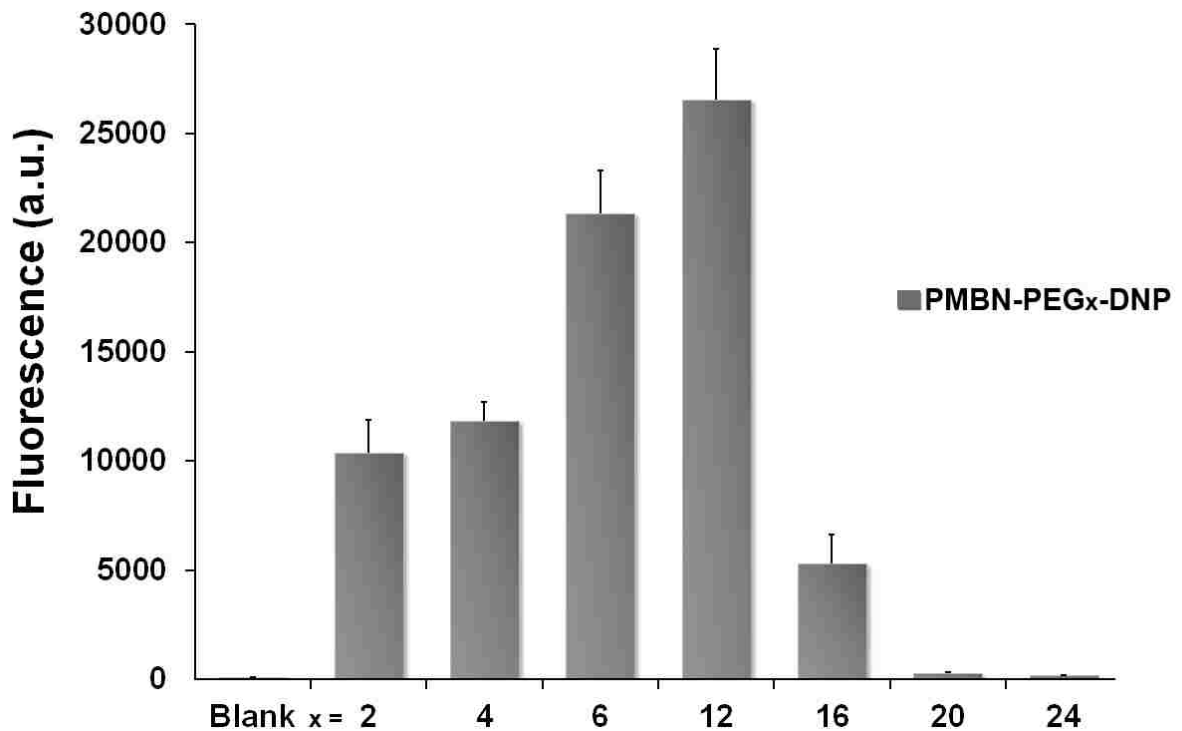


Figure 4.12 PMBN-PEG_x-DNP mediated antibody recruitment in *E. coli*. Stationary phase *E. coli* were incubated in LB supplemented with 40 μM of PMBN-PEG_x-DNP of varying lengths for 2 h at 37 °C. Incubation with anti-DNP antibodies followed and cells were analyzed via flow cytometry. Data are represented as mean + SD (n = 3).

The length dependence observed suggests that there is a particular tether length that optimizes hapten presentation by displaying it away from the immediate OM. Remarkably PMBN-PEG₁₂-DNP treatment resulted in a robust recruitment of antibodies. To the best of our knowledge, this is the first demonstration of a strategy that induces the recruitment of antibodies to surfaces of Gram-negative bacteria using small molecules. Most importantly, this level of recruitment was observed in bacterial cells from the stationary phase.

Next, we assessed the toxicity of PMBN-PEG₁₂-DNP to *E. coli*. As PMBN displays minimal bacterial toxicity, we expected an attenuated response in cells treated with PMBN-PEG₁₂-DNP. As such, we observed low toxicity in *E. coli* treated with up to 30 µg /mL of PMBN-PEG₁₂-DNP (Figure 4.13). The MIC was defined as the lowest

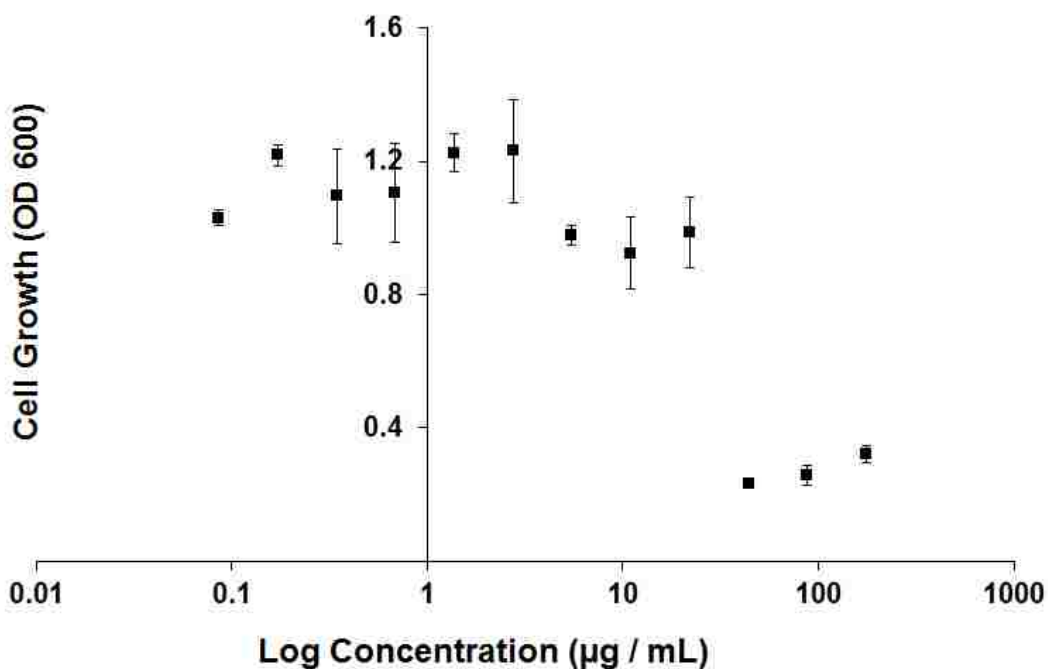


Figure 4.13 PMBN-PEG₁₂-DNP Toxicity towards *E. coli*. *E. coli* cells were incubated with varying concentrations of PMBN-PEG₁₂-DNP for 18 h at 37 °C. Bacterial viability was evaluated by measuring the absorbance at 600 nm. Data are represented as mean + SD (n = 3).

concentration at which visible bacterial growth was inhibited following 18 h incubation at 37 °C. For PMBN-PEG₁₂-DNP, 43.95 µg / mL (25 µM) is the MIC in *E. coli*. Separately, high cell density stationary-phase cultures of *E. coli* were treated with various concentrations of PMBN-PEG₁₂-DNP (0, 17.3, 34.6, 69.2, 103.7, 138.3, 172.9 µg /mL or 10, 20, 40, 60, 80, 100 µM). Time-kill studies were performed at 37 °C with shaking at 250 rpm. At the indicated times, bacterial aliquots were removed and plated on LB agar plates which were then incubated for 18 h at 37 °C. Cell viability was assessed by enumerating the CFU (colony forming units) per milliliter. It was demonstrated that the number of viable cells was reduced quickly by several logs for *E. coli* treated with 60 µM or greater of PMBN-PEG₁₂-DNP (Figure 4.14). Conversely, we observed a slow killing effect with *E. coli* treated with 40 µM of PMBN-PEG₁₂-DNP.

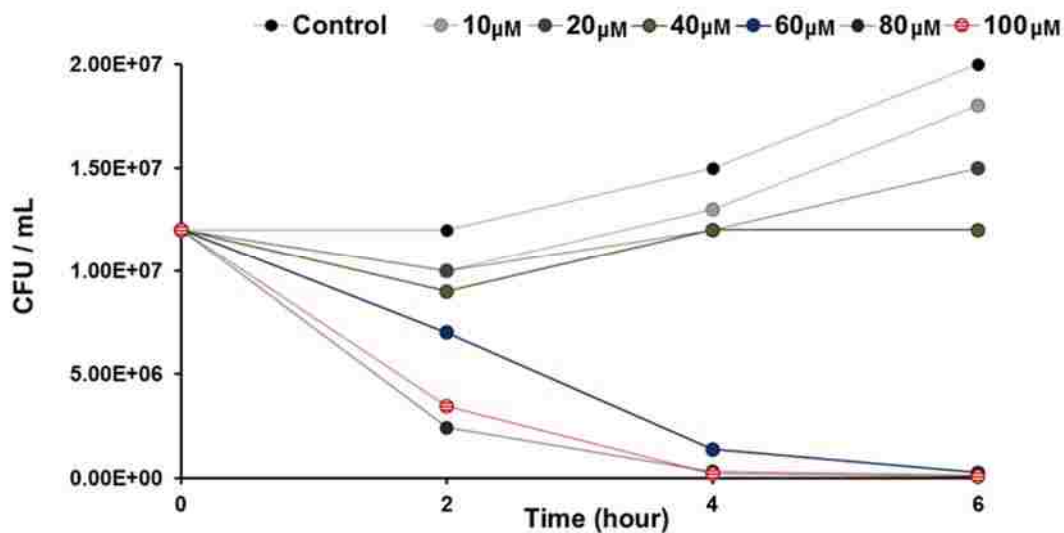


Figure 4.14 Toxicity of PMBN-PEG₁₂-DNP towards Stationary phase *E. coli*. *E. coli* cells in the stationary phase of growth were treated with increasing concentrations of PMBN-PEG₁₂-DNP for indicated times. Cell viability was assessed by enumerating colonies from overnight incubation on LB agar culture plates. Data displayed as CFU/mL (concentration) over time.

Killing of Gram-negative bacteria that are in a stationary phase of growth has been described as a specific characteristic of the bactericidal action of polymyxin B.²⁰ In this study it could be demonstrated that stationary phase *E. coli* reacts differently to PMBN-PEG₁₂-DNP presence, whereas killing curves with logarithmically growing bacteria exhibited a lower tolerance to high concentrations to PMBN-PEG₁₂-DNP.

Next, we set out to assess the toxicity of PMBN-PEG₁₂-DNP against host mammalian cells. One concern we had is the overall negative charge of mammalian cells and the probability of interacting with positive charged molecules. To evaluate the toxicity of PMBN-PEG₁₂-DNP, HEK293 cells were incubated in the presence of varying concentrations of PMBN-PEG₁₂-DNP for 72 h and analyzed by standard viability assays (Figure 4.15). At all concentrations examined, we observed no significant loss of viability.

In conclusion the assessment of PMBN-PEG₁₂-DNP toxicity, we show that the conjugate is relatively non-toxic (Table 4.1). We determined that the conjugate is non-toxic to bacterial cells in the growth phase. The MIC of PMBN-PEG₁₂-DNP in *E. coli* is consistent with the MIC observed for PMBN.²¹ Thus, the addition of PEG linker and DNP moiety does not affect the attenuated toxicity of PMBN. Conversely, we observed a high tolerance for PMBN-PEG₁₂-DNP in stationary phase *E. coli*. This data hints at another mechanism of action given the nature of the interaction between PMBN and LPS on cell surfaces is independent of cell growth and division.

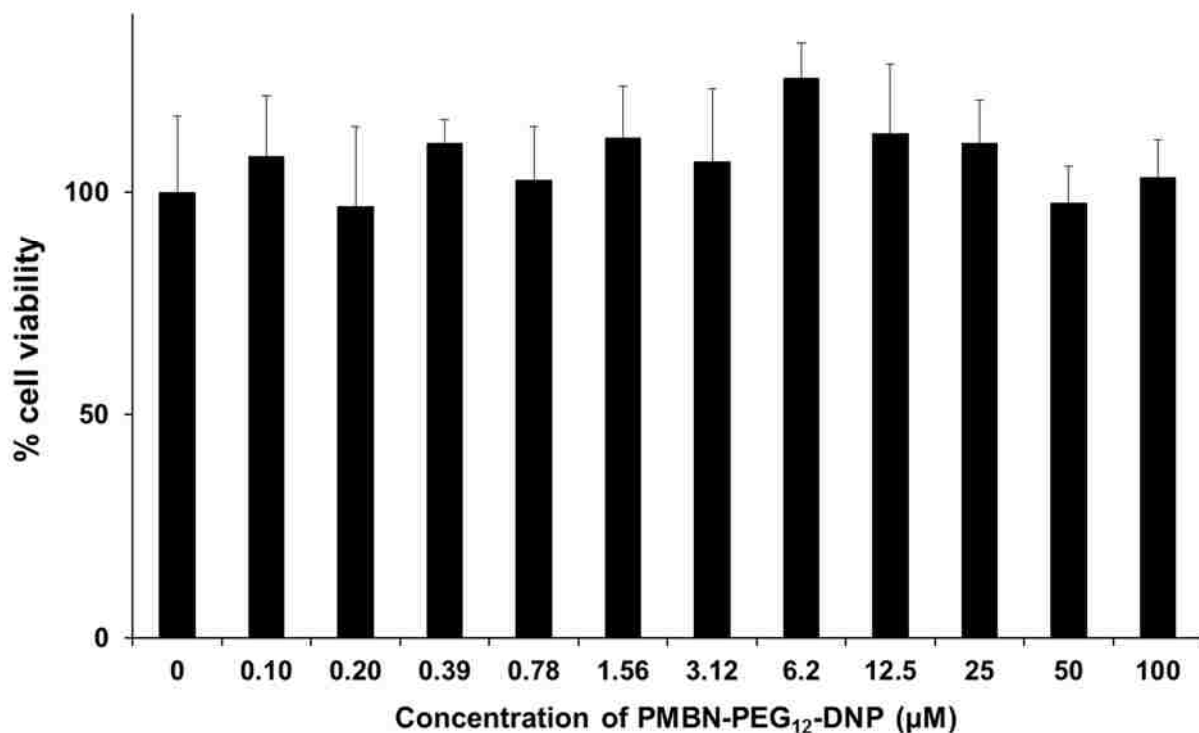


Figure 4.15 PMBN-PEG₁₂-DNP Induced Mammalian Cell Toxicity. HEK293 cells were incubated for 72 hours in the absence or the presence of increasing concentrations of PMBN-PEG₁₂-DNP. Cellular viability was evaluated with MTT by measuring absorbance at 580 nm. Data are represented as mean + SD (n = 3).

Concentration					
MIC <i>E. coli</i>		Stationary Phase Killing <i>E. coli</i>		Mammalian Cell Toxicity HEK293	
μg / mL	μM	μg / mL	μM	μg / mL	μM
43.95	25	103.7	60	> 172	> 100

Table 4.1 PMBN-PEG₁₂-DNP Toxicity towards *E. coli* and Mammalian Cells.

4.3.3 PMBN-DNP Potentiation of Antibiotics

Studies have been carried out showing that the addition of PMBN renders Gram-negative bacteria susceptible to several antibiotics by permeabilizing their outer membranes.^{22, 23} Given the ability of PMBN to potentiate large-molecular-weight antibiotics, we reasoned that PMBN-PEG₁₂-DNP would also act as an antibiotic adjuvant capable of sensitizing Gram-negative bacteria to antibiotics typically restricted to Gram-positive bacteria.

To test this, we grew *E. coli* in the presence of increasing concentrations of rifampicin accompanied with PMBN-PEG₁₂-DNP at 0.5×MIC. Rifampicin is a polyketide antibiotic, which inhibits RNA synthesis. We observed that PMBN-PEG₁₂-DNP potentiated the activity of rifampicin against *E. coli* at 37 °C (Figure 4.16). Specifically, PMBN-PEG₁₂-DNP synergized with rifampicin (fractional inhibitory concentration (FIC) index of ≤0.5), which is hydrophobic, but not with the hydrophilic glycopeptide vancomycin (Table 4.2). These data are consistent with antibiotic potentiation by PMBN, where synergy with hydrophobic molecules is generally more pronounced than that with hydrophilic molecules.²²

Drug	MIC _D	FIC _D	MIC _P	FIC _P	FIC Index
Rifampicin	12.5	0.0624	50	0.0156	0.078
Vancomycin	>100	>1	50	0.0156	>1.0156

Table 4.2 Evidence of Synergy against *E. coli*. Fractional inhibitory concentration (FIC) indices were calculated against *E. coli* using microdilution assays with maximum concentrations of PMBN-PEG₁₂-DNP at 25 µg/mL, and drugs, rifampicin and vancomycin, set to 50 µg/mL and 100 µg/mL, respectively. MIC_D is the minimum inhibitory concentration of each drug alone. MIC_P is the MIC of PMBN-PEG₁₂-DNP alone. FIC_D is the FIC of each drug. FIC_P is the FIC of PMBN-PEG₁₂-DNP. FIC_x = [x]/MIC_x, where [x] is the lowest inhibitory concentration of drug in the presence of co-drug, and MIC_x is the MIC of x in the absence of co-drug.

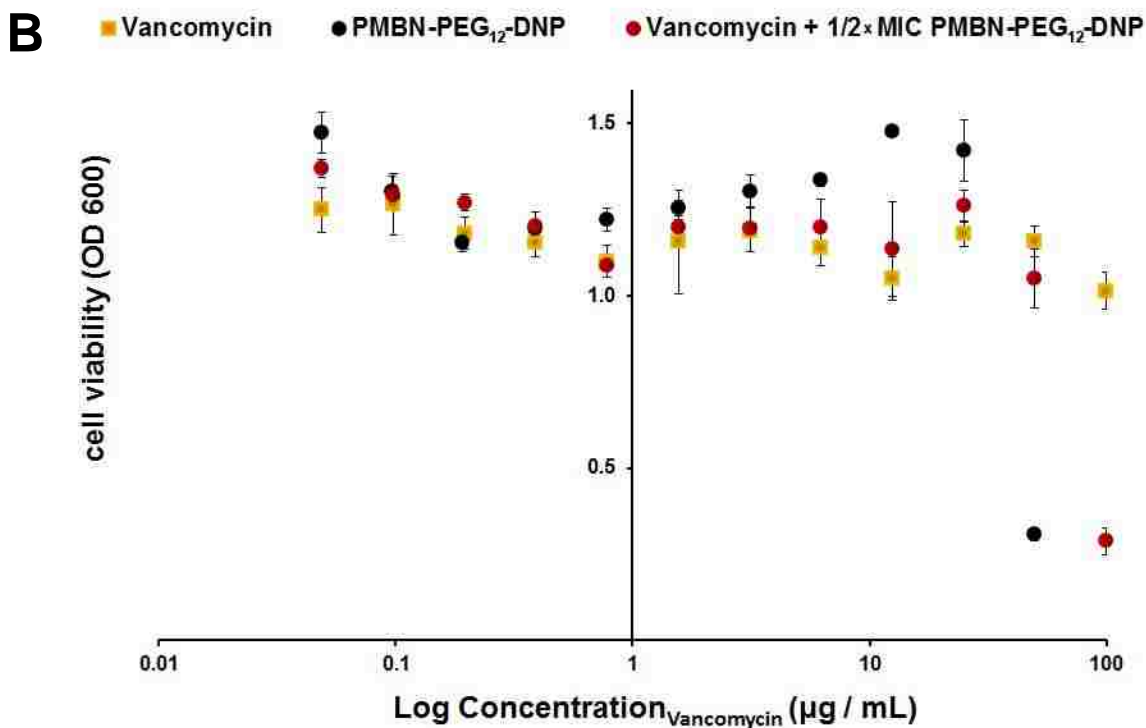
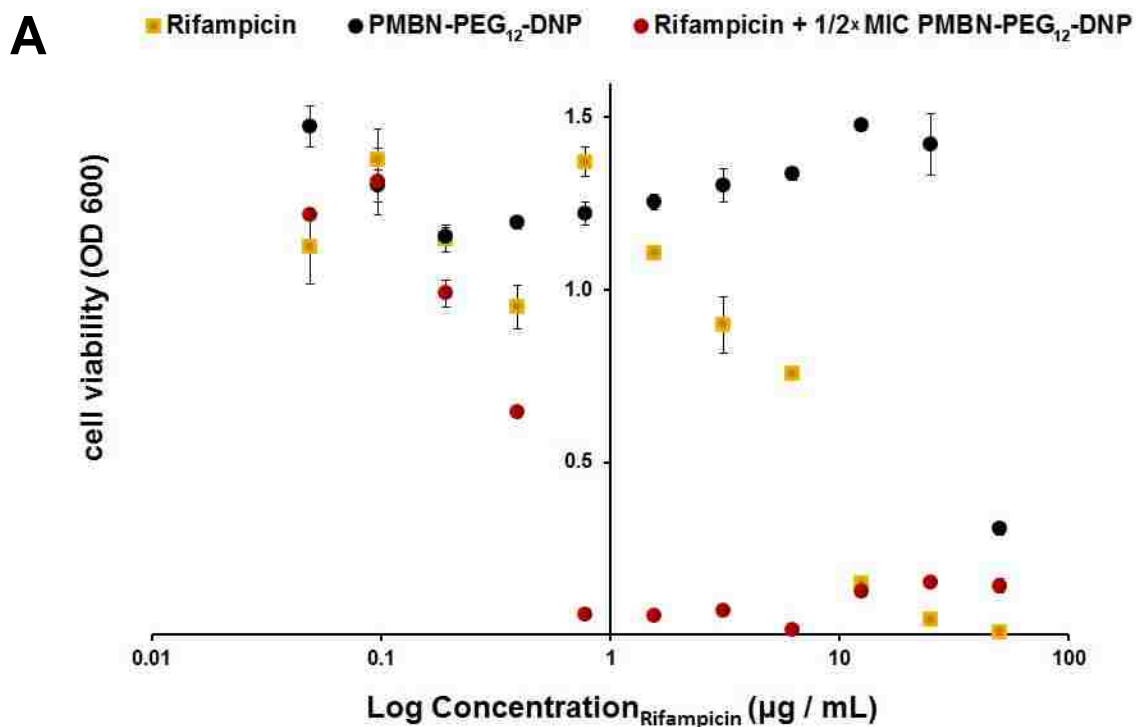


Figure 4.16 Potentiation of Antibiotics. *E. coli* toxicity of rifampicin (A) and vancomycin (B) in the presence of 12.5µM (0.5×MIC) PMBN-PEG₁₂-DNP for 18 h at 37 °C. Bacterial viability was evaluated by measuring the absorbance at 600 nm. Data are represented as mean + SD (n = 3).

4.3.4 PMBN-DNP Mediated Opsonization of *P. aeruginosa*

Next, we set out to determine if this strategy was compatible in other pathogenic Gram-negative bacteria. We chose to study *Klebsiella pneumoniae*, *Acinetobacter baumannii*, and *Pseudomonas aeruginosa*. As seen in Chapter 1, therapies for these bacteria are among those listed in the World Health Organization's account of critical priority. Although the strains used in this study were non-resistant strains, the feasibility of this strategy towards these bacteria will serve as a proof-of-principle in targeting more dangerous bacterial strains.

As previously mentioned, the conserved domains of the LPS are shared regions among bacterial species, which intervene in the development and in the survival of the bacteria. The O-antigen may display modifications, such as alterations in the length of the oligosaccharide chain, changes in the surface composition, and changes in the chemical configuration the O-antigen of Gram-negative bacteria.²⁴ It also renders additional protection from the antimicrobial action of certain antibiotics and participates in the inhibition of the membrane attack complex (MAC) during an immune response.²⁵

Up until this point, we were using an *E.coli* strain (K12) devoid of the O-antigen layer for assessing antibody recruitment (Figure 4.17). Acting as a model system, the K12 strain displayed pronounced antibody recruitment with our synthesized panel of PMBN-DNP conjugates. In order to determine the usefulness of this strategy against clinically relevant bacterial strains, we assessed antibody recruitment in *Klebsiella pneumoniae*, *Acinetobacter baumannii*, and *Pseudomonas aeruginosa*.

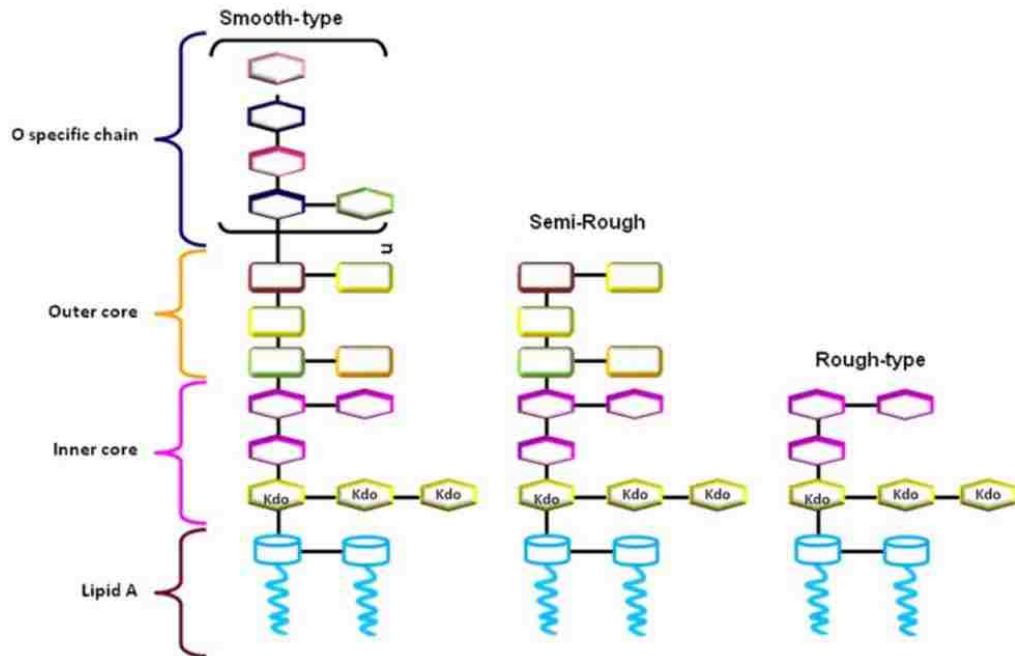


Figure 4.17 Schematic Representation of Variety in Lipopolysaccharide Structures. Gram-negative bacteria can have varying designs of LPS, which represents 75% of the total surface. There is smooth-type (left), which contains a strain specific O-antigen that varies in length. The bacterial surface can also be of the semi-rough type with only one O-chain subunit (center) and rough-type (right), which halts LPS biosynthesis at the inner saccharide core.¹ (*Mechanisms of O-Antigen Structural Variation of Bacterial Lipopolysaccharide (LPS)*, Reyes, R. E, 2012, Ch.3.)

We incubated each strain with 40 μ M of PMBN-PEG_x-DNP, where x = 12, 16, 20, 24, for 2 h during the stationary phase lifecycle for the bacteria. We did not observe any recruitment capability for any of conjugates in *Klebsiella pneumoniae* or *Acinetobacter baumannii*. However, we observed roughly an 8-fold increase in fluorescence in *Pseudomonas aeruginosa* treated with PMBN-PEG₁₂-DNP over the other conjugate-treated and untreated bacteria (Figure 4.18). This is, to our knowledge, the first synthetic conjugate capable of facilitating endogenous antibody recruitment to a pathogenic Gram-negative organism.

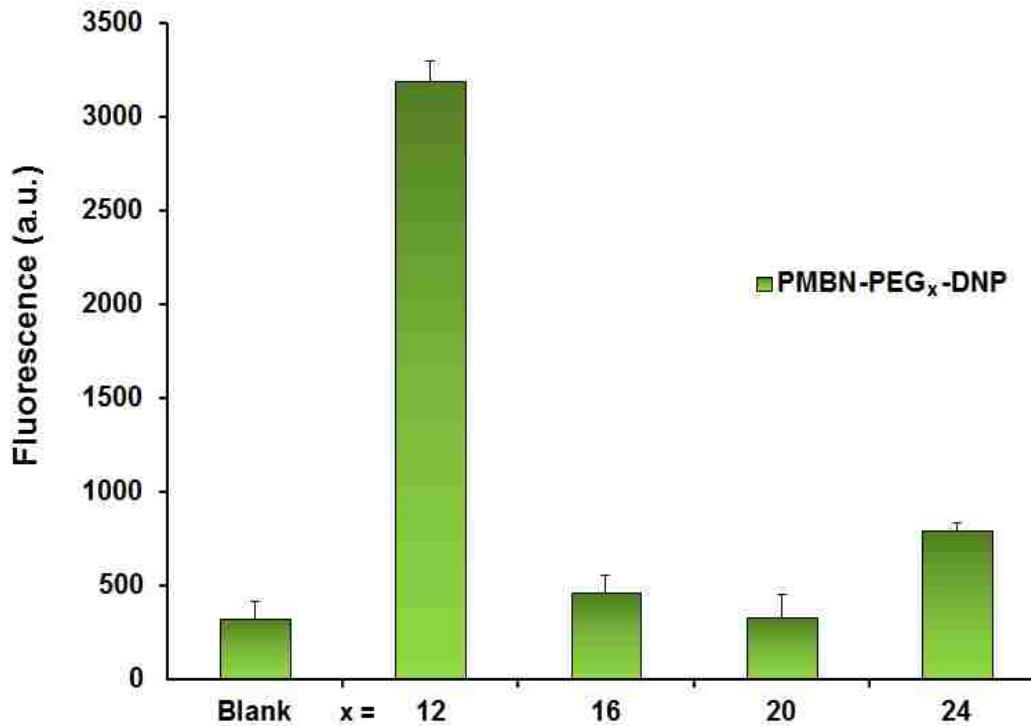


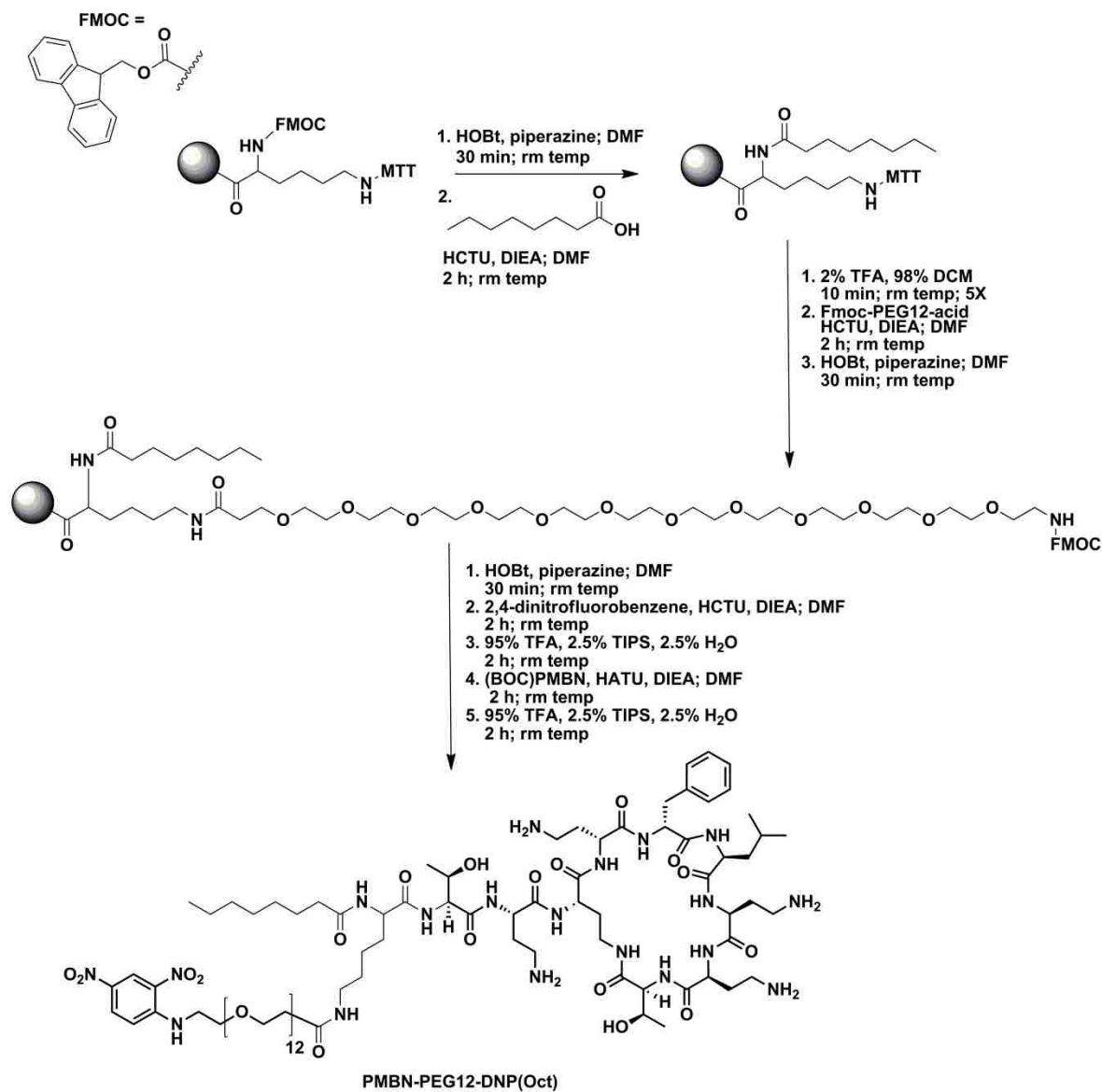
Figure 4.18 PMBN-PEG_x-DNP mediated antibody recruitment in *Pseudomonas aeruginosa*. Stationary phase *Pseudomonas aeruginosa* were incubated in LB supplemented with 40 μ M of PMBN-PEG_x-DNP of varying lengths for 2 h at 37 °C. Incubation with anti-DNP antibodies followed and cells were analyzed via flow cytometry. Data are represented as mean + SD (n = 3).

Due to the complexity related to LPS, we have a limited molecular-level understanding of how the bacterial outer membranes behave for various types of bacteria. Therefore, we have collaborated with the Im laboratory at Lehigh University, who developed a unique technique to build and simulate complex outer membranes of Gram-negative bacteria, including different cores and O-antigens of *E. coli* and *P. aeruginosa*. In attaining this information, we will look forward to the de novo design of linkers to achieve high levels of surface labeling and proper display of antigens for antibody recruitment, specific for the surface of the bacteria we aim to target.

4.3.5 Induced Toxicity with Fatty Acid Derivative

We expected that the re-introduction of the fatty acid tail will improve the inherent antimicrobial activity of the conjugates. More importantly, antibody recruitment will be expected to be efficient at lower concentrations. The ability of the fatty acid tail to imbed within the outer membrane should result in better affinity towards Lipid A and longer residency time of the entire construct onto the bacterial cell surface.

We synthesized an octanoic acid derivative via solid-phase peptide synthesis (Scheme 4.4). Chlorotrityl resin was loaded with N- α -Fmoc-N- ϵ -4-methyltrityl-L-lysine (Fmoc-L-Lys(Mtt)-OH). The N-terminus of lysine was deprotected to allow for the coupling of caprylic acid (octanoic acid). Selective unmasking of the N ϵ -methyltrityl protecting group was completed in mild acidic conditions. The free amine was then reacted with Fmoc-N-amido-PEG₁₂-acid in the presence of coupling agent and base. Deprotection of the construct, followed by conjugation of 2, 4-dinitrofluorobenzene allowed for the completion of portion of the construct on solid support. The construct was cleaved from the resin and reacted with (BOC)PMBN. After reaction time and removal of BOC protecting groups, the final construct was purified on RP-HPLC and characterized by MALDI-TOF MS.



Scheme 4.4 Synthesis of PMBN-PEG₁₂-DNP(Oct). Peptide construct was built via solid-phase peptide synthesis as previously discussed. Construct was reacted with (BOC)PMBN. Protecting group removal and purification, afforded the final derivative.

We assessed the toxicity of PMBN-PEG₁₂-DNP(Oct) to *E. coli*. We expected this conjugate to replace the inherent antimicrobial activity of the conjugates. As such, we observed high toxicity in *E. coli* treated with concentrations as low as 5 µg /mL of PMBN-PEG₁₂- DNP(Oct) (Figure 4.12). The MIC was defined as the lowest concentration at which visible bacterial growth was inhibited following 18 h incubation at 37 °C. For PMBN-PEG₁₂- DNP(Oct), 3.09 µg / mL (1.56 µM) is the MIC in *E. coli*.

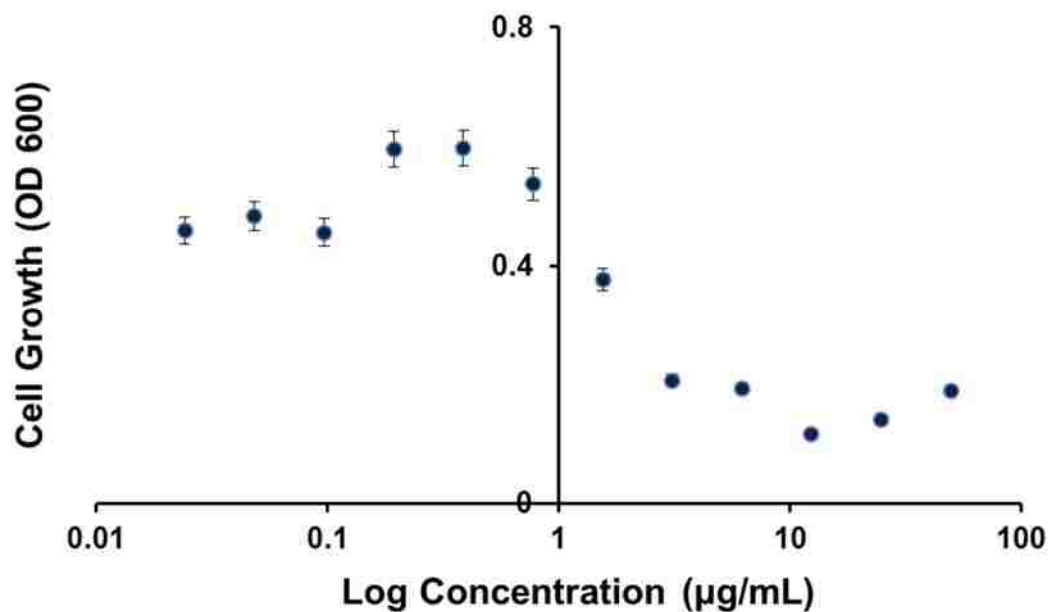


Figure 4.19 PMBN-PEG₁₂-DNP(Oct) Toxicity towards *E. coli*.

E. coli cells were incubated with varying concentrations of PMBN-PEG₁₂-DNP octanoic acid for 18 h at 37 °C. Bacterial viability was evaluated by measuring the absorbance at 600 nm. Data are represented as mean + SD (n = 3).

4.3.6 Pooled Human Serum Bacterial Cell Opsonization

Next, we set out to investigate the ability of the conjugates to induce opsonization in a physiologically-relevant environment. Up to this point, we have shown that by associating the the bacterial surface, PMBN-PEG_x-DNP conjugates can trigger the recruitment of purified FITC-labeled anti-DNP IgG antibodies. While these results establish the feasibility of the overall strategy, the recruitment of IgG antibodies in a human host would have to be derived directly from the serum. The recruitment of serum-associated IgG antibodies could potentially fail due to interference with serum proteins, lack of specificity, and overall lack of anti-DNP abundance. Therefore, it was critical to evaluate this strategy in the biologically relevant conditions. The lack of a fluorescent handle on IgG antibodies from the pooled human serum necessitated the introduction of a secondary antibody.

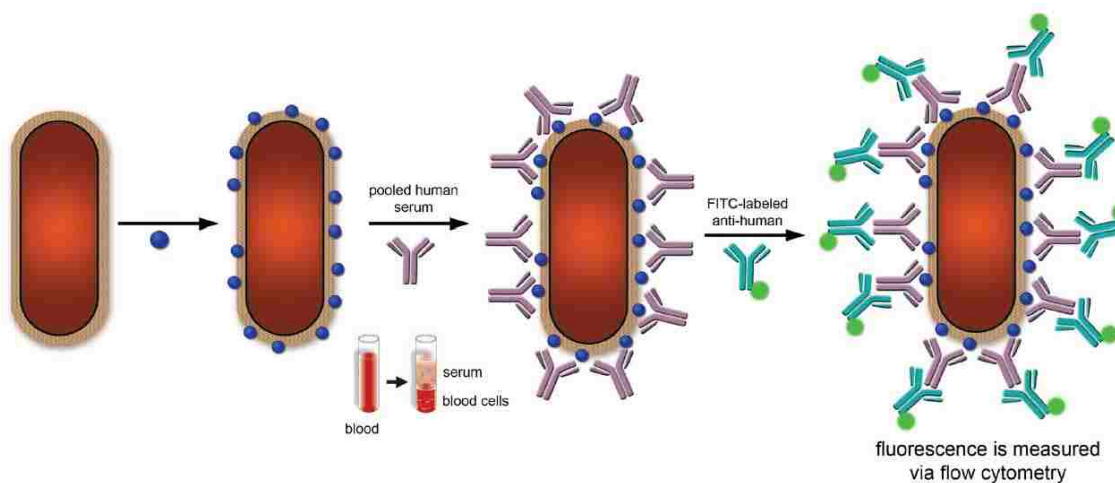


Figure 4.20 Cartoon Representation of Antibody Recruitment using Pooled Human Serum.

In this assay, IgG antibodies from pooled human serum that had opsonized the bacteria cell surface were detected using a FITC-labeled anti-human IgG antibody via flow cytometry (Figure 4.20). We chose to assess the recruitment capability of PMBN-PEG₁₂-DNP octanoic acid for this assay. As this conjugate displays acute toxicity to *E.coli*, the potential of this conjugate to possess dual- modes of thwarting bacterial cells was exciting.

We observed that in the absence of pooled human serum, there was slight cell-associated fluorescence signal from untreated *E. coli* cells. These results indicated that there is non-specific binding of the FITC-labeled anti-human antibody on the surface of *E. coli* cells. Upon treatment with 25% pooled human serum to cells treated with PMBN-PEG₁₂-DNP(Oct) led to an increase in fluorescence signal (Figure 4.21). There was a 3-fold increase in cell-associated fluorescence for cells incubated with the conjugate of 1 h. This data points to this strategy being compatible with conditions that mimic the human host environment.

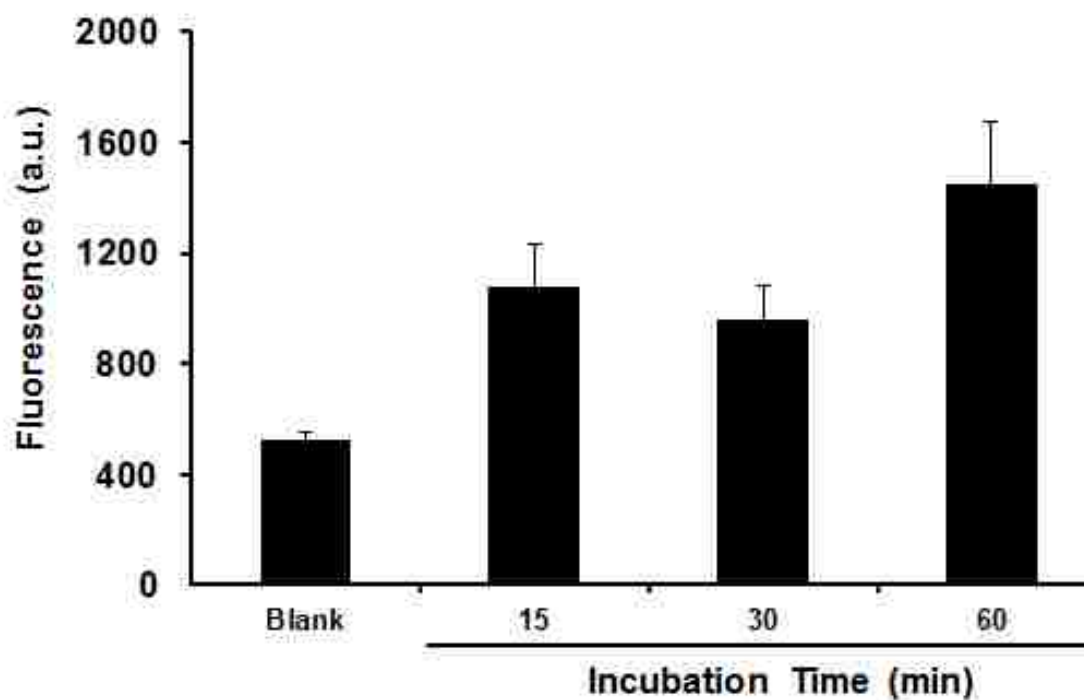


Figure 4.21 Antibody Recruitment from Pooled Human Serum in *E. coli*.

E.coli cells were incubated with 20 μ M of PMBN-PEG₁₂-DNP(Oct) for indicated time points at 37 °C. Cells were subsequently incubated with either 25% pooled human serum or PBS, followed by the incubation with FITC-labeled anti-human IgG antibodies and analyzed using flow cytometry. Data are represented as mean + SD (n = 3).

4.4 FUTURE WORK

We have developed a series of conjugates capable of facilitating the recruitment of endogenous antibodies to the surface of Gram-negative bacteria. As mentioned, we are lacking in our ability to fully understand the on-goings of the outer membrane. Our current collaboration with the Im laboratory will hopefully illuminate key structural differences among the bacteria surfaces, in order to rationally design more efficacious immune attractant molecules.

In generating a more robust immune response, we have synthesized a PMBN construct displaying the rhamnose antigen in place of the DNP epitope. It has been recently shown there is a greater abundance of endogenous anti-rhamnose antibodies compared to anti-DNP antibodies in human serum.^{26, 27} Therefore, the switch to rhamnose antigens should result in even higher levels of antibody recruitment due to the higher abundance of anti-rhamnose in human serum. As we have shown the recruitment of antibodies directly from pooled human serum, we can apply this assay to evaluate the PMBN-rhamnose constructs, as anti-rhamnose antibodies are not commercially available. Additionally, anti-rhamnose opsonization can induce more effective pathogen killing.²⁷ If successful in facilitating the recruitment of anti-rhamnose antibodies from pooled human serum, the opsonized pathogens will be targeted for complement-dependent cytotoxicity (CDC) or antibody-dependent cell-mediated cytotoxicity (ADCC). By elevating the levels of antibodies on the surface of bacteria, we expect to see an induction in bacterial lysis by the serum-components and directly by human immune cells.

4.5 CONCLUSION

In this immunotherapy strategy, we utilized the homing properties of polymyxin B to design polymyxin B nonapeptide-antigen conjugates capable of inducing the recruitment of antibodies to the surface of Gram-negative bacteria. We show that PMBN-FITC targets Gram-negative *E. coli* and maintains association with the bacterial surface through ionic interactions with the negatively charged *E. coli* surface. From these data, the possibility of PMBN-antigen conjugates interacting with the surface long enough to facilitate the recruitment of antibodies was conceivable. Therefore, we synthesized a panel of PMBN-antigen conjugates, employing a PEG spacer and DNP antigen. Our results demonstrate that PMBN-PEG_x-DNP induce the recruitment of anti-DNP antibodies to the surface of *E. coli*. We hypothesize that spacer length requirements arise from differences in complexity of the LPS on the bacterial surface. We identified that PMBN-PEG₁₂-DNP is the optimal construct for efficient recruitment in *E. coli* and *P. aeruginosa*. Further studies need to be conducted in order to answer fundamental questions and may be achieved by computational simulations of outer membrane behavior.

Furthermore, we show that PMBN-PEG₁₂-DNP potentiates the activity of the hydrophobic antibiotic, rifampicin. Similar to PMBN, this construct displays minimal toxicity to *E. coli* and mammalian cells. We also show that re-introduction of the fatty acid tail accentuates the toxicity of the construct to *E. coli*. This is an important feature that can be tailored based on the level of toxicity desired for studying dual-mode approaches to combatting Gram-negative bacteria. Finally, we show that our conjugate can trigger the recruitment of anti-DNP antibodies directly from pooled human serum.

Further investigations into this strategy, may prove great potential to be an effective therapy against bacterial infections caused by challenging Gram-negative pathogens. Although, there have been extreme cases where bacteria have evolved their LPS, resistance to polymyxin B is rare.^{28, 29} We plan to explore the ability of these conjugates to label *E. coli* bacterial in the future by using live organism models. We anticipate that these agents will be excellent lead compounds as a bacterial immunotherapy strategy against Gram-negative pathogenic bacteria.

4.6 REFERENCES

1. Lerouge I, V. J., O-antigen structural variation: mechanisms and possible roles in animal/plant-microbe interactions. *Microbiol Rev* **2002**, *26* (1), 17-47.
2. Ohno, N.; Morrison, D. C., Lipopolysaccharide interaction with lysozyme. Binding of lipopolysaccharide to lysozyme and inhibition of lysozyme enzymatic activity. *Journal of Biological Chemistry* **1989**, *264* (8), 4434-4441.
3. Marston, H. D.; Dixon, D. M.; Knisely, J. M.; Palmore, T. N.; Fauci, A. S., Antimicrobial Resistance. *JAMA* **2016**, *316* (11), 1193-1204.
4. Kalan, L.; Wright, G. D., Antibiotic adjuvants: multicomponent anti-infective strategies. *Expert Rev Mol Med* **2011**, *13*, e5.
5. An, Y. H.; Friedman, R. J., Concise review of mechanisms of bacterial adhesion to biomaterial surfaces. *J Biomed Mater Res* **1998**, *43* (3), 338-48.
6. Backhed, F.; Ley, R. E.; Sonnenburg, J. L.; Peterson, D. A.; Gordon, J. I., Host-bacterial mutualism in the human intestine. *Science* **2005**, *307* (5717), 1915-20.
7. Wu, M.; Hancock, R. E., Interaction of the cyclic antimicrobial cationic peptide bactenecin with the outer and cytoplasmic membrane. *J Biol Chem* **1999**, *274* (1), 29-35.
8. Sahalan, A. Z.; Dixon, R. A., Role of the cell envelope in the antibacterial activities of polymyxin B and polymyxin B nonapeptide against *Escherichia coli*. *Int J Antimicrob Agents* **2008**, *31* (3), 224-7.
9. Schindler, P. R.; Teuber, M., Action of polymyxin B on bacterial membranes: morphological changes in the cytoplasm and in the outer membrane of *Salmonella typhimurium* and *Escherichia coli* B. *Antimicrob Agents Chemother* **1975**, *8* (1), 95-104.
10. Vaara, M.; Viljanen, P., Binding of polymyxin B nonapeptide to gram-negative bacteria. *Antimicrobial Agents and Chemotherapy* **1985**, *27* (4), 548-554.
11. Viljanen P, K. H., Vaara M, Vaara T., Susceptibility of gram-negative bacteria to the synergistic bactericidal action of serum and polymyxin B nonapeptide. *Can J Microbiol.* **1986**, *32* (1), 66-69.
12. Levin, B. R.; Rozen, D. E., Non-inherited antibiotic resistance. *Nat Rev Microbiol* **2006**, *4* (7), 556-62.
13. Tenover, F. C., Mechanisms of antimicrobial resistance in bacteria. *Am J Med* **2006**, *119* (6 Suppl 1), S3-10; discussion S62-70.
14. Velkov, T.; Roberts, K. D.; Nation, R. L.; Thompson, P. E.; Li, J., Pharmacology of polymyxins: new insights into an 'old' class of antibiotics. *Future microbiology* **2013**, *8* (6), 10.2217/fmb.13.39.
15. Velkov, T.; Thompson, P. E.; Nation, R. L.; Li, J., Structure—Activity Relationships of Polymyxin Antibiotics. *Journal of medicinal chemistry* **2010**, *53* (5), 1898-1916.
16. Primož, P.; Jurka, K., The Search for Molecular Determinants of LPS Inhibition by Proteins and Peptides. *Current Topics in Medicinal Chemistry* **2004**, *4* (11), 1185-1201.
17. Deris, Z. Z.; Swarbrick, J. D.; Roberts, K. D.; Azad, M. A. K.; Akter, J.; Horne, A. S.; Nation, R. L.; Rogers, K. L.; Thompson, P. E.; Velkov, T.; Li, J., Probing

- the Penetration of Antimicrobial Polymyxin Lipopeptides into Gram-Negative Bacteria. *Bioconjugate Chemistry* **2014**, *25* (4), 750-760.
18. Moison, E.; Xie, R.; Zhang, G.; Lebar, M. D.; Meredith, T. C.; Kahne, D., A Fluorescent Probe Distinguishes between Inhibition of Early and Late Steps of Lipopolysaccharide Biogenesis in Whole Cells. *ACS Chemical Biology* **2017**.
 19. Finlay, B. B.; McFadden, G., Anti-Immunology: Evasion of the Host Immune System by Bacterial and Viral Pathogens. *Cell* **2006**, *124* (4), 767-782.
 20. Tam, V. H.; Schilling, A. N.; Vo, G.; Kabbara, S.; Kwa, A. L.; Wiederhold, N. P.; Lewis, R. E., Pharmacodynamics of Polymyxin B against *Pseudomonas aeruginosa*. *Antimicrobial Agents and Chemotherapy* **2005**, *49* (9), 3624-3630.
 21. Duwe, A. K., Rupar, C. A., Horsman, G. B., Vas, S. I., In Vitro Cytotoxicity and Antibiotic Activity of Polymyxin B Nonapeptide. *Antimicrobial Agents and Chemotherapy* **1986**, *30* (2), 340-341.
 22. Ofek, I.; Cohen, S.; Rahmani, R.; Kabha, K.; Tamarkin, D.; Herzig, Y.; Rubinstein, E., Antibacterial synergism of polymyxin B nonapeptide and hydrophobic antibiotics in experimental gram-negative infections in mice. *Antimicrobial Agents and Chemotherapy* **1994**, *38* (2), 374-377.
 23. Vaara, M.; Vaara, T., Polycations as outer membrane-disorganizing agents. *Antimicrobial Agents and Chemotherapy* **1983**, *24* (1), 114-122.
 24. Dixon, D. R.; Darveau, R. P., Lipopolysaccharide Heterogeneity: Innate Host Responses to Bacterial Modification of Lipid A Structure. *Journal of Dental Research* **2005**, *84* (7), 584-595.
 25. Erridge, C.; Stewart, J.; Bennett-Guerrero, E.; McIntosh, T. J.; Poxton, I. R., The biological activity of a liposomal complete core lipopolysaccharide vaccine. *Journal of Endotoxin Research* **2002**, *8* (1), 39-46.
 26. Jakobsche, C. E.; Parker, C. G.; Tao, R. N.; Kolesnikova, M. D.; Douglass, E. F., Jr.; Spiegel, D. A., Exploring binding and effector functions of natural human antibodies using synthetic immunomodulators. *ACS Chem Biol* **2013**, *8* (11), 2404-11.
 27. Sheridan, R. T.; Hudon, J.; Hank, J. A.; Sondel, P. M.; Kiessling, L. L., Rhamnose glycoconjugates for the recruitment of endogenous anti-carbohydrate antibodies to tumor cells. *ChemBiochem* **2014**, *15* (10), 1393-8.
 28. Gunn, J. S., Bacterial modification of LPS and resistance to antimicrobial peptides. *Journal of Endotoxin Research* **2001**, *7* (1), 57-62.
 29. Steimle, A.; Autenrieth, I. B.; Frick, J.-S., Structure and function: Lipid A modifications in commensals and pathogens. *International Journal of Medical Microbiology* **2016**, *306* (5), 290-301.

Chapter 5

Fluorescence-based Assay Monitors PAD2 and PAD4 Activity

5.1 ABSTRACT

Post-translational modifications (PTMs) can greatly increase the functional diversity of the modified protein by changing its size, charge, and/or structure. As a result, PTMs may lead to physiological consequences. Peptidylarginine deiminases (PADs) are a family of post-translational modifiers which catalyze the calcium-dependent conversion of arginine residues to non-tRNA encoded citrulline residues. The full extent of the role PADs play in normal physiology and diseased states is not yet fully understood, however in some diseases, such as rheumatoid arthritis, a clear correlation between arginine citrullination and manifestation of the disease exists. Although this correlation is known, few assays described to date have been operationally facile with satisfactory sensitivity. This chapter explores a new, facile, fluorescence-based assay that reports on the activity and inhibition of two isoforms of the PAD family: PAD2 and PAD4. The data, herein, show the assay to be readily performed under ambient conditions displaying a high signal to noise ratio. Furthermore, through collaboration with Penn State Hershey Medical Center, we utilized the assay in a high-throughput screen for potential PAD4 inhibitors.

5.2 INTRODUCTION

5.2.1 Post-Translational Modifications

Within any particular cell, there exists a delicate balance among protein expression, modification, and degradation, all of which are crucial in maintaining cellular homeostasis. Modifications that are made to proteins after ribosomal biosynthesis are called post-translational modifications (PTMs). These post-translational modifications (PTMs) can greatly increase the functional diversity of the modified protein by changing its size, charge, structure, and oligomerization state, amongst other features.^{1, 2, 3} As a result, the change in protein structure can lead to physiological consequences, such as protein degradation, cellular differentiation, signaling, modulation in gene expression, and protein-protein interactions. While these modifications are prevalent in a large percentage of all human proteins, the terminal ends on histone proteins undergo an unusually high number of covalent modifications.⁴

Histone proteins are a family of structural proteins that facilitate the condensation of genomic DNA. Covalent modifications of the unstructured histone tails are carried out and regulated by a series of enzymes that can catalyze the covalent modification of residues (writers), reverse the same modifications (erasers), and distinguish among the changes being imprinted onto the histone tails (readers).^{5, 6, 7} In fact, most of the known PTMs can be observed within this short segment of the histone including methylation, phosphorylation, acetylation, sumoylation, ubiquitination, and citrullination.⁸

Within the past decade, the identification and characterization of post-translational modifications (PTMs) have received a significant amount of research interest⁹. The vast and versatile protein products generated by PTMs allow for the diversification of proteins

potentially influencing both normal cellular homeostasis and diseased states. A dysregulation in PTMs can lead to proteins with altered or expired functions. While most PTMs are fully reversible, a few appear to permanently alter the protein structure.

5.2.2 Peptidylarginine Deiminases

Peptidylarginine deiminases (PADs) catalyze the post-translational conversion of arginine residues to the non-*t*RNA encoded citrulline residues in the presence of calcium. The full extent of the role PADs play in diseased states is not yet fully established, yet rheumatoid arthritis patients harbor an elevated level of citrullinated proteins.^{10, 11, 12} Aberrant protein citrullination has also been found to be elevated in multiple sclerosis (MS)¹³, Alzheimer's disease¹⁴, lupus¹⁵, and various types of cancer^{16, 17}, thus suggesting a possible intervention pathway via therapeutics. Amid the five PAD isoforms, PAD2 and PAD4 are commonly overexpressed in the aforementioned diseases.

Assays that readily and reliably measure the activity of PAD2 / PAD4 would not only enhance our understanding of PADs, but also aid in the search for potent and specific inhibitors. To date, five members of the PAD family have been described (PAD1, PAD2, PAD3, PAD4, and PAD6). Each member of this family appears to target distinct cellular proteins and displays unique tissue distribution profiles. PAD4 is the only member of this protein family known to be localized within the nucleus via a nuclear localization sequence.¹⁸ Accordingly, it has been shown to deiminate a number of nuclear targets, including arginine side chains on the N-terminal tails of histones H2A arginine residue 3 (H2R3), H3 (H3R2, H3R17, and H3R26) and H4 (H4R3)^{19,20}. While each of the PAD isozymes have specific and critical physiological functions, PAD4 has received

considerably more attention due to its role in a number of human processes in both diseased and healthy cells. Recently, PAD4 was shown to be a member of the pluripotency transcriptional network²¹. In a recent experiment, PAD4 expression levels and activity were shown to be elevated during reprogramming and ground-state pluripotent states in mice. By controlling the regulation of stem-cell genes, PAD4 may retain a pivotal role in cellular reprogramming efficiency. PAD4 has also been implicated in the formation of neutrophil extracellular traps, which upon binding of pathogens enable their system clearance. The hypercitrullination of histone proteins by PAD4 induces decondensation of the chromatin, which serves as the base material for the encapsulation of pathogenic bacteria by the extracellular trap, thus warding off bacterial infections²².

PAD2 is widely expressed in the brain, secretory glands, and skeletal muscles. PAD2 overexpression is responsible for hypercitrullination of myelin basic protein (MBP), which leads to myelin sheath integrity loss in multiple sclerosis²³. Recently, the overexpression of PAD2 in cell carcinoma cells led to an elevated tumorigenic profile, including markers consistent with epithelial-to-mesenchymal transition (EMT)²⁴. The same study found that the overexpression of PAD2 in transgenic mice induced spontaneous skin lesions, which also showed high EMT and invasion markers.

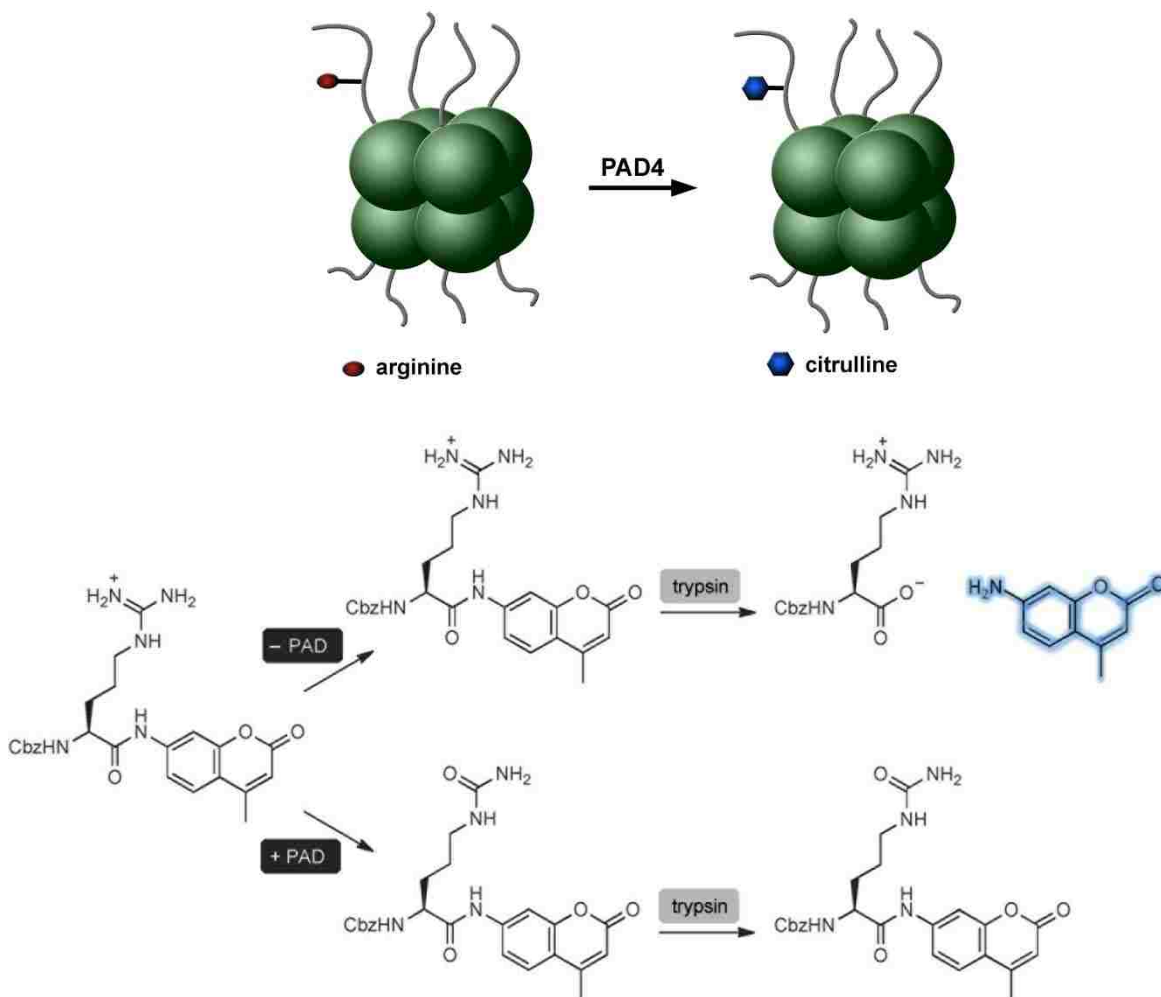
The use of small molecules to turn off the function of PADs may prove to be a powerful new strategy in thwarting the consequences due to aberrant protein expression. Toward this end, several activity assays have been developed with the goal of discovering new PAD inhibitors. A number of covalent inhibitors have been developed by the

Thompson group using the chloro/fluoro imidine handle that mimics the arginine substrate^{25,26,27} and have proven to be practical tools in understanding the role of PAD4 in both healthy and diseased state cells. PAD4 assays have also been described that link the release of ammonia from the reaction to a colorimetric readout²⁸, utilize a fluorescently labeled chloroamidine substrate analog for fluorescence polarization assay,²⁹ rely on the acid-assisted reaction between glyoxal and citrulline³⁰, and couple the PAD4 activity to a fluorescence dequenching step³¹. Of these, only the covalent modifier haloacetamidine strategy has been proven to be compatible with high-throughput screening platforms³² and few are operationally facile with satisfactory sensitivity. The lack of adequate assays has likely contributed to the absence of potent non-covalent PAD4 inhibitors.

Here, we describe a new mechanism-based fluorescence assay that quickly and reliably measures the activity of PAD2 / PAD4. We reason that we could monitor PAD2 / PAD4 activity by utilizing the pro-fluorescent substrate analog. When acting upon substrate histones 3 and 4, PAD4 converts a positively charged arginine side chain to a neutral side chain through the citrullination reaction, which is currently thought to be irreversible (Figure 5.1). The neutralization of this positive charge has important implications for the association of histones with the negatively charged genomic DNA, potentially modulating transcriptional regulation and promoting the formation of neutrophil extracellular traps (NETs).³³ The citrullination of arginine could similarly be leveraged to monitor PAD4 activity. Furthermore, citrullination of arginine would also interfere with the ability of trypsin to hydrolyze the carboxyl side of the amide bond. Trypsin has a distinct preference in hydrolyzing the C-terminal amide bonds of both lysine and arginine, with optimal activity near a pH range of 7.5 to 8.5.

The incorporation of a masked fluorophore (7-amino-4-methylcoumarin, AMC) on the carboxyl side of arginine could be used to generate a signal upon trypsin-mediated hydrolysis. Acylation of AMC is known to greatly reduce its fluorescence intensity, a feature that has been utilized in a number of protease assays.³⁴ Likewise, acylation of AMC onto the arginine is expected to greatly reduce the fluorescence of the potential PAD4 substrate (Scheme 5.1). In addition, a carboxybenzyl (Cbz, Z) group on the amino side of the arginine was included to mimic the typical protein-based substrate of PAD4. The N-terminus acetylation was crucial since it has been previously reported that neither free arginine nor arginine-methyl ester is citrullinated by PAD4 to any appreciable levels²⁰.

As shown by Wildemen et al., the modification of arginine with the unnatural moieties AMC and Cbz is well-tolerated in the active site of PAD4 and responds to trypsin-mediated hydrolysis.³⁵ The substrate, ZRCoum, was also shown to efficiently convert to the expected product upon co-incubation with PAD4.³⁵ In furthering the initial framework of this design, we set up to optimize the assay for high-throughput screening platforms and extend the assay to other PAD isoforms.



Scheme 5.1 PAD Assay Design. (A) A schematic representation of the octameric histones found in a basic unit of a nucleosome. PAD4 is able to citrullinate a number of arginine residues on histone proteins. (B) Schematic representation of the PAD assay. The citrullination reaction catalyzed by PAD renders the substrate (ZRCoum) resistant to trypsin-mediated amide hydrolysis, thus leading to a change in fluorescence levels.

5.3 MATERIALS AND METHODS

5.3.1 Materials

The PAD2 – GST and PAD4 – GST fusions containing pGEX-6P plasmid were a kind gift from Dr. Yanming Wang and Dr. Walter Fast, respectively. Luria Broth (LB), Isopropyl- β -D-thiogalactopyranoside (IPTG) and Ampicillin trihydrate were purchased from Sigma Aldrich. LB Agar, Miller granulated was purchased from Fisher Scientific. Z-Arg-L-7-amino-4-methylcoumarin, 7-amino-4-methylcoumarin, benzamidine, and phenylmethylsulfonyl fluoride (PMSF) were purchased from Sigma Aldrich. Cl-amidine, PAD inhibitor, was purchased from Chem Impex. Compound YW4-03 was supplied by Yanming Wang. Trypsin, crystalline from Bovine Pancreas (Amresco) was purchased from Sigma Aldrich. All salts were purchased from Fisher Scientific.

5.3.2 PAD2 / PAD4 Expression and Purification

The PAD2 – GST / PAD4 – GST fusion containing pGEX-6P plasmid were transformed into chemically competent *Escherichia coli* BL21(DE3) cells. The cells were plated on an ampicillin-containing agar-LB plate and incubated overnight at 37 °C. A single colony was picked and grown overnight in 50 mL of lysogeny broth (LB) containing 1 mM ampicillin at 37 °C. LB (8 L) containing 1 mM ampicillin was inoculated with the overnight growth medium. Cells grew to an OD = ~0.2, when they were moved to a 16 °C environment and continued to OD = ~0.6. Protein production was induced with 0.3 mM isopropyl- β -D-thiogalactopyranoside and incubated overnight at 16 °C while shaking at 250 RPM. Cells were harvested by centrifugation at 3, 500 x g for 30 min at 4 °C. The remaining cell pellet was resuspended in 100 mL lysis buffer containing

50 mM NaH₂PO₄, 300 mM NaCl, 10 mM Imidazole, 1 mM PMSF, and 1 mM DTT. The mixture was sonicated for 15 min and centrifuged at 20,000 x g's for 30 min at 4 °C. The transparent supernatant was transferred to a Protino's glutathione agarose 4B column. After washing steps with 1 X PBS (3 × 10 mL per mL of bead volume) the protein was eluted with 10 mL elution buffer (50 mM Tris HCl, 10 mM glutathione, pH = 8.0). The eluent was further purified and concentrated by using a 100 MWCO spin column. SDS-PAGE was utilized to verify the expected molecular weight and purity of the protein. Aliquots were stored in -80 °C.

5.3.3 PAD Activity Assay

GST-tagged PAD2 or PAD4 was introduced to reaction buffer with a final concentration of 50 mM tris(hydroxymethyl)aminomethane hydrochloride (Tris HCl), 50 mM NaCl, 1 mM tris(2-carboxyethyl)phosphine (TCEP) and 10 mM CaCl₂ (pH = 8.0) and incubated for 10 min at 37 °C. ZRCoum (25 μM) was added to the wells and the reaction continued for 2 h at 37 °C. Quenching of the reaction occurred upon the addition of 10 μL 10 mg/mL trypsin/100 mM EDTA. After 10 min, fluorescence values were obtained via Tecan Infinite 200 ($\lambda_{\text{ex}} = 340\text{nm}$, $\lambda_{\text{em}} = 475\text{nm}$). .

5.3.4 Calcium Dependence Analysis

GST-tagged PAD2 or PAD4 was incubated for 10 min at 37 °C in reaction buffer with a final concentration of 50 mM Tris HCl, 50 mM NaCl, 1 mM TCEP and varying concentrations of calcium chloride (0 – 10 mM) (pH = 8.0). ZRCoum (25 μM) was added and the reaction continued for 2 h at 37 °C. Quenching of the reaction occurred upon the

addition of 10 μ L 10 mg/mL trypsin/100 mM EDTA. After 10 min, fluorescence values were obtained via Tecan Infinite 200 ($\lambda_{\text{ex}} = 340\text{nm}$, $\lambda_{\text{em}} = 475\text{nm}$).

5.3.5 Kinetic Analysis

GST-tagged PAD2 / PAD4 was incubated for 10 min at 37 °C in reaction buffer with a final concentration of 50 mM Tris HCl, 50 mM NaCl, 1 mM TCEP and 10 mM CaCl₂ (pH = 8.0). ZRCoum (25 μ M, 100 μ M, 250 μ M, 500 μ M, 800 μ M and 1 mM) was added to specific wells and the reaction was quenched at time points (15, 30, 45, 90, 120, and 180 min) by the addition of 10 μ L 10 mg/mL trypsin/100 mM EDTA. After 10 min, the fluorescence values were obtained via Tecan Infinite 200 ($\lambda_{\text{ex}} = 340\text{nm}$, $\lambda_{\text{em}} = 475\text{nm}$). The slopes of the data points that displayed a linear relationship of fluorescence plotted against time (min) were the values of V_o ($\mu\text{mol} / \text{min}$). From this data, the kinetic parameters, k_{cat} and K_M , were calculated.

5.3.6 Trypsin Inhibition Analysis

PMSF or benzamidine (0 – 1 mM) was introduced to wells containing 25 μ M ZRCoum for 10 min at 37 °C (Buffer: 50 mM Tris-HCl, 50 mM NaCl, 1 mM TCEP and 10 mM CaCl₂). Quenching of the reaction occurred upon the addition of 10 μ L 10 mg/mL trypsin/100 mM EDTA. After 10 min, fluorescence values were obtained via Tecan Infinite 200 ($\lambda_{\text{ex}} = 340\text{nm}$, $\lambda_{\text{em}} = 475\text{nm}$).

5.3.7 Small Molecule Inhibition Curves

GST-tagged PAD2 or PAD4 was incubated for 10 min at 37 °C in reaction buffer with a final concentration of 50 mM Tris HCl, 50 mM NaCl, 1 mM TCEP and 10 mM

CaCl₂ (pH = 8.0). Varying concentrations of inhibitor (0 μM – 100 μM) was introduced to the wells for 1 h at 37 °C. ZRCoum (25 μM) was added to the wells and the reaction continued for 6 h at 37 °C. Quenching of the reaction occurred upon the addition of 10 μL 10 mg/mL trypsin/100 mM EDTA. After 10 min, fluorescence values were obtained via Tecan Infinite 200 ($\lambda_{\text{ex}} = 340\text{nm}$, $\lambda_{\text{em}} = 475\text{nm}$). IC₅₀ values were calculated.

5.4 RESULTS AND DISCUSSION

5.4.1 Assay reports on PAD2 / PAD4 Activity

We set out to determine the suitability of our assay for reporting on the enzymatic activity of PAD2 / PAD4 in 96-well plates to demonstrate its potential utility for high-throughput screening methods. Reaction wells were incubated with the substrate, ZRCoum, in the presence and absence of PAD2 / PAD4. The wells were incubated at 37°C for 1 h. Next, an excess of trypsin/EDTA was added to designated wells and the reaction continued for an additional 10 minutes at 37 °C.

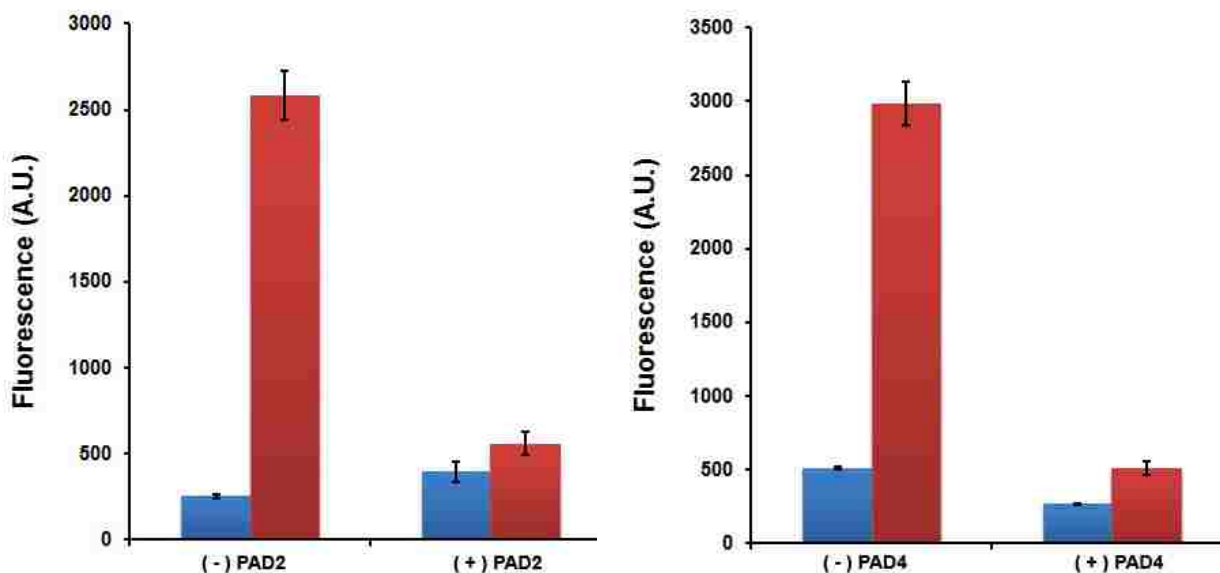


Figure 5.1 Fluorescence assay reports on Activity of PAD2 and PAD4. PAD 2 / PAD4 was incubated in reaction buffer (pH=8.0) with ZRCoum (25 μ M) at 37 °C. Fluorescence was measured (λ_{ex} = 340 nm, λ_{em} = 475 nm) in the absence (blue) and presence (red) of trypsin/EDTA. Data represented as mean +/- SD.

Upon treatment with trypsin, the fluorophore, AMC, is uncoupled from the molecule, thus restoring its fluorescence. We observe a 5- fold increase in fluorescence levels. The change in fluorescence can be readily monitored in solution via its maximum excitation ~440 nm under physiological pH conditions. The enzymatic activity of PAD2 / PAD4 in converting arginine to citrulline should prevent the unmasking of the fluorophore, therefore reducing the fluorescence output.

Conversely, in wells treated with PAD2 / PAD4 and sequential trypsin/EDTA addition, low fluorescence levels are observed (Figure 5.1). This low fluorescence is due to substrate conversion in the presence of the enzyme, thus no longer retaining specificity for trypsin and foregoing hydrolysis of the fluorophore. The addition of EDTA is intended to assist in the cessation of the PAD reaction due its ability to chelate the essential calcium ions. From these data, we observe a 6.5-fold decrease in fluorescence output in the presence of PAD2 and a 5.6-fold decrease in fluorescence output in the presence of PAD4. Trypsin release of the fluorophore is complete within 10 minutes and further incubation does not increase the fold difference (Figure 5.2). From this data, it is evident that ZRCoum has the potential to be a fast and facile reporter of PAD2 / PAD4 activity.

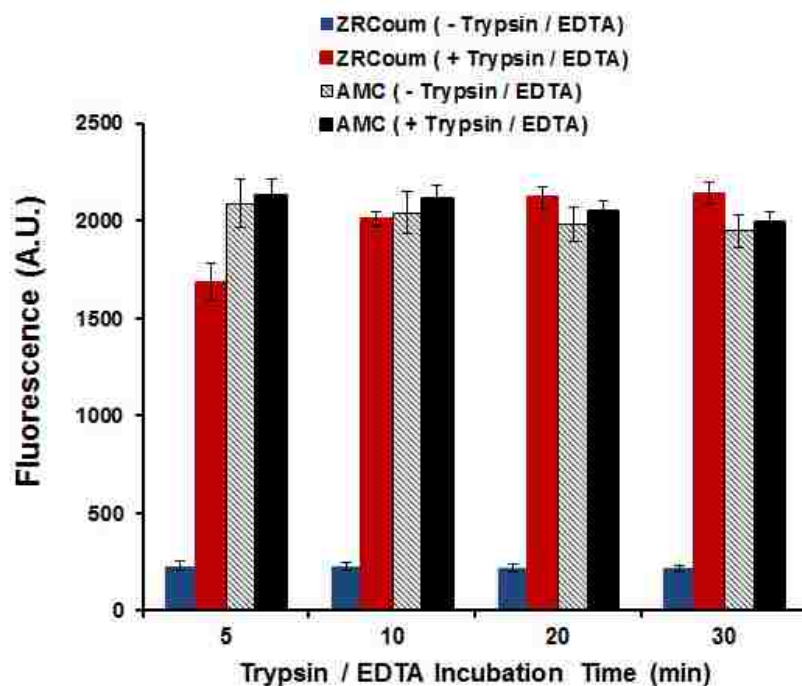


Figure 5.2 Trypsin Hydrolysis of ZRCoum. ZRCoum (25 μ M) or AMC (25 μ M) was incubated in reaction buffer at 37 °C. Fluorescence was measured ($\lambda_{\text{ex}} = 340 \text{ nm}$, $\lambda_{\text{em}} = 475 \text{ nm}$) after trypsin/EDTA addition at designated time intervals. Data represented as mean +/- SD.

Next, we examined the effect the presence of calcium has on PAD activity. The binding of calcium ions (up to five binding sites have been identified) leads to a restructuring of the protein to generate the active site³⁶. In vitro, calcium binding is known to cause a conformational change that moves Cys645 and His471 into positions that are competent for catalysis.³⁷

Indeed, as more calcium ions are titrated in a decrease in the fluorescence is observed, consistent with the fluorescence signal being linked to citrullination by active PAD2 / PAD4 (Figure 5.3).

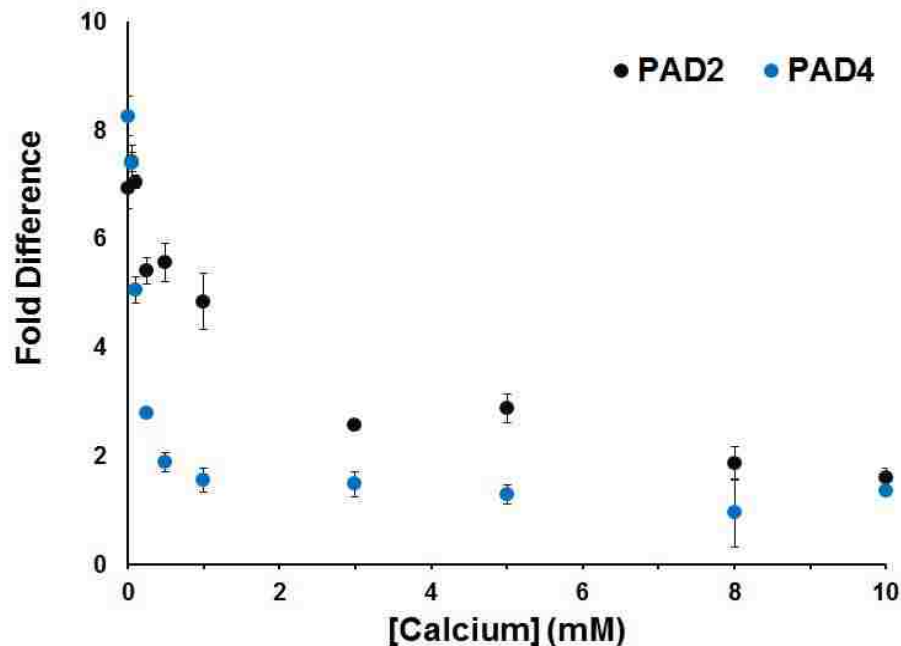


Figure 5.3 Calcium Dependence of PAD2 and PAD4. PAD2 / PAD4 was incubated in reaction buffer (pH = 8.0) containing varying concentrations (0 – 10 mM) of calcium chloride followed by ZRCoum (25 μ M) addition. After 2 h, fluorescence was measured in the presence of trypsin/EDTA. Data represented as mean +/- SD.

Conversely, at very low levels of calcium, fluorescence levels are elevated, indicating the PAD enzyme is not as active and the pro-fluorescent ZRCoum is released upon trypsin hydrolysis. Interestingly, it is evident that PAD4 restores its full catalytic activity at lower concentrations of exogenous calcium ions than PAD2. It is conceivable that either the calcium binding sites in PAD4 have tighter affinities for the calcium ions or the catalytic activity of PAD2 is more strictly associated with full occupation of the calcium binding sites.

5.4.2 Assay Optimization for High-Throughput Screening

5.4.2.1 Assay Miniaturization at Room Temperature

Next, we demonstrated the compatibility of our assay with high-throughput screening platforms. We were primarily interested in analyzing five reaction variables that would be most favorable for screening purposes: (1) the further miniaturization of the assay volume, (2) the possibility of performing the assay at room temperature, (3) the stability of the protein and buffer mixture prior to completing the assay, (4) the kinetics of the assay, and (5) the potential interference of trypsin inhibitors.

For mid-throughput or high-throughput screening efforts, high-density well plates are commonly utilized in small molecule screens. We verified that the assay can be performed almost identically in a 384-well plate as compared to a 96-well plate (Figure 5.4). In further determining the working conditions for the assay in a high-throughput format, we sought to investigate whether PAD4 activity can be monitored in a reasonable time frame at room temperature.

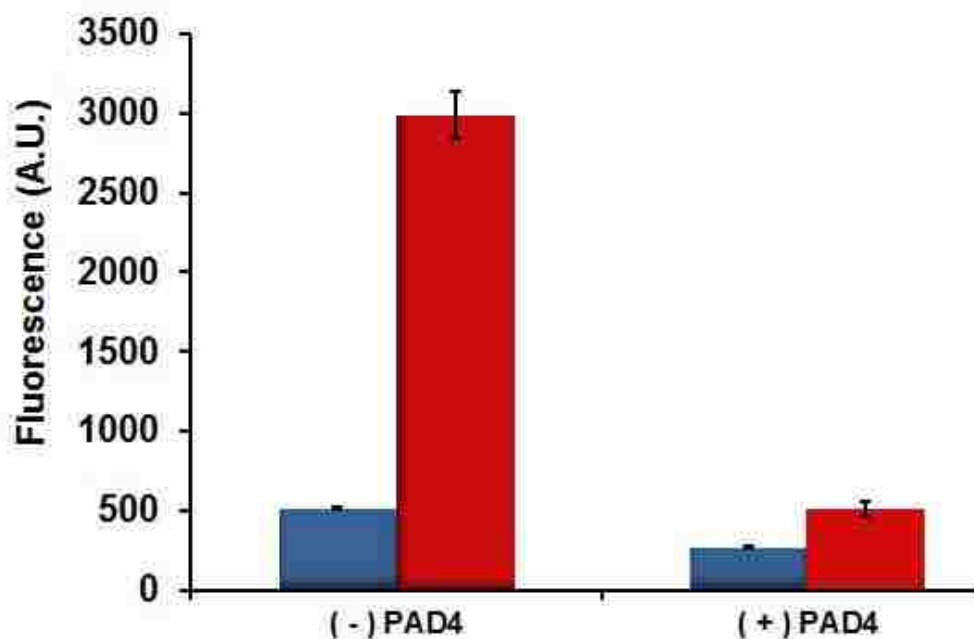


Figure 5.4 Assay Monitors PAD4 Activity in 384 – well plate. PAD4 was incubated in reaction buffer (pH=8.0) with ZRCoum (25 μ M) at 37 °C in a 384-well plate. Fluorescence was measured (λ_{ex} = 340 nm, λ_{em} = 475 nm) in the absence (blue) and presence (red) of trypsin. Data represented as mean +/- SD.

Since not all liquid-handling instruments have a temperature controller, it can become cumbersome and costly to have an incubation step at elevated temperature. Furthermore, accounting for fluctuation in temperature can be a cause for discrepancy between plates and runs. In order to determine the effect of lower temperatures for the assay described here, we performed a similar assay at room temperature. We found that the signals were virtually unchanged between 37° C and room temperature (Figure 5.5).

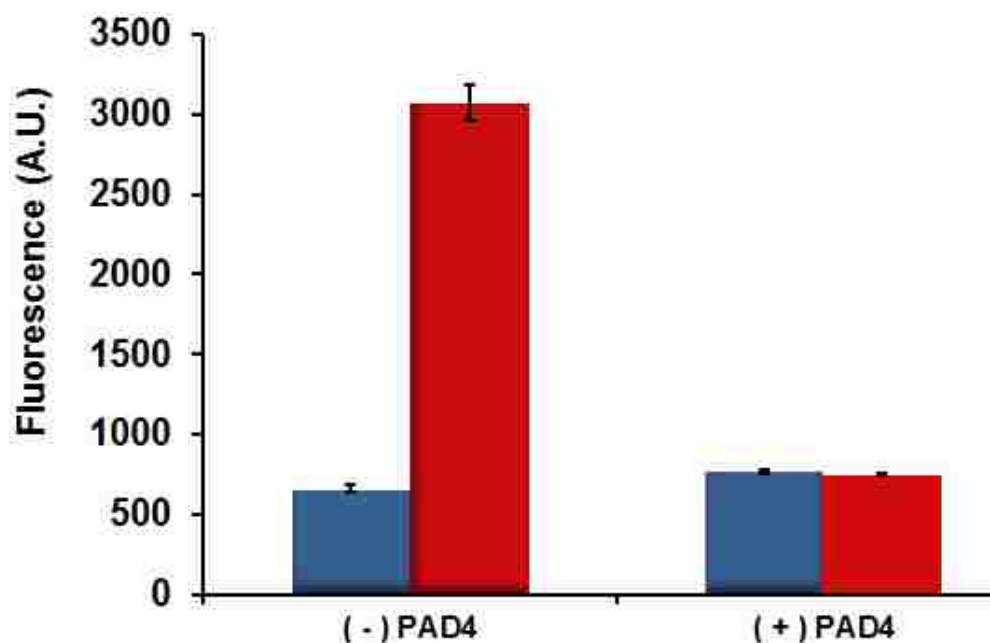


Figure 5.5 Assay Monitors PAD4 Activity in 384 – well plate at Room Temperature. PAD4 was incubated in reaction buffer (pH=8.0) with ZRCoum (25 μ M) at room temperature. Fluorescence was measured (λ_{ex} = 340 nm, λ_{em} = 475 nm) in the absence (blue) and presence (red) of trypsin. Data represented as mean +/- SD.

5.4.2.2 Reagent Stability

Next, we evaluated the stability of PAD4 when dissolved in the reaction buffer over a prolonged period of time. Realistically, high-throughput screening will require reagents to be generally stable for many hours while the instrument is completing the screen. Due to short half-lives of certain reagents, it can be quite expensive and time consuming to terminate a screen in order to prepare fresh reagents. Depending on the assay conditions, it is not unusual for some assays to be incompatible with high-throughput screening for this very reason. Minding this potential obstruction, we tested the stability of PAD4 in the reaction buffer over several hours.

The enzyme was suspended in reaction buffer and left at room temperature in a sealed vial covered from light. At indicated time points, an aliquot was removed for testing in the PAD4 activity assay. We observe almost no loss in enzymatic activity throughout the time period, thus indicating that the protein is stable even after sitting at room temperature for over 15 hours (Figure 5.6).

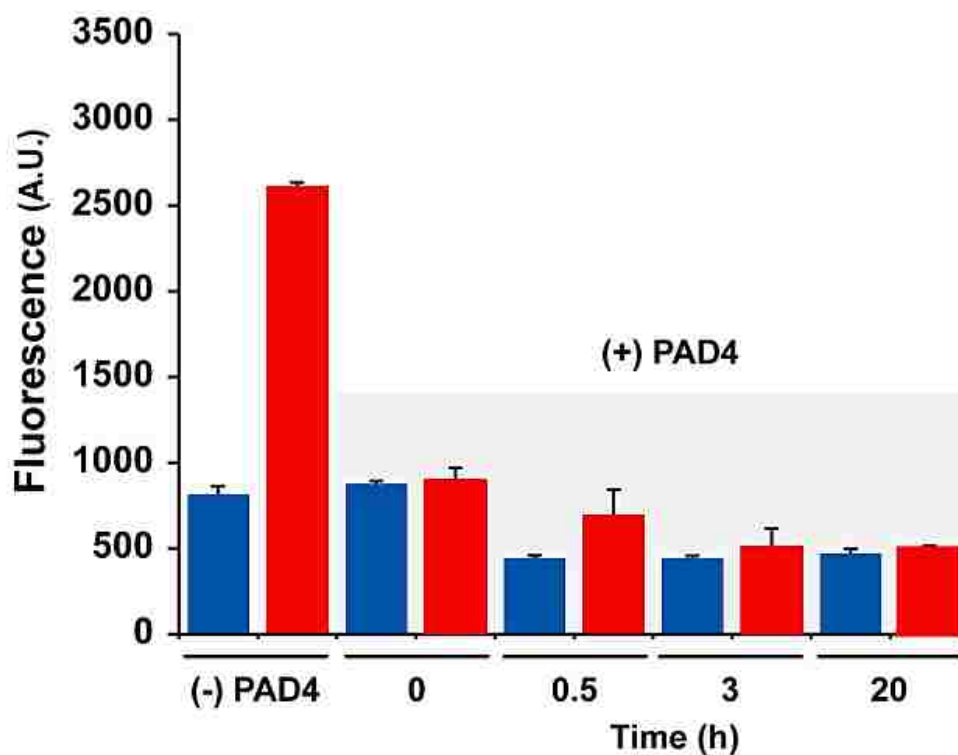


Figure 5.6 Analysis of Reagent Stability. PAD4 was incubated in reaction buffer (pH=8.0) with ZRCoum (25 μ M) at room temperature for a time. Fluorescence was measured (λ_{ex} = 340 nm, λ_{em} = 475 nm) in the absence (blue) and presence (red) of trypsin. Data represented as mean +/- SD.

5.4.2.3 Kinetics of Reaction

To further optimize the assay performance by minimizing the required incubation time between PAD2 or PAD4 and the substrate, we analyzed the kinetics of the reaction. We monitored PAD4 activity over time both at room temperature and 37° C. As expected, it appears that PAD4 is more active at 37° C (consistent with human physiological temperature) with the reaction mostly complete by 20 minutes. Satisfyingly, the reaction is not strongly affected by the reduction in temperature down to room temperature. The reaction proceeds at approximately half the speed as at the elevated temperature and is essentially complete 40-45 minutes post initiation (Figure 5.7).

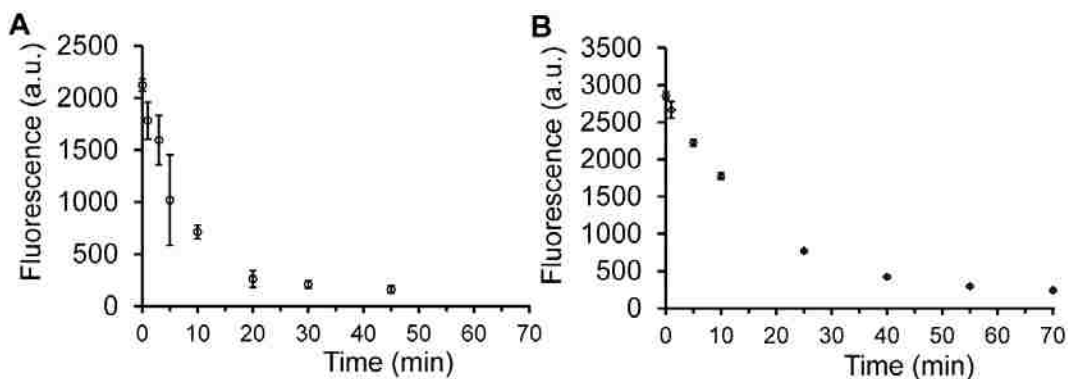


Figure 5.7 Time Course of PAD4 Reaction. PAD4 was incubated in reaction buffer (pH=8.0) with ZRCoum (25 μ M) at 37 ° C (A) and room temperature (B). Fluorescence was measured (λ_{ex} = 340 nm, λ_{em} = 475 nm) in the presence of trypsin/EDTA. Data represented as mean +/- SD.

From the time course analyses, kinetics constants were calculated and the parameters ($K_M = 397 \mu\text{M}$, $k_{cat} = 2.98 \text{ sec}^{-1}$, $k_{cat} / K_M = 7400 \text{ M}^{-1}\text{sec}^{-1}$) were found to be similar to other PAD4 substrates.²⁸ We observed slightly different parameters with PAD2 ($K_M = 260 \mu\text{M}$, $k_{cat} = 0.51 \text{ sec}^{-1}$, $k_{cat} / K_M = 1950 \text{ M}^{-1}\text{sec}^{-1}$) compared to PAD4 (Figure 5.8), which is expected considering their inherent differences in substrate preferences. These values are also comparable to a similar substrate evaluated with PAD2 using the ammonia-release colorimetric assay.³⁸

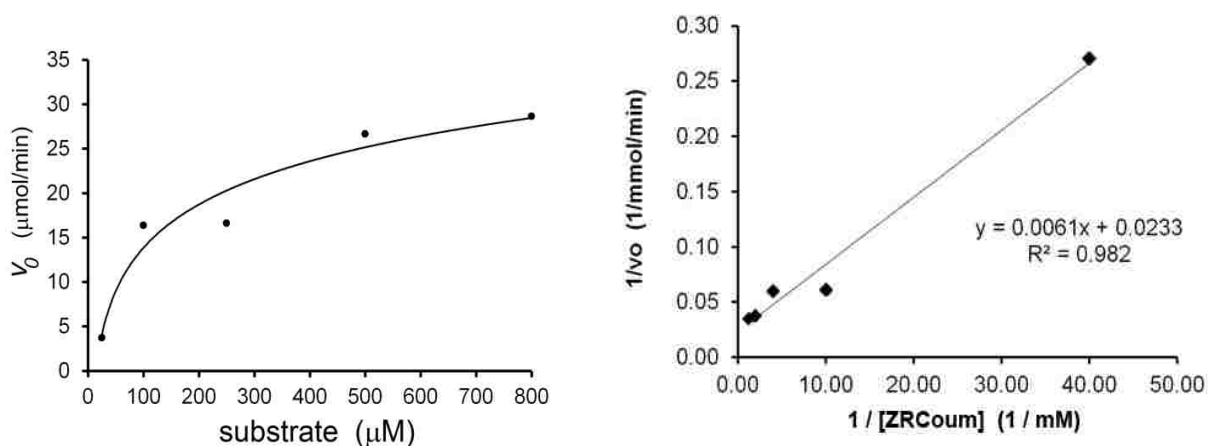


Figure 5.8 Kinetics of PAD2 Reaction. (Left) Michaelis–Menten data obtained from varying ZRCoum concentration and time to determine rate, V_0 , as a function of ZRCoum concentration. (Right) Lineweaver-Burk plot (double reciprocal plot) of PAD2 activity in the presence of varying concentrations of the substrate, ZRCoum.

5.4.2.4 Trypsin Inhibition

In adapting our assay to high-throughput screening platforms, we addressed the possibility of a false negative small molecule inhibitor resulting from unintended inhibition of trypsin. The assay we developed couples the citrullination reaction by PAD2 / PAD4 with the protease action of trypsin. We imagined that large concentrations of trypsin would not reduce the signal-to-noise ratio. Furthermore, we anticipated that small molecules that could inhibit trypsin would not disrupt the assay given the quantity of trypsin present. To test this, we incubated our assay in the presence of trypsin inhibitors. Phenylmethylsulfonyl fluoride (PMSF), a known covalent-inhibitor of trypsin, was incubated with the reaction mixture prior to trypsin introduction. We observed that co-incubation of trypsin with PMSF did not alter the fluorescence output within our assay conditions. The assay was also tested against benzamidine, a trypsin inhibitor with increased water stability (Figure 5.9). These findings are consistent with the amount of trypsin added in the unmasking of the fluorophore, which far exceeds the usual amount of potential inhibitor being evaluated and should not result in false positive hits.

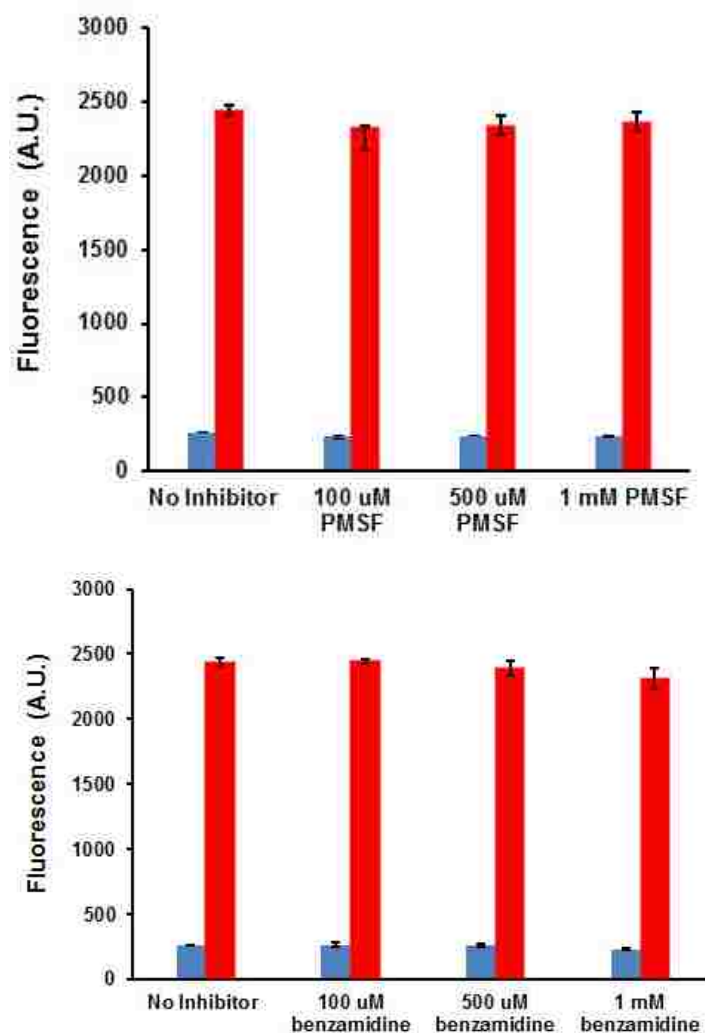


Figure 5.9 Analysis of Trypsin Inhibition. ZRCoum (25 μ M) was incubated in reaction buffer at 37 $^{\circ}$ C in the presence of trypsin inhibitors. After trypsin/EDTA addition, the fluorescence was measured (λ_{ex} = 340 nm, λ_{em} = 475 nm) in the absence (blue) and presence (red) of trypsin/EDTA. Data represented as mean \pm SD.

Having shown that the assay is tolerant to a variety of conditions that are typically encountered in small molecule drug discovery efforts, we set out to highlight the selectivity of the reaction by performing the reaction in crude whole cell lysates. *E. coli* cells containing the GST-PAD4 expression vector were induced with isopropyl β -D-1-thiogalactopyranoside (IPTG), similar to the procedure used for the isolation of GST-PAD4. Following the disruption of the cell membrane via sonication, the cellular debris was separated by centrifugation to afford a clarified cell lysate. When the PAD4-containing cell lysate was submitted to the same assay conditions as the purified GST-PAD4 assay, the fluorescence signal varied in agreement with the presence of active PAD4 in solution. Cell lysates contain a number of biomacromolecules at high concentrations that could potentially interfere with the assay (i.e. the activity of PAD4, the fluorescent properties of ZRCoum, and the trypsin hydrolysis). We found that the assay was functional in crude cell lysates thus indicating a high selectivity in the reaction between PAD4 and ZRCoum. To further demonstrate that the signal decrease in the presence of crude cell lysates was specific to the presence of active PAD4, we evaluated the effect of Cl-amidine, an established PAD4 inhibitor. The addition of Cl-amidine leads to a restoration in the fluorescence signal, consistent with the inactivation of PAD4 (Figure 5.10). Together, we show that the assay can be further simplified by utilizing crude cell lysates for the monitoring of PAD4 activity.

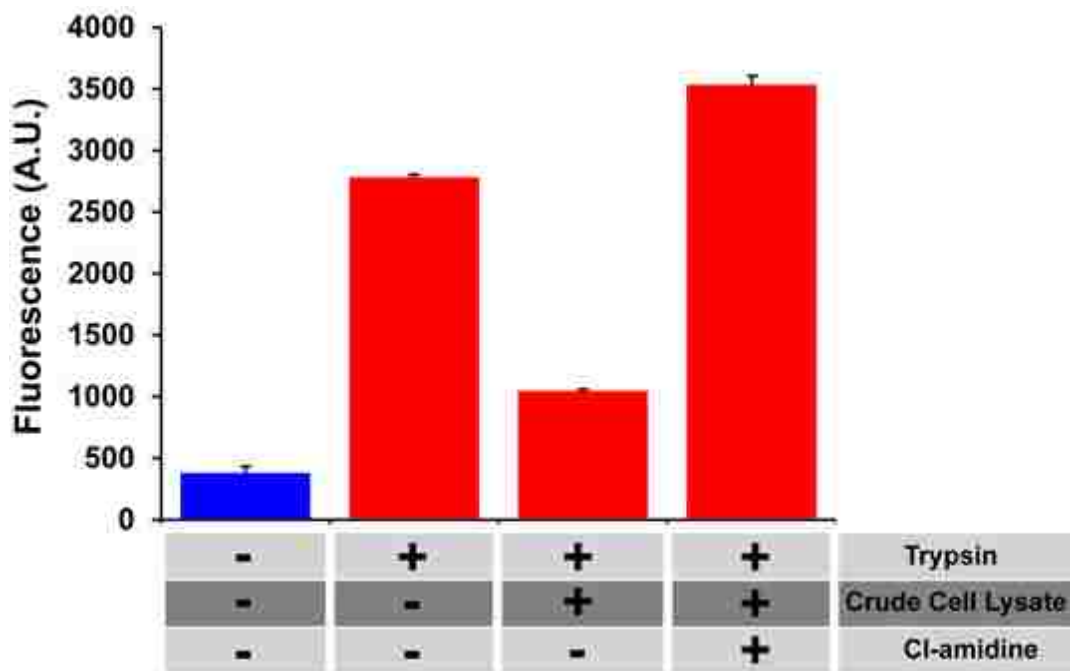


Figure 5.10 Assay using Crude Cell Lysate as PAD4 Source. ZRCoum (25 μ M) and cell lysate was incubated in reaction buffer at room temperature in a 384-well plate. After trypsin/EDTA addition, the fluorescence was measured (λ_{ex} = 340 nm, λ_{em} = 475 nm) in the absence (blue) and presence (red) of trypsin/EDTA. Data represented as mean \pm SD.

5.4.3 Assay Response to known PAD Inhibitors

Finally, we evaluated the ability of the assay to respond to the presence of known inhibitors: Cl-amidine and YW4-03.^{37, 39} It was found that both of these compounds effectively reduce the citrullination reaction by PAD2 / PAD4, consistent with previous findings for these compounds (Figure 5.11). The IC₅₀ values for Cl-amidine are 14 μ M and 19 μ M for PAD2 and PAD4, respectively. The IC₅₀ values for YW4-03 are 6 μ M and 14 μ M for PAD2 and PAD4, respectively. Furthermore, the data suggests that YW4-03 is a more effective inhibitor for PAD2 than PAD4. This slight selectivity in inhibition is especially significant in diseases where PAD2 and PAD4 are both overexpressed and supports the existence of novel PAD selective inhibitors.

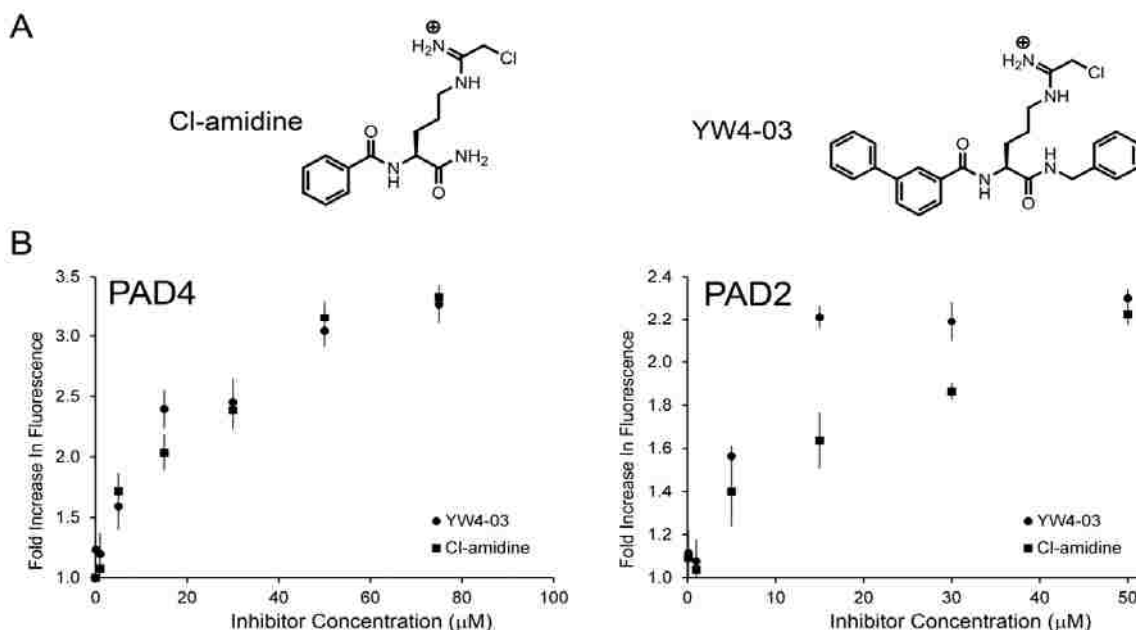


Figure 5.11 Assay Reports on PAD Inhibition. (A) Chemical structures of Cl-amidine and YW4-03. (B) IC₅₀ curves of Cl-amidine and YW4-03. Conditions: PAD2 / PAD4 (2 μ M) were incubated with ZRCoum (25 μ M) in 384-well plate at 37 $^{\circ}$ C for 6 h. Fluorescence was measured ($\lambda_{\text{ex}} = 340$ nm, $\lambda_{\text{em}} = 475$ nm) in the presence of trypsin/EDTA. Data represented as mean \pm SD.

5.5 CONCLUSION

We report a novel rapid and facile fluorescence-based assay of PAD2 / PAD4, which relies on the re-design of an arginine substrate. In particular, we incorporated a fluorescent moiety whose fluorescence is controlled by the reaction of the substrate with the enzyme. The citrullination reaction leads to a change in the level of blue fluorescence, yielding a reliable read-out of PAD activity. This strategy has proven to be compatible with high-throughput screening platforms. The assay has several advantages over existing technologies, including a strong signal-to-noise ratio, speed of analysis, and robustness of measurement. Most importantly, it is technically facile and can be performed with readily available reagents. Having shown that the assay is tolerant to a variety of conditions that are typically encountered in small molecule drug discovery efforts, we set out to employ it for high-throughput screening of potential PAD4 inhibitors. Working with the Drug Discovery Core Facility at Penn State Hershey Medical, we conducted a pilot screen of 80 compounds in order to quantify the suitability of the assay for use in a high-throughput screen. To measure suitability, a Z-factor or Z' (Z-prime) is calculated based off of four parameters: the means and standard deviations of both the positive and negative controls.

1.0	Ideal Assay
$0.5 < X < 1.0$	Excellent Assay
$0 < X < 0.5$	Marginal Assay
$X < 0$	Too much overlap between positive and negative controls for the assay to be considered useful

Table 5.1 Interpretation of Z-factor.

In regarding the pilot screen, a robust Z' value of 0.7 was identified making the assay very compatible for high-throughput robotics. To date, over 2,000 natural and FDA-approved compounds have been screened via our assay using the robotic lab at the Drug Discovery Core Facility. No positive hits have been discovered.

5.6 REFERENCES

1. Jensen, O. N., Interpreting the protein language using proteomics. *Nat Rev Mol Cell Biol* **2006**, 7 (6), 391-403.
2. Sims, R. J., 3rd; Reinberg, D., Is there a code embedded in proteins that is based on post-translational modifications? *Nat Rev Mol Cell Biol* **2008**, 9 (10), 815-20.
3. Pandey, A.; Mann, M., Proteomics to study genes and genomes. *Nature* **2000**, 405 (6788), 837-46.
4. Berger, S. L., The complex language of chromatin regulation during transcription. *Nature* **2007**, 447 (7143), 407-12.
5. Taverna, S. D.; Li, H.; Ruthenburg, A. J.; Allis, C. D.; Patel, D. J., How chromatin-binding modules interpret histone modifications: lessons from professional pocket pickers. *Nat Struct Mol Biol* **2007**, 14 (11), 1025-40.
6. Strahl, B. D.; Allis, C. D., The language of covalent histone modifications. *Nature* **2000**, 403 (6765), 41-5.
7. Seet, B. T.; Dikic, I.; Zhou, M. M.; Pawson, T., Reading protein modifications with interaction domains. *Nat Rev Mol Cell Biol* **2006**, 7 (7), 473-83.
8. Fischle, W.; Wang, Y.; Allis, C. D., Binary switches and modification cassettes in histone biology and beyond. *Nature* **2003**, 425 (6957), 475-9.
9. Mann, M.; Jensen, O. N., Proteomic analysis of post-translational modifications. *Nat Biotech* **2003**, 21 (3), 255-261.
10. Auger, I.; Charpin, C.; Balandraud, N.; Martin, M.; Roudier, J., Autoantibodies to PAD4 and BRAF in rheumatoid arthritis. *Autoimmunity Reviews* **2012**, 11 (11), 801-803.
11. Kinloch, A. L., K.; Wait, R.; Wegner, N.; Lim, N. H.; Zendman, A. J.; Saxne, T.; Malmstrom, V.; Venables, P. J., Synovial fluid is a site of citrullination of autoantigens in inflammatory arthritis. *Arthritis Rheum.* **2008**, 58, 2287-2295.
12. Shelef, M. A.; Sokolove, J.; Lahey, L. J.; Wagner, C. A.; Sackmann, E. K.; Warner, T. F.; Wang, Y.; Beebe, D. J.; Robinson, W. H.; Huttenlocher, A., Peptidylarginine Deiminase 4 Contributes to Tumor Necrosis Factor α -Induced Inflammatory Arthritis. *Arthritis & Rheumatology* **2014**, 66 (6), 1482-1491.
13. Wood, D. D.; Ackerley, C. A.; Brand, B. v. d.; Zhang, L.; Rajmakers, R.; Mastronardi, F. G.; Moscarello, M. A., Myelin localization of peptidylarginine deiminases 2 and 4: comparison of PAD2 and PAD4 activities. *Lab Invest* **2008**, 88 (4), 354-364.
14. Wang, S.; Wang, Y., Peptidylarginine deiminases in citrullination, gene regulation, health and pathogenesis. *Biochim Biophys Acta* **2013**, 1829 (10), 1126-35.
15. Knight, J. S.; Zhao, W.; Luo, W.; Subramanian, V.; x; Dell, A. A.; Yalavarthi, S.; Hodgkin, J. B.; Eitzman, D. T.; Thompson, P. R.; Kaplan, M. J., Peptidylarginine deiminase inhibition is immunomodulatory and vasculoprotective in murine lupus. *The Journal of Clinical Investigation* **2013**, 123 (7), 2981-2993.
16. Wang, Y., Li, P. Wang, J., Hu, X. A., Chen, J., Wu, M., Fisher, K., Oshaben, N., Zhao, Y., Gu, D., Wang, G., Chen, G., Anticancer Peptidylarginine Deiminase (PAD) Inhibitors Regulate the Autophagy Flux and the Mammalian Target of Rapamycin Complex 1 Activity. *J. Biol.Chem.* **2012**, 287, 25941-25953.

17. Cherrington, B. D.; Zhang, X.; McElwee, J. L.; Morency, E.; Anguish, L. J.; Coonrod, S. A., Potential Role for PAD2 in Gene Regulation in Breast Cancer Cells. *PLoS ONE* **2012**, *7* (7), e41242.
18. Nakashima, K.; Hagiwara, T.; Yamada, M., Nuclear Localization of Peptidylarginine Deiminase V and Histone Deimination in Granulocytes. *Journal of Biological Chemistry* **2002**, *277* (51), 49562-49568.
19. Hagiwara, T.; Hidaka, Y.; Yamada, M., Deimination of histone H2A and H4 at arginine 3 in HL-60 granulocytes. *Biochemistry* **2005**, *44* (15), 5827-34.
20. Kearney, P. L.; Bhatia, M.; Jones, N. G.; Yuan, L.; Glascock, M. C.; Catchings, K. L.; Yamada, M.; Thompson, P. R., Kinetic Characterization of Protein Arginine Deiminase 4: A Transcriptional Corepressor Implicated in the Onset and Progression of Rheumatoid Arthritis†. *Biochemistry* **2005**, *44* (31), 10570-10582.
21. Christophorou, M. A.; Castelo-Branco, G.; Halley-Stott, R. P.; Oliveira, C. S.; Loos, R.; Radzisheuskaya, A.; Mowen, K. A.; Bertone, P.; Silva, J. C.; Zernicka-Goetz, M.; Nielsen, M. L.; Gurdon, J. B.; Kouzarides, T., Citrullination regulates pluripotency and histone H1 binding to chromatin. *Nature* **2014**.
22. Li, P.; Li, M.; Lindberg, M. R.; Kennett, M. J.; Xiong, N.; Wang, Y., PAD4 is essential for antibacterial innate immunity mediated by neutrophil extracellular traps. *J Exp Med* **2010**, *207* (9), 1853-62.
23. Musse, A. A., Li, Z., Ackerley, C. A., Bienzle, D., Lei, H., Poma, R., Harauzi, G., Moscarello, M. A., Mastronardi, F. G., Peptidylarginine deiminase 2 (PAD2) overexpression in transgenic mice leads to myelin loss in the central nervous system. *Dis. Model. Mech.* **2008**, *1*, 229-240.
24. McElwee, J. L.; Mohanan, S.; Horibata, S.; Sams, K. L.; Anguish, L. J.; McLean, D.; Cvitaš, I.; Wakshlag, J. J.; Coonrod, S. A., PAD2 Overexpression in Transgenic Mice Promotes Spontaneous Skin Neoplasia. *Cancer Research* **2014**.
25. Li, P.; Yao, H.; Zhang, Z.; Li, M.; Luo, Y.; Thompson, P. R.; Gilmour, D. S.; Wang, Y., Regulation of p53 target gene expression by peptidylarginine deiminase 4. *Mol Cell Biol* **2008**, *28* (15), 4745-58.
26. Slack, J. L.; Causey, C. P.; Thompson, P. R., Protein arginine deiminase 4: a target for an epigenetic cancer therapy. *Cell Mol Life Sci* **2011**, *68* (4), 709-20.
27. Luo, Y.; Knuckley, B.; Lee, Y. H.; Stallcup, M. R.; Thompson, P. R., A fluoroacetamide-based inactivator of protein arginine deiminase 4: design, synthesis, and in vitro and in vivo evaluation. *J Am Chem Soc* **2006**, *128* (4), 1092-3.
28. Knuckley, B.; Causey, C. P.; Jones, J. E.; Bhatia, M.; Dreyton, C. J.; Osborne, T. C.; Takahara, H.; Thompson, P. R., Substrate specificity and kinetic studies of PADs 1, 3, and 4 identify potent and selective inhibitors of protein arginine deiminase 3. *Biochemistry* **2010**, *49* (23), 4852-63.
29. Knipp, M.; Vasak, M., A colorimetric 96-well microtiter plate assay for the determination of enzymatically formed citrulline. *Anal Biochem* **2000**, *286* (2), 257-64.
30. Knuckley, B., Jones, J. E., Bachovchin D. A., Slack, J., Causey C., Brown, S., Rosen, H., Cravatt, B., Thompson, P. R. , A Fluopol-ABPP HTS Assay to Identify PAD Inhibitors. *Chem. Commun.* **2010**, *46* (38), 7175-7.

31. Bicker, K. L.; Subramanian, V.; Chumanevich, A. A.; Hofseth, L. J.; Thompson, P. R., Seeing citrulline: development of a phenylglyoxal-based probe to visualize protein citrullination. *J Am Chem Soc* **2012**, *134* (41), 17015-8.
32. Jones, J. E.; Slack, J. L.; Fang, P.; Zhang, X.; Subramanian, V.; Causey, C. P.; Coonrod, S. A.; Guo, M.; Thompson, P. R., Synthesis and screening of a haloacetamide containing library to identify PAD4 selective inhibitors. *ACS Chem Biol* **2012**, *7* (1), 160-5.
33. Tanikawa, C.; Espinosa, M.; Suzuki, A.; Masuda, K.; Yamamoto, K.; Tsuchiya, E.; Ueda, K.; Daigo, Y.; Nakamura, Y.; Matsuda, K., Regulation of histone modification and chromatin structure by the p53-PADI4 pathway. *Nat Commun* **2012**, *3*, 676.
34. Cui, X.; Witalison, E. E.; Chumanevich, A. P.; Chumanevich, A. A.; Poudyal, D.; Subramanian, V.; Schetter, A. J.; Harris, C. C.; Thompson, P. R.; Hofseth, L. J., The induction of microRNA-16 in colon cancer cells by protein arginine deiminase inhibition causes a p53-dependent cell cycle arrest. *PLoS One* **2013**, *8* (1), e53791.
35. Wildeman, E.; Pires, M. M., Facile Fluorescence-Based Detection of PAD4-Mediated Citrullination. *ChemBioChem* **2013**, *14* (8), 963-967.
36. Arita, K.; Hashimoto, H.; Shimizu, T.; Nakashima, K.; Yamada, M.; Sato, M., Structural basis for Ca²⁺-induced activation of human PAD4. *Nat Struct Mol Biol* **2004**, *11* (8), 777-783.
37. Luo, Y.; Arita, K.; Bhatia, M.; Knuckley, B.; Lee, Y.-H.; Stallcup, M. R.; Sato, M.; Thompson, P. R., Inhibitors and Inactivators of Protein Arginine Deiminase 4: Functional and Structural Characterization. *Biochemistry* **2006**, *45* (39), 11727-11736.
38. Dreyton, C. J.; Knuckley, B.; Jones, J. E.; Lewallen, D. M.; Thompson, P. R., Mechanistic Studies of Protein Arginine Deiminase 2: Evidence for a Substrate-Assisted Mechanism. *Biochemistry* **2014**, *53* (27), 4426-4433.
39. Wang, Y.; Li, P.; Wang, S.; Hu, J.; Chen, X. A.; Wu, J.; Fisher, M.; Oshaben, K.; Zhao, N.; Gu, Y.; Wang, D.; Chen, G., Anticancer peptidylarginine deiminase (PAD) inhibitors regulate the autophagy flux and the mammalian target of rapamycin complex 1 activity. *J Biol Chem* **2012**, *287* (31), 25941-53.

Chapter 6

Materials and Methods

6.1 Materials

Protected amino acids were purchased from Chem-Impex. Fluorescein 5-isothiocyanate and 5, 6-carboxyfluorescein were purchased from Chem-Impex. Amino-PEG₁₆₋₂₄-acid, DNP-PEG₂₋₁₂-acid, and Fmoc-N-amido-PEG₁₂-acid compounds were purchased from Broadpharm. Fmoc-8-amino-3,6-dioxaoctanoic acid was purchased from Chem Impex, International. Antibody was purchased from Vector Laboratories. Purified Human IgG, Normal Serum was purchased from Bethyl Laboratories. All other organic chemical reagents were purchased from Fisher Scientific or Sigma Aldrich and used without further purification. Dimethyl sulfoxide (DMSO) and Dulbecco's modified Eagle's medium (DMEM) were purchased from Thermo Fisher Scientific Inc. Fetal Bovine Serum (FBS) was purchased from Corning. Penicillin-Streptomycin was purchased from Sigma-Aldrich. 3-(4,5-dimethylthiazol-2-yl)-2,5-diphenyltetrazolium bromide (MTT) was purchased from EMD Millipore.

6.2 Mammalian Cell Culture

Human embryonic kidney 293 cells were cultured in Dulbecco's modified Eagle's medium (DMEM) supplemented with 10% FBS, 100 U/mL penicillin, and 0.1 mg/mL streptomycin in a humidified atmosphere of 5% CO₂ at 37 °C.

6.3 Bacterial Cell Culture

Bacterial cells were cultured in specific media in an aerobic environment shaking at 250 rpm at 37 °C. *S. aureus*, *S. epidermidis*, *B. subtilis*, *E. coli*, *Acinetobacter baumannii*, *Klebsiella pneumoniae*, were all grown in Luria Bertani (LB) medium. *P. aeruginosa* were grown in Trypsin Soy Broth (TSB) medium. *L. monocytogenes* was grown in Brain Heart Infusion (BHI) medium.

6.4 Bacterial Strains

Bacterial strains utilized in this work are as followed.

Bacterial Strain	Classification	Chapter Reference
<i>B. subtilis</i> NCIB 3610	Gram Positive	3
<i>S. aureus</i> Newman	Gram Positive	3, 4
<i>S. aureus</i> Sc01	Gram Positive	3
<i>S. epidermidis</i> NRS101	Gram Positive	3
<i>L. monocytogenes</i> 10403s	Gram Positive	3
<i>E. coli</i> MG1655	Gram Negative	3,4
<i>Acinetobacter baumannii</i> ATCC 19606	Gram Negative	4
<i>Klebsiella pneumoniae</i> ATCC 13883	Gram Negative	4
<i>Pseudomonas aeruginosa</i> ATCC 27853	Gram Negative	4
<i>Pseudomonas aeruginosa</i> ATCC 27853	Gram Negative	4
<i>E. coli</i> XL1 Blue	Gram Negative	5
<i>E. coli</i> BL21 (DE3)	Gram Negative	5

6.5 Synthesis of FITC-conjugated anti-DNP Antibody

Anti-DNP rabbit (1 mg/mL) was suspended in 1 mL cold solution of 0.05 M boric acid, 0.2 M NaCl at a pH = 9.2 in a 30 KDa molecular weight cut-off centrifuge tube. Antibody was spun at 5,000g for 10 min at 4 °C (4X) to complete the wash process. A solution of 5 mg/mL of fluorescein 5-isothiocyanate (40 µL) was added to the washed

antibody solution (1mL). Solution rotated for 2 h protected from light. After reaction time, solution was washed in with 10 mM phosphate, 0.15 M NaCl, 0.08% NaN₃ at pH = 7.8, as before. Concentration was determined by absorbance at 280 nm and 480 nm via Shimadzu Biotech BioSpec-nano spectrophotometer.

6.6 Solid Phase Peptide Synthesis of FITC-Conjugated Sortase Recognition Peptides

A 25 ml synthetic vessel was charged with 564 g (0.41 mmol) of Rink Amide resin. The resin was initially deprotected in a solution of 6 M piperazine/100 mM HOBt in DMF (7 ml). The flask was agitated for 30 minutes and the deprotection solution was drained. The resin was washed with DMF, CH₂Cl₂, MeOH, CH₂Cl₂, and DMF (3 x 5 ml each). Initial loading of Fmoc-Gly (example for Sortase A peptide) (4 eq., 0.91 mmol), HCTU (3.9 eq., 0.88 mmol), and DIEA (8 eq., 1.80 mmol) in DMF (10 mL) was performed. The vessel was agitated for 2 h at room temperature. The resin was then washed with DMF, CH₂Cl₂, MeOH, CH₂Cl₂ and DMF (3 x 5 ml each). The Fmoc-protecting group was removed with a solution of 6 M piperazine/100 mM HOBt in DMF (7 ml). The flask was agitated for 25 minute and the deprotection solution was drained. The resin was washed and the addition of the second amino acid was performed by adding Fmoc-protected amino acid (4 eq., 0.91 mmol), HCTU (3.9 eq., 0.88 mmol), and DIEA (8 eq., 1.80 mmol) in DMF (10 mL) and agitating for 2 hours. Peptide synthesis was continued for remaining Fmoc-protected amino acids and/or Fmoc-protected PEG groups. For the FITC modification addition, the resin was deprotected and 5, 6-carbocylfluorescein (2 eq., 0.46 mmol), HCTU (1.9 eq., 0.44 mmol), and DIEA (4 eq., 0.93 mmol) in DMF (10 mL) was added to the resin. The flask was agitated in the dark

overnight. The resin was drained and subsequently washed with DMF, CH₂Cl₂, MeOH, CH₂Cl₂ and DMF (3 x 5 ml each). The cleavage of the peptide from resin was carried out by addition of trifluoroacetic acid (TFA) cocktail solution (95% TFA, 2.5% TIPS, 2.5% H₂O, 20 ml). The mixture was agitated for 1 hour at room temperature. The resulting solution was concentrated via compressed air to remove the TFA. The residue was triturated in cold diethyl ether and the precipitate was collected by centrifugation and dissolved in H₂O. Compounds were then purified using RP-HPLC with a Phenomenex C8 prep column and an eluent consisting of solvent A (H₂O / 0.1% TFA) and solvent B (MeOH / 0.1% TFA) using a 60 minute gradient transitioning from 5% B to 100% B at a flow rate of 10 ml min⁻¹. The purity of the peptides was verified by analytical reverse phase HPLC using a Phenomenex C18 column with an eluent consisting of solvent A (CH₃CN/0.1% TFA) and solvent B (H₂O/0.1% TFA) with a 30 minute gradient consisting of 5 to 100 % B, and a flow rate of 1 ml min⁻¹ and monitored at 230 nm. Purified peptides were subsequently characterized using ESI-MS and MALDI-TOF MS.

6.7 Solid Phase Peptide Synthesis of DNP-Conjugated Sortase Recognition Peptides

The resin was initially deprotected in a solution of 6 M piperazine/100 mM HOBt in DMF (7 ml). The flask was agitated for 30 minutes and the deprotection solution was drained. The resin was washed with DMF, CH₂Cl₂, MeOH, CH₂Cl₂, and DMF (3 x 5 ml each). Initial loading of Fmoc-Gly (example for Sortase A peptide) (4 eq., 0.91 mmol), HCTU (3.9 eq., 0.88 mmol), and DIEA (8 eq., 1.80 mmol) in DMF (10 mL) was performed. The vessel was agitated for 2 h at room temperature. The resin was then washed with DMF, CH₂Cl₂, MeOH, CH₂Cl₂ and DMF (3 x 5 ml each). The Fmoc-protecting group was removed with a solution of 6 M piperazine/100 mM HOBt in DMF

(10 ml). The flask was agitated for 25 minute and the deprotection solution was drained. The resin was washed and the addition of the second amino acid was performed by adding Fmoc-protected amino acids (4 eq., 0.91 mmol), HCTU (3.9 eq., 0.88 mmol), and DIEA (8 eq., 1.80 mmol) in DMF (10 mL) and agitating for 2 hours. Peptide synthesis was continued for remaining Fmoc-protected amino acids and/or Fmoc-protected PEG groups. For the DNP modification step, the resin was treated with 2, 4-dinitrofluorobenzene (10 eq. 2.5 mmol) and DIEA (15 eq., 3.75 mmol) in DMF, and the flask was agitated in the dark for 1 hour at room temperature. The resin was drained and subsequently washed with DMF, CH₂Cl₂, and MeOH (3 x 5 mL each). The peptide was built with sequence, DNP-PEG-K(Mtt)LPMTG. The N^ε-methyltrityl protecting group of the lysine was then deprotected by adding 10 mL of a TFA cocktail solution (1% TFA, 2% TIPS in CH₂Cl₂) to the resin and agitating for 10 minutes protected from light. The solution was drained and this procedure was repeated four additional times. The solution was then drained and washed as previously stated. Upon MTT deprotection, Fmoc-8-amino-3, 6-dioxaoctanoic acid (3 eq., 0.36 mmol), HCTU (0.36 eq., 0.36 mmol), and DIEA (6 eq., 0.72 mmol) in DMF was added to the resin. After 2 h of agitation, the resin was deprotected and washed as previously stated. Depending on the length of the PEG linker, additional PEG groups were added before cleaving the peptide from the resin. After 1 h agitation with TFA cocktail solution (95% TFA, 2.5% TIPS, and 2.5 % H₂O), the resin was concentrated to remove the TFA. The residue was triturated in cold diethyl ether and the precipitate was collected by centrifugation. Peptides were purified using RP-HPLC using a Phenomenex C8 prep column with an eluent consisting of solvent A (H₂O / 0.1% TFA) and solvent B (MeOH / 0.1% TFA) using a 60 minute gradient

transitioning from 5% B to 100% B at a flow rate of 10 ml min⁻¹. The purity of the peptides was verified by analytical RP-HPLC using a Phenomenex C4 column with an eluent consisting of solvent A (H₂O /0.01% TFA) and solvent B (CH₃CN / 0.01% TFA) with a 30 minute gradient transitioning from 5% B to 100% B at a flow rate of 3 ml min⁻¹ and monitored at 230 nm and molecular weight was confirmed using MALDI-TOF MS.

6.8 Synthesis of Vancomycin-conjugated SrtA Recognition Peptides

Vancomycin (20 mg, 0.0138 mmol) was dissolved in 1 mL 50/50 DMSO: DMF. Solution was cooled on ice and HCTU (5.13mg, 0.0124 mmol) and DIEA (7.2μL, 0.0414 mmol) were added. SrtA recognition peptide, FITC(PEG_m)K(PEG_n)LPMTG or DNP(PEG₂)K(PEG)LPMTG (1.5 eq.), was added to the mixture. Reaction continued on ice for 2 h with stirring. After time, mixture was filtered and injected into RP-HPLC for purification. Peptides were purified using RP-HPLC using a Phenomenex C8 prep column with an eluent consisting of solvent A (H₂O / 0.001% TFA) and solvent B (MeOH / 0.001% TFA) using a 60 minute gradient transitioning from 5% B to 100% B at a flow rate of 10 ml min⁻¹. The purity of the peptides was verified by analytical RP-HPLC using a Phenomenex C4 column with an eluent consisting of solvent A (H₂O /0.001% TFA) and solvent B (CH₃CN / 0.001% TFA) with a 30 minute gradient transitioning from 5% B to 100% B at a flow rate of 3 ml min⁻¹ and monitored at 230 nm and molecular weight was confirmed using MALDI-TOF MS.

6.9 Synthesis of PMBN-FITC

Fluorescein isothiocyanate (FITC) (1.5 eq., 4.08 mg, 0.0105 mmol) was dissolved in DMF (100 μ L). (BOC)PMBN (1 eq., 10 mg, 0.007 mmol) was added to the fluorophore solution. DIEA (3 eq., 3.65 μ L, 0.021 mmol) was then added to the solution. Reaction progressed for 2 h while rotating protected from light. Reaction solution was purified on normal phase silica column with an eluent consisting of solvent A (CH_2Cl_2 / 0.01% DIEA) and solvent B (MeOH) with a 20 minute gradient transitioning from 0% B to 20% B at a flow rate of 18 ml min⁻¹ and monitored at 280 nm and 254 nm. Product eluted at 10% MeOH and molecular weight was confirmed using ESI-MS. Solvent was removed under reduced pressure and yellow oil was treated with acidic cocktail (50%, TFA, 2.5% TIPS, and 47.5 % CH_2Cl_2) for 2 h at room temperature to remove protecting groups. After reaction time, solvent was removed to yield 11 mg of PMBN-FITC.

6.10 Synthesis of PMBN-PEG_x-DNP

Amino-PEG16-acid (Broadpharm 21880) (12.8 mg, 0.016 mmol) was dissolved in 200 μ L of MeCN:0.1 M NaHCO_3 . 2, 4-dinitrofluorobenzene (1.5 eq, 3 μ L) was added to the reaction and progressed for 2 h at room temperature protected from light. After reaction time, product was extracted in CH_2Cl_2 : 2 M HCl and organic layer was isolated. Solvent was removed under reduced pressure and product was used without further purification. Synthesis repeated for DNP- PEG20-acid and PEG24-acid. DNP-PEG₂₋₁₂-acid compounds were purchased from Broadpharm.

DNP-PEG16-acid (1.5 eq., 12 mg, 0.012 mmol) was dissolved in DMF (50 μ L). HATU (1.4 eq., 4.7 mg, 0.0112 mmol) and DIEA (3 eq., 4.6 μ L) were added to DNP-

PEG16-acid solution. (BOC)PMBN (1 eq., 10.9 mg, 0.0079 mmol) was dissolved in DMF (100 μ L). Solutions were mixed together and rotated for 2 h protected from light. After reaction time, product was resuspended in $\text{CH}_2\text{Cl}_2:\text{NaHCO}_3$ and organic layer was isolated. Solvent was removed under reduced pressure. The resulting yellow oil was purified on normal phase silica column with an eluent consisting of solvent A (CH_2Cl_2 / 0.01% DIEA) and solvent B (MeOH) with a 20 minute gradient transitioning from 0% B to 20% B at a flow rate of 18 ml min^{-1} and monitored at 280 nm and 254 nm. Product eluted at 19% MeOH and molecular weight was confirmed using MALDI-TOF MS. Solvent was removed under reduced pressure and yellow oil was treated with acidic cocktail (50% TFA, 2.5% TIPS, and 47.5 % CH_2Cl_2) for 2 h at room temperature to remove protecting groups. After reaction time, solvent was removed to yield 13 mg of PMBN-PEG₁₆-DNP.

6.11 Synthesis of PMBN-PEG_x-DNP(Oct)

A 25 mL vessel was charged with 1 g (0.9 mmol) of 2-Chlorotriethyl chloride resin. Initial loading with N- α -Fmoc-N- ϵ -4-methyltrityl-L-lysine (Fmoc-L-Lys(Mtt)-OH) (2 eq., 1.8 mmol) and DIEA (4eq., 3.6 mmol) in anhydrous CH_2Cl_2 (10 mL) was performed. The vessel was agitated for 2 h at room temperature. The resin was washed with DMF, CH_2Cl_2 , MeOH, CH_2Cl_2 , and DMF (3 x 5 ml each). The N-terminus of lysine was deprotected in a solution of 6 M piperazine/100 mM HOBt in DMF (7 ml) for 30 min. Caprylic acid (5 eq.) was added to the vessel in DMF (10 mL) with HCTU (4.9 eq.) and DIEA (10 eq.). The vessel was agitated for 2 h at room temperature. The resin was washed as previously stated. Selective unmasking of the N ϵ -methyltrityl protecting group was completed in mild acidic conditions of 2 % TFA in CH_2Cl_2 . Fmoc-N-amido-PEG12-

acid (2 eq.) was added to the resin in DMF (10 mL) with HCTU (1.9 eq.) and DIEA (4 eq.). After shaking for 4 h, the resin was washed and deprotected, as previously stated. 2,4-dinitrofluorobenzene (8 eq.) was added to the reaction and progressed for 3 h at room temperature protected from light. After reaction time, resin was again washed and cleaved from resin in acidic conditions. After removing solvent, product was isolated and used without further purification. Lys(PEG₁₂)-DNP(Oct) was conjugated to (BOC)PMBN following reaction steps as mentioned in 6.10.

6.12 SrtA Mediated Fluorescent Labeling

Bacteria were grown in presence of FITC-labeled SrtA recognition peptides or FITC-labeled vancomycin-conjugated SrtA recognition peptides (5 μ M) overnight at 37 °C with shaking at 250 rpm in LB media. The next morning, the bacteria were harvested, washed 3X in 1X phosphate buffered saline (PBS), and fixated with 2% formaldehyde solution and analyzed via flow cytometry on a BDFacs Canto II flow cytometer (BD Biosciences, San Jose, CA) equipped with a 488 nm argon laser and a 530 bandpass filter (FL1). A minimum of 10,000 events were counted for each data point. The data were analyzed using the FACSDiva version 6.1.1 software. Cells were also imaged with fluorescent confocal microscopy.

6.13 Antibody Binding Assay in *S. aureus* (Wood Strain)

S. aureus (Wood Strain) bacteria were grown at 37 °C overnight in LB broth, supplemented with 0.4 μ g mL⁻¹ tunicamycin and DNP-2PEG1Vanc at designated concentrations with shaking at 250 rpm. The bacteria were harvested and washed 3X with 1X phosphate buffer saline (PBS). Approximately 2×10^6 colony forming units (CFU)

were then incubated in 100 μ L of PBS containing 10% (v/v) FBS and 0.02 μ g / mL of FITC-conjugated rabbit anti-dinitrophenyl IgG. All experiments were protected from light and incubated at 37 °C for 1 hour. Samples were then immediately analyzed by flow cytometry. Fluorescence data are expressed as mean arbitrary fluorescence units and were gated to include all healthy bacteria.

6.14 Antibody Binding Assay in *S. aureus*

S. aureus bacteria were grown at 37 °C overnight in LB broth, supplemented with 0.4 μ g mL⁻¹ tunicamycin and DNP-2PEG1Vanc (5 μ M) with shaking at 250 rpm. The bacteria were harvested and washed 3X with 1X phosphate buffer saline (PBS). Polyclonal antibody (0.02 μ g / mL) was added to bacteria for 20 min at 4 °C. Cells were washed and roughly 2×10^6 colony forming units (CFU) were then incubated in 100 μ L of PBS containing 10% (v/v) FBS and 0.02 μ g / mL of FITC-conjugated rabbit anti-dinitrophenyl IgG. All experiments were protected from light and incubated at 4 °C for 30 min. Cells were washed 1X PBS and fixated in 2 % formaldehyde. Samples were then analyzed by flow cytometry. Fluorescence data are expressed as mean arbitrary fluorescence units and were gated to include all healthy bacteria.

6.15 Bacterial Labeling in live *C. elegans*

N2 Caenorhabditis elegans were maintained by standard protocol using nematode growth agar with bacterial lawns of *E.coli* OP50 (source) on a 60mm x 15mm cell culture dish. For bacterial labeling assays, *C. elegans* were grown to contain primarily L4 larval stage nematodes by incubation at 25 °C for ~48-52 h. On the day of experiments, *C. elegans* were washed off the plates with M9 buffer, and washed three times with M9

buffer. For washing steps, the *C. elegans* were pelleted at 1000g. The *C. elegans* were resuspended in 450 μ L of M9 buffer containing 10% LB broth and transferred to a sterile 24 multiwell plate. For infection, *Staphylococcus aureus* Sc01 of an overnight growth was harvested at 6000g and washed three times with original culture volume of M9 buffer. The bacteria were resuspended in original culture volume in M9 buffer containing 10% LB broth and 50 μ L of the bacterial cells were added to the 450 μ L suspension of *C. elegans*. The *C. elegans* were incubated at 25 °C for 4 h, harvested at 1000g and washed three times with M9 buffer to remove excess bacteria in the extracellular space. The *C. elegans* were then resuspended in 500 μ L of M9 buffer containing 10% LB broth and 50 μ M FITC(PEG₂)K(PEG-Vanc)LPMTG (FITC-2PEG1Vanc). *C. elegans* were incubated for an additional 30 min at 25 °C. The *C. elegans* were harvested at 1000g, and washed three times with M9 buffer, and put into a final suspension of 10 mM sodium azide in M9 buffer and analyzed by confocal microscopy.

(Source) Lewis, J. A. & Fleming, J. T. (1995) *Caenorhabditis elegans: Modern Biological Analysis of an Organism*, eds. Epstein, H. F. & Shakes, D. C. (Academic, San Diego), Vol. 48, pp. 3–29.

6.16 Minimal Inhibitory Concentration Assay

The MICs of conjugates were determined by broth microdilution. Experiments were performed with Cation-adjusted Mueller-Hinton Broth (CaMHB) in 96-well polypropylene microtiter plates. Wells were inoculated with 200 μ L of bacterial suspension prepared in CaMHB (containing $\sim 10^6$ colony forming units (CFU) / mL) and 200 μ L of CaMHB containing increasing concentrations of the conjugates (0 to 100

µg/mL). The MIC was defined as the lowest concentration at which visible growth was inhibited following 18 h incubation at 37 °C.

6.17 Mammalian Cell Viability Assay

HEK293 cells were seeded in 96-well plates at a density of 10,000 cells/well and incubated overnight. Prior to treatment, constructs were dissolved in DMSO to obtain desired aliquoted stock solutions. Appropriate volumes of these stock solutions were added to DMEM media so the final concentration of DMSO was equal to 1%. After removal of cell media, 200 µL of treatment solutions were added to each well and incubated at 37 °C for 72 h. After treatment, the media was removed and the cells were washed with 100 µL of complete DMEM. Next, 100 µL of complete DMEM was added to each well. Cell viability was determined using the colorimetric 3-(4,5-dimethylthiazol-2-yl)-2,5-diphenyltetrazolium bromide (MTT) assay, in which 10 µL of a 5 mg/mL MTT stock solution was added to the treated cells and incubated for 2 h at 37 °C. The resulting formazan crystals were solubilized in 200 µL of DMSO. Absorbance was measured at 580 nm using an Infinite 200 PRO microplate reader (Tecan). Cell viability was calculated against control cells treated with complete medium.

6.18 Fluorescent Imaging

Medium containing fluorescent conjugate was prepared to desired concentration. Bacteria were inoculated (1:100) in the corresponding medium and allowed to grow at designated time points or overnight at 37 °C. The bacteria were harvested at 1,000g and washed with 1X PBS (3X). The bacteria were analyzed on a glass slide by fluorescent

confocal microscopy using a B-2E/C filter (ex 465-495/em 515-555) for bacteria labeled with FITC fluorophore.

6.19 PMBN-FITC *E. coli* Labeling

E. coli were grown overnight in LB media. Concentrated (0 - 40 μ M) aliquots of PMN-FITC were prepared in LB. Stationary phase *E. coli* (OD600 = 1.4) were harvested, suspended in PMN-FITC concentrated media, and shaken at 250 rpm for designated time points at 37 °C. After treatment, bacteria were harvested, washed with 1X phosphate buffered saline (PBS) 3X, and fixated with 2% formaldehyde solution and analyzed via flow cytometry on a BDFacs Canto II flow cytometer (BD Biosciences, San Jose, CA) equipped with a 488 nm argon laser and a 530 bandpass filter (FL1). A minimum of 10,000 events were counted for each data point. The data were analyzed using the FACSDiva version 6.1.1 software. Cells were also imaged with fluorescent confocal microscopy.

6.20 Dissociation of PMBN-FITC from *E. coli* Surface

Stationary phase *E. coli* (2 mL) were treated with 40 μ M PMN-FITC for 2 h in LB media at 37 °C. After treatment, 2 mL of cells were harvested, washed with 1X PBS, and resuspended in 2 mL of PBS. Cells were shaken at 250 rpm at 37 °C. At designated time points, 0 – 24 h, 100 μ L of cells were harvested, washed and fixated with 2% formaldehyde solution. All fixed samples were analyzed via flow cytometry as previously stated.

6.21 PMBN-PEG_x-DNP Antibody Binding Assay

Stationary phase bacteria (600 μ L) were treated with 40 μ M PMN-PEG_x-DNP for 2 h in media at 37 °C. After treatment, cells were harvested and washed with PBS 3X. 2×10^6 colony forming units (CFU) were then incubated in 100 μ L of PBS containing 10% (v/v) FBS and 0.02 μ g / mL of FITC-conjugated rabbit anti-dinitrophenyl IgG. All experiments were protected from light and incubated at 37 °C for 1 h. Cells were washed 1X PBS and fixated in 4 % formaldehyde. Samples were then analyzed by flow cytometry. Fluorescence data are expressed as mean arbitrary fluorescence units and were gated to include all healthy bacteria.

6.22 Bacterial Opsonization with Pooled Human Serum

E. coli MG1655 was grown at 37 °C in LB broth with shaking. Stationary phase *E. coli* (OD = 1.4) were incubated with 40 μ M of PMN-PEG₁₂-DNP or PMN-PEG₁₂-DNP-octanoic acid for 15 min, 30 min or 60 min. The bacteria were harvested and washed 3X with PBS solution, and fixated in 4 % formaldehyde. Bacteria were then washed 2X with LB media. Pooled human serum was diluted to 25% in PBS solution with 10 % FBS and incubated with bacteria at 4 °C for 20 min. The opsonized bacteria were then washed with PBS and 2×10^6 colony forming units (CFU) were incubated with Anti-Human IgG-FITC diluted 1:1000 in PBS containing 10% FBS at 4 °C for 30 min protected from light. Cells were washed 1X PBS and fixated in 4 % formaldehyde. Samples were then analyzed by flow cytometry as previously stated.

6.23 Time-kill Studies of Stationary-phase *E. coli*

High cell density stationary-phase cultures of *E. coli* in MH broth were treated with various concentrations of PMBN-PEG₁₂-DNP (0, 17.3, 34.6, 69.2, 103.7, 138.3, 172.9 µg /mL or 10, 20, 40, 60, 80, 100 µM). Time-kill studies were performed at 37 °C with shaking at 250 rpm. Culture aliquots (10 µL) were removed at the times shown in the figures, serially diluted in 1X PBS (pH 7.4 to 7.6), and then plated on LB agar and incubated overnight in a 37 °C incubator. Cell viability was assessed by enumerating the CFU per milliliter. Bactericidal activity was defined as a log reduction with antibiotic treatment compared with the untreated control at the start of each assay.

6.24 Antibiotic Potentiation Assay

Antibiotic synergy was determined by broth microdilution assays. Experiments were performed with cation-adjusted Mueller-Hinton Broth (CaMHB) in 96-well polypropylene microtiter plates. Wells were inoculated with 200 µL of bacterial suspension prepared in CaMHB (containing ~10⁶ colony forming units (CFU) / mL) and 200 µL of CaMHB containing increasing concentrations of the antibiotics (0 to 100 µg/mL) and 25 µg / mL of PMBN-PEG₁₂-DNP. The MIC was defined as the lowest concentration at which visible growth was inhibited following 18 h incubation at 37 °C. Data are representative of at least three biological replicates. Fractional inhibitory concentration (FIC) indices were calculated according to:

$$\mathbf{FIC\ index = (MIC_{ac} / MIC_a) + (MIC_{bc} / MIC_b) = FIC_a + FIC_b}$$

where MIC_a is the minimum inhibitory concentration (MIC) of compound A alone; MIC_{ac} is the MIC of compound A in combination with compound B; MIC_b is the MIC of

compound B alone; MIC_{bc} is the MIC of compound B in combination with compound A; FIC_a is the FIC of compound A; FIC_b is the FIC of compound B. Synergy is defined as an FIC index of ≤ 0.5 . Antagonism is defined as an FIC index of ≥ 4 .

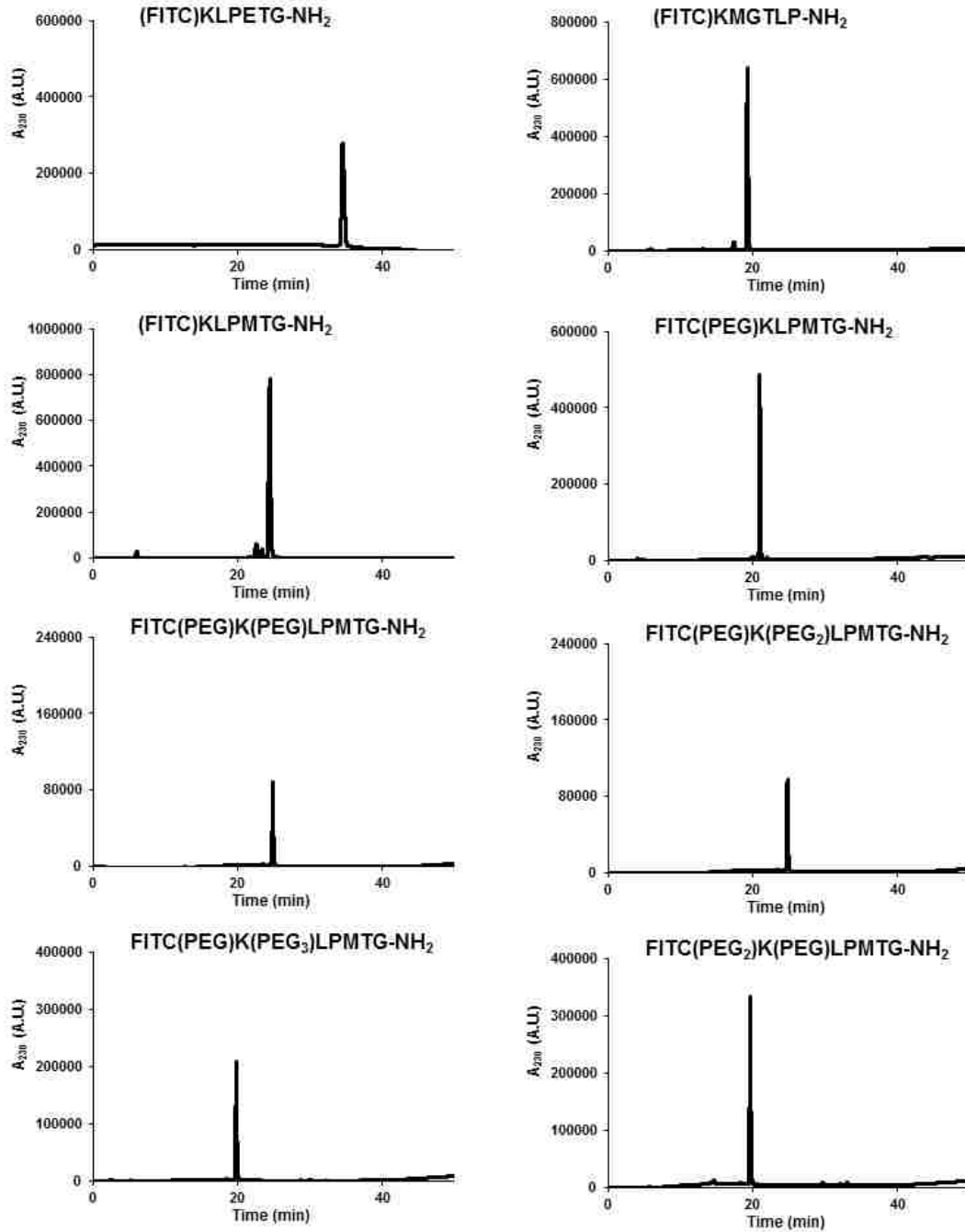
Appendices

A.1 Molecular Weights and Purities of FITC-Conjugated SrtA Recognition Peptides

Compound	Calculated [M + H ⁺]	Found [M + H ⁺]	Purity
FITC-KLPETG	1003.43	1003.046	>95%
FITC-KLPMTG	1005.43	1005.337	>95%
FITC(PEG)K(PEG)LPMTG	1295.58	1295.159	>95%
FITC(PEG)K(PEG ₂)LPMTG	1440.65	1439.911	>95%
FITC(PEG)K(PEG ₃)LPMTG	1585.73	1585.035	>95%
FITC(PEG ₂)K(PEG)LPMTG	1440.65	1440.24	>95%

Compound	Calculated [M + Na ⁺]	Found [M + Na ⁺]	Purity
FITC-KMGTLP	1027.42	1027.139	>95%
FITC(PEG)KLPMTG	1172.5	1172.911	>95%

Analytical RP-HPLC Profiles of FITC-conjugated SrtA Recognition Peptides: The specified derivatives were analyzed on a Phenomenex C4 column by reverse phase HPLC with an eluent consisting of solvent A (H₂O /0.1% TFA) and solvent B (CH₃CN /0.1% TFA) with a 30 minute gradient consisting of 5 to 100 % B, a flow rate of 3 mL/min, and monitoring at 230 nm.



A.2 Molecular Weights and Purities of Vancomycin-Conjugated SrtA Recognition Peptides

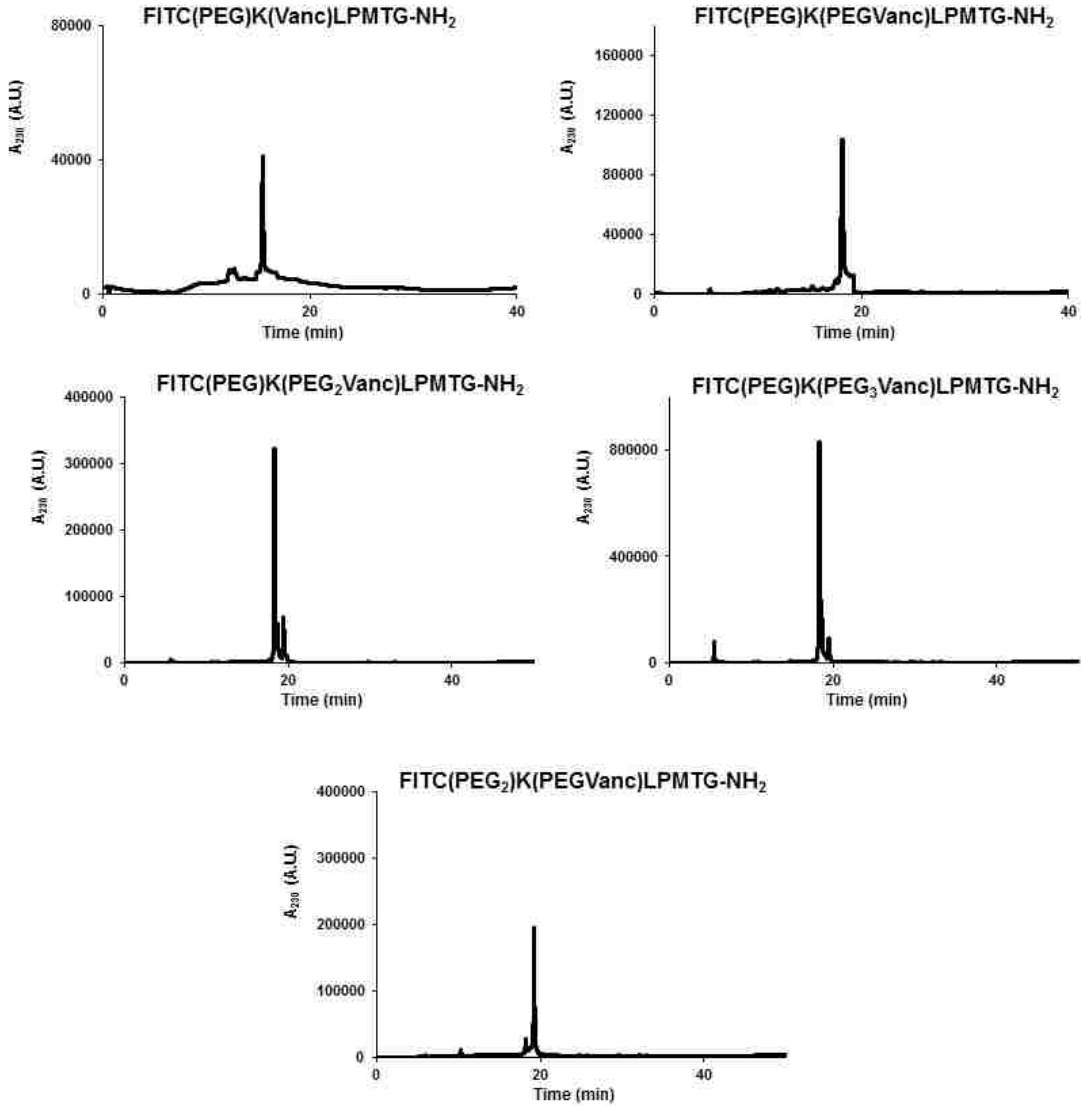
Compound	Calculated [M + H ⁺]	Found [M + H ⁺]	Purity
FITC(PEG)-K(Vanc)LPMTG	2582.54	2582.163	>95%

Compound	Calculated [M + K ⁺]	Found [M + K ⁺]	Purity
FITC(PEG)-K(PEGVanc)LPMTG	2765.78	2765.241	>95%
FITC(PEG)-K(PEG ₃ Vanc)LPMTG	3057.01	3057.809	>95%

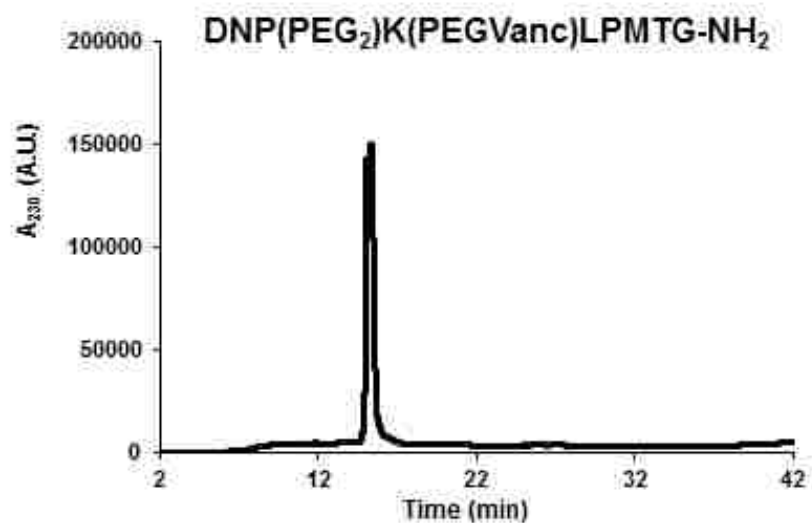
Compound	Calculated [M + Na ⁺]	Found [M + Na ⁺]	Purity
FITC(PEG)-K(PEG ₂ Vanc)LPMTG	2894.84	2894.55	>95%
FITC(PEG ₂)K(PEGVanc)LPMTG	2894.84	2894.622	>95%
DNP(PEG ₂)K(PEGVanc)LPMTG	2700.62	2700.454	>95%

Analytical RP-HPLC Profiles of FITC(PEG)K(PEG_NVanc)LPMTG-NH₂ Peptides :

The specified derivatives were analyzed on a Phenomenex C4 column by reverse phase HPLC with an eluent consisting of solvent A (H₂O /0.001% TFA) and solvent B (CH₃CN /0.001% TFA) with a 30 minute gradient consisting of 5 to 100 % B, a flow rate of 3 mL/min, and monitoring at 230 nm.



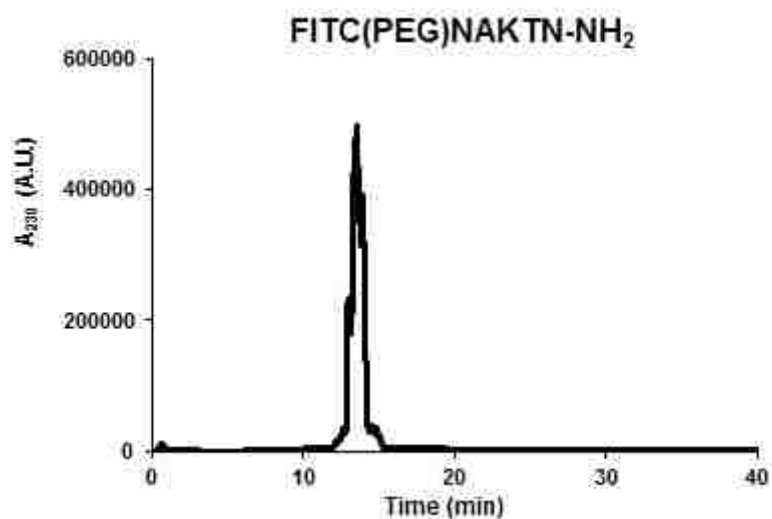
Analytical RP-HPLC Profile of DNP(PEG₂)K(PEGVanc)LPMTG-NH₂ : The specified derivative was analyzed on a Phenomenex C18 column by reverse phase HPLC with an eluent consisting of solvent A (H₂O /0.001% TFA) and solvent B (CH₃CN /0.001% TFA) with a 30 minute gradient consisting of 5 to 100 % B, a flow rate of 1 mL/min, and monitoring at 230 nm.



A.3 Molecular Weights and Purities of FITC-Conjugated SrtB Recognition Peptides

Compound	Calculated [M + H ⁺]	Found [M + H ⁺]	Purity
FITC(PEG)-NAKTN	1052.06	1052.136	>95%

Analytical RP-HPLC Profiles of FITC-conjugated Sortase B Peptide: The specified peptide was analyzed on a Phenomenex C18 column by reverse phase HPLC with an eluent consisting of solvent A (H₂O /0.1% TFA) and solvent B (CH₃CN /0.1% TFA) with a 30 minute gradient consisting of 5 to 100 % B, a flow rate of 1 mL/min, and monitoring at 230 nm.



A.4 Molecular Weights and Purities of PMBN Conjugates

Compound	Calculated [M + Na⁺]	Found [M + Na⁺]	Purity
PMBN-PEG₂-DNP	1311.399	1311.815	>98%
PMBN-PEG₄-DNP	1399.499	1399.842	>98%
PMBN-PEG₆-DNP	1487.609	1487.829	>98%
PMBN-PEG₁₂-DNP	1751.919	1751.447	>98%
PMBN-PEG₁₆-DNP	1928.123	1928.094	>98%
PMBN-PEG₂₀-DNP	2104.349	2104.221	>98%
PMBN-PEG₂₄-DNP	2280.559	2279.925	>98%

Compound	Calculated [M + H⁺]	Found [M + H⁺]	Purity
PMBN-FITC	1353.52	1354.304	>98%
PMBN-PEG₁₂-DNP(Oct)	1983.2	1983.476	>95%

Mary J. Sabulski

EDUCATION

- PhD, Chemistry**, Lehigh University, Bethlehem PA *April 2017*
- Thesis Title: Development of Immunotherapy Strategies: Targeting Gram-positive and Gram-negative Pathogenic Bacteria
 - Advisor: Marcos M. Pires, PhD
- MS, Chemistry**, Lehigh University, Bethlehem PA *May 2016*
- BS, Chemistry**, *magna cum laude*, King's College, Wilkes-Barre, PA *May 2011*
Minor: Mathematics

RESEARCH EXPERIENCE

- Graduate Research Assistant, Lehigh University** *August 2011 – Present*
Advisor: Marcos M. Pires, Ph. D.
- Constructed therapeutic agents utilizing last resort antibiotics for bacterial immunotherapy
 - Optimized the protocol for the synthesis and purification of epitope-displaying agents specifically targeting Gram-positive and -negative bacteria.
 - Extensively designed/performed treatment and viability assays.
 - Designed a facile assay to determine activity of proteins implicated in the onset of rheumatoid arthritis and breast cancer.
- Undergraduate Research Student, King's College** *August 2010 – May 2011*
Advisor: Ronald M. Supkowski, Ph. D.
- Studied the effects of low levels of personal care pharmaceuticals (PPCPs) on aquatic life.
 - Detected and quantified traces of PPCPs in environmental samples.
- Undergraduate Research Student, Pennsylvania State University** *Summer 2010*
Advisor: Harry R. Allcock, Ph. D.
- Synthesized polymers based on the polyphosphazene scaffold to be utilized in several energy-related applications.

TEACHING EXPERIENCE

- Teaching Assistant, Lehigh University** *August 2011 – May 2016*
- Supervised general chemistry, organic and biochemistry laboratories consisting of roughly 20 students.
 - Instructed students in chemical techniques, safety and efficiency.
 - Emphasized accuracy and completion of scientific notebooks.
- Guest Lecturer, Lehigh University**
- Bio-organic Chemistry (Prof. Marcos Pires) *March 2015 and January 2017*
Title: "Nucleic Acids as Therapeutics in Cancer Biology"
 - Organic Chemistry Laboratory II (Prof. Aliana Lungu) *November 2014*
Title: "Preparation and Properties of Acetylene"

After-School Program Teacher, Broughal Middle School

Spring 2016

- The Pires Lab established *Mad Science* – an after school program for students in 6th - 8th grade. The 75 min program was held once a week for 6 weeks. During that duration, I explored topics in chemistry and biology with 10 to 15 students.

PRESENTATIONS

- Emerging Paradigms in Drug Discover & Chemical Biology
New York Academy of Sciences, New York, NY *October 2016*
- Graduate Research Seminar, Lehigh University, Bethlehem, PA *November 2012*
- Undergraduate Poster Presentation, Misericordia University, Dallas, PA *May 2011*
- Undergraduate Research Seminar, Wilkes University, Wilkes-Barre, PA *November 2010*

PUBLICATIONS

Sabulski, M.J., Yu, Y., Regen, S. L., Pires, M. M., “Synthetic Immuno-Attractants Against Gram-negative Pathogens” 2017. *In Preparation*

Sabulski, M.J., Pidgeon, S. E., Pires, M. M., “Narrow-Spectrum Immune Stimulants Target *Staphylococcus aureus*” 2017. *In Preparation*

Sabulski, M.J., Wang, Y., Pires, M. M., “PAD2 Activity Monitored via a Fluorescent Substrate Analog” *Chemical Biology & Drug Design* 2015, 86 (4), 599-605.

Sabulski, M. J., Fura, J. M., Pires, M.M., “Fluorescence-based Monitoring of PAD4 Activity via a Pro- Fluorescence Substrate Analog” *Journal of Visualized Experiments* 2014, (93).

Yu, Y., **Sabulski, M. J.**, Schell, W. A., Pires, M. M., Perfect, J. R., Regen, S. L., “Simple Strategy for Taming Membrane-Disrupting Antibiotics” *Bioconjugate Chemistry* 2016, 27 (12), 2850-2853.

Fura, J. M., **Sabulski, M. J.**, Pires, M.M., “D-Amino Acid Mediated Recruitment of Endogenous Antibodies to Bacterial Surfaces” *ACS Chemical Biology* 2014, 9 (7), 1480-1489.